Heterogeneous reactions of mineral dust aerosol: implications for tropospheric oxidation capacity

Mingjin Tang,[1,*] Xin Huang,[2] Keding Lu,[3] Maofa Ge,[4] Yongjie Li,[5] Peng Cheng,[6] Tong Zhu,[3,*] Aijun Ding,[2] Yuanhang Zhang,[3] Sasho Gligorovski,[1] Wei Song,[1] Xiang Ding,[1] Xinhui Bi,[1] Xinming Wang[1,7,*]

[1] State Key Laboratory of Organic Geochemistry and Guangdong Key Laboratory of Environmental Protection and Resources Utilization, Guangzhou Institute of Geochemistry, Chinese Academy of Sciences, Guangzhou, China

[2] Joint International Research Laboratory of Atmospheric and Earth System Sciences (JirLATEST)，School of Atmospheric Sciences, Nanjing University, Nanjing, China

[3] State Key Joint Laboratory of Environmental Simulation and Pollution Control, College of Environmental Sciences and Engineering, Peking University, Beijing, China

[4] Beijing National Laboratory for Molecular Sciences, State Key Laboratory for Structural Chemistry of Unstable and Stable Species, Institute of Chemistry, Chinese Academy of Sciences, Beijing, China

[5] Department of Civil and Environmental Engineering, Faculty of Science and Technology, University of Macau, Avenida da Universidade, Taipa, Macau, China

[6] Institute of Mass Spectrometer and Atmospheric Environment, Jinan University, Guangzhou, China

[7] Center for Excellence in Regional Atmospheric Environment, Institute of Urban Environment, Chinese Academy of Sciences, Xiamen 361021, China

Correspondence: Mingjin Tang (mingjintang@gig.ac.cn), Tong Zhu (tzhu@pku.edu.cn)

Abstract

Heterogeneous reactions of mineral dust aerosol with trace gases in the atmosphere could directly and indirectly affect tropospheric oxidation capacity, in addition to aerosol composition and physicochemical properties. In this article we provide a comprehensive and critical review of laboratory studies of heterogeneous uptake of OH, NO_3, O_3, and their directly related species as well (including HO_2, H_2O_2, HCHO, HONO, and N_2O_5) by mineral dust particles. Atmospheric importance of heterogeneous uptake as sinks for these species are assessed i) by comparing their lifetimes with respect to heterogeneous reactions with mineral dust to lifetimes with respect to other major loss processes and ii) by discussing relevant field and modelling studies. We have also outlined major open questions and challenges in laboratory studies of heterogeneous uptake by mineral dust and discussed research strategies to address them in order to better understand the effects of heterogeneous reactions with mineral dust on tropospheric oxidation capacity.

1 Introduction

1.1 Mineral dust in the atmosphere

Mineral dust, emitted from arid and semi-arid regions with an annual flux of ~2000 Tg per year, is one of the most abundant types of aerosol particles in the troposphere (Zhang et al., 2003b; Textor et al., 2006; Huneeus et al., 2011; Ginoux et al., 2012; Huang et al., 2016). After being emitted into the atmosphere, mineral dust aerosol has an average lifetime of a few days in the troposphere and can be transported over several thousand kilometers, thus having important impacts globally (Prospero, 1999; Uno et al., 2009; Huneeus et al., 2011). Mineral dust aerosol has a myriad of significant impacts on atmospheric chemistry and climate. For example, dust aerosol particles can influence the radiative balance of the Earth system directly by scattering and absorbing solar and terrestrial radiation (Balkanski et al., 2007; Jung et al., 2010; Lemaitre et al., 2010; Huang et al., 2014; Huang et al., 2015b; Zhang et al., 2015; Bi et al., 2016; Bi et al., 2017; Kok et al., 2017; Moteki et al., 2017), and indirectly by serving as cloud condensation nuclei (CCN) to form cloud droplets (Koehler et al., 2009; Kumar et al., 2009; Twohy et al., 2009; Garimella et al., 2014; Tang et al., 2016a) and ice nucleation particles (INP) to form ice particles (DeMott et al., 2003; Hoose and Moehler, 2012; Murray et al., 2012; Ladino et al., 2013; DeMott et al., 2015). Mineral dust particles are believed to be the dominant ice nucleation particles in the troposphere (Hoose et al., 2010; Creamean et al., 2013; Cziczo et al., 2013), therefore having a large impact on the radiative balance, precipitation, and the hydrological cycle (Rosenfeld et al., 2001; Lohmann and Feichter, 2005; Rosenfeld et al., 2008). In addition, deposition of mineral dust is a major source for several important nutrient elements (e.g., Fe and P) in remote regions such as open ocean waters and the Amazon (Jickells et al., 2005; Mahowald et al., 2005; Mahowald et al., 2008; Boyd and Ellwood, 2010; Nenes et al., 2011; Schulz et al., 2012; Shi et al., 2012), strongly affecting several biogeochemical cycles and the climate system of the Earth (Jickells et al., 2005; Mahowald, 2011; Mahowald

et al., 2011; Schulz et al., 2012). The impacts of mineral dust aerosol on air quality, atmospheric visibility, and public health have also been widely documented (Prospero, 1999; Mahowald et al., 2007; Meng and Lu, 2007; De Longueville et al., 2010; de Longueville et al., 2013; Giannadaki et al., 2014; Yang et al., 2017).

It is worthy being emphasized that impacts of mineral dust aerosol on various aspects of atmospheric chemistry and climate depend on its mineralogy (Journet et al., 2008; Crowley et al., 2010a; Formenti et al., 2011; Highwood and Ryder, 2014; Jickells et al., 2014; Morman and Plumlee, 2014; Fitzgerald et al., 2015; Tang et al., 2016a), which shows large geographical and spatial variability (Claquin et al., 1999; Ta et al., 2003; Zhang et al., 2003a; Jeong, 2008; Nickovic et al., 2012; Scheuvens et al., 2013; Formenti et al., 2014; Journet et al., 2014; Scanza et al., 2015). According to a recent global modeling study (Scanza et al., 2015), major minerals contained by tropospheric mineral dust particles include quartz, illite, montmorillonite, feldspar, kaolinite, calcite, hematite, and gypsum. Formenti et al. (2011) summarized published measurements of tropospheric mineral dust particles, and the size of mineral dust particles depends dust sources and transport, with typical volume median diameters being a few micrometers or larger.

Mineral dust particles can undergo heterogeneous and/or multiphase reactions during their transport (Dentener et al., 1996; Usher et al., 2003a; Crowley et al., 2010a). These reactions will modify the composition of dust particles (Matsuki et al., 2005; Ro et al., 2005; Sullivan et al., 2007; Shi et al., 2008; Li and Shao, 2009; He et al., 2014) and subsequently change their physicochemical properties, including hygroscopicity, CCN and IN activities (Krueger et al., 2003b; Sullivan et al., 2009b; Chernoff and Bertram, 2010; Ma et al., 2012; Tobo et al., 2012; Sihvonen et al., 2014; Wex et al., 2014; Kulkarni et al., 2015), and the solubility of Fe and P, and etc. (Meskhidze et al., 2005; Vlasenko et al., 2006; Duvall et al., 2008; Nenes et al., 2011; Shi et al., 2012; Ito and Xu, 2014). The effects of heterogeneous and

multiphase reactions on the hygroscopicity and CCN and IN activities of dust particles have been comprehensively summarized by a very recent review paper (Tang et al., 2016a), and the impacts of atmospheric aging processes on the Fe solubility of mineral dust has also been reviewed (Shi et al., 2012).

Heterogeneous reactions of mineral dust in the troposphere can also remove or produce a variety of reactive trace gases, directly and/or indirectly modifying the gas phase compositions of the troposphere and thus changing its oxidation capacity. The global impact of mineral dust aerosol on tropospheric chemistry through heterogeneous reactions was proposed in the mid-1990s by a modelling study (Dentener et al., 1996). According to this study, heterogeneous reactions with mineral dust could largely impact tropospheric photochemical oxidation cycles, resulting in up to 10% decreases in O_3 concentrations in dust source regions and nearby. The pioneering work by Dentener et al. (1996) has motivated many following laboratory, field, and modelling work (de Reus et al., 2000; Tie et al., 2001; Bian and Zender, 2003; Usher et al., 2003a; Bauer et al., 2004; Crowley et al., 2010a; Zhu et al., 2010; Wang et al., 2012; Nie et al., 2014). It should be noted that the regional impact of heterogeneous reactions of mineral dust aerosol was even recognized earlier (Zhang et al., 1994). It has also been suggested that dust aerosol could indirectly impact tropospheric chemistry by affecting radiative fluxes and thus photolysis rates (Liao et al., 1999; Bian and Zender, 2003; Jeong and Sokolik, 2007; Real and Sartelet, 2011).

A few minerals (e.g., TiO_2) with higher refractive indices, compared to stratospheric sulfuric acid particles, have been proposed as potentially suitable materials (Pope et al., 2012; Tang et al., 2014d; Weisenstein et al., 2015) instead of sulfuric acid and its precursors, to be delivered into the stratosphere in order to scatter more solar radiation back into space, as one of solar radiation management methods for climate engineering (Crutzen, 2006). Heterogeneous uptake of reactive trace gases by minerals is also of interest in this aspect for

assessment of impacts of particle injection on stratospheric chemistry and especially stratospheric ozone (Pope et al., 2012; Tang et al., 2014d; Tang et al., 2016b). In addition, some minerals, such as $CaCO_3$ and TiO_2, are widely used as raw materials in construction, and their heterogeneous interactions with reactive trace gases can be important for local outdoor and indoor air quality (Langridge et al., 2009; Raff et al., 2009; Ammar et al., 2010; Baergen and Donaldson, 2016; George et al., 2016) and deterioration of construction surfaces (Lipfert, 1989; Webb et al., 1992; Striegel et al., 2003; Walker et al., 2012).

1.2 An introduction to heterogeneous kinetics

The rates of atmospheric heterogeneous reactions are usually described or approximated as pseudo-first-order reactions. The pseudo-first-order removal rate of a trace gas (X), k_I(X), due to the heterogeneous reaction with mineral dust, depends on its average molecular speed, c(X), the surface area concentration of mineral dust aerosol, S_a, and the uptake coefficient, γ, given by Eq. (1) (Crowley et al., 2010a; Kolb et al., 2010; Ammann et al., 2013; Tang et al., 2014b):

$$k_I(X) = 0.25 \cdot c(X) \cdot S_A \cdot \gamma \quad (1)$$

The uptake coefficient is the net probability that a molecule X is actually removed from the gas phase upon collision with the surface, equal to the ratio of number of molecules removed from the gas phase to the total number of gas-surface collisions (Crowley et al., 2010a).

Heterogeneous reaction of a trace gas (X) will lead to depletion of X close to the surface, and thus the effective uptake coefficient, γ_{eff}, will be smaller than the true uptake coefficient, γ, as described by Eq. (2) (Crowley et al., 2010a; Davidovits et al., 2011; Tang et al., 2014b):

$$\frac{1}{\gamma_{eff}} = \frac{1}{\gamma} + \frac{1}{\Gamma_{diff}} \quad (2)$$

where Γ_{diff} represents the gas phase diffusion limitation. For the uptake onto spherical particles, Eq. (3) (the Fuchs-Sutugin equation) can be used to calculate Γ_{diff} (Tang et al., 2014b; Tang et al., 2015):

$$\frac{1}{\Gamma_{diff}} = \frac{0.75+0.286Kn}{Kn\cdot(Kn+1)} \qquad (3)$$

where *Kn* is the Knudsen number, given by Eq. (4)

$$Kn = \frac{2\lambda(X)}{d_p} = \frac{6D(X)}{c(X)\cdot d_p} \qquad (4)$$

where λ(X), *D*(X) and d_p are the mean free path of X, the gas phase diffusion coefficient of X, and the particle diameter, respectively. Experimentally measured gas phase diffusion coefficients of trace gases with atmospheric relevance have been recently compiled and evaluated (Tang et al., 2014b; Tang et al., 2015); if not available, they can be estimated using Fuller's semi-empirical method (Fuller et al., 1966; Tang et al., 2015). A new method has also been proposed to calculate *Kn* without the knowledge of *D*(X), given by Eq. (5):

$$Kn = \frac{2}{d_p}\cdot\frac{\lambda_P}{P} \qquad (5)$$

where *P* is the pressure in atm and λ_P is the pressure-normalized mean free path which is equal to 100 nm·atm (Tang et al., 2015).

1.3 Scope of this review

Usher et al. (2003a) provided the first comprehensive review in this field, and heterogeneous reactions of mineral dust with a myriad of trace gases, including nitrogen oxides, SO_2, O_3, and some organic compounds are included. After that, the IUPAC Task Group on Atmospheric Chemical Kinetic Data Evaluation published the first critical evaluation of kinetic data for heterogeneous reactions of solid substrates including mineral dust particles (Crowley et al., 2010a), and kinetic data for heterogeneous uptake of several trace gases (including O_3, H_2O_2, NO_2, NO_3, HNO_3, N_2O_5, and SO_2) onto mineral dust have been recommended. It should be pointed out that in addition to this and other review articles published by Atmospheric Chemistry and Physics, the IUPAC task group keeps updating recommended kinetic data online (http://iupac.pole-ether.fr/). We note that a few other review papers and monographs have also mentioned atmospheric heterogeneous reactions of mineral dust particles (Cwiertny et al., 2008; Zhu et al., 2011; Chen et al., 2012; Rubasinghege and Grassian, 2013; Shen et al.,

2013; Burkholder et al., 2015; Ge et al., 2015; George et al., 2015; Akimoto, 2016), in a less comprehensive manner compared to Usher et al. (2003a) and Crowley et al. (2010). For example, Cwiertny et al. (2008) reviewed heterogeneous reactions and heterogeneous photochemical reactions of O_3 and NO_2 with mineral dust. Atmospheric heterogeneous photochemistry was summarized by Chen et al. (2012) for TiO_2 and by George et al. (2015) for other minerals. Heterogeneous reactions of mineral dust with a few volatile organic compounds (VOCs), such as formaldehyde, acetone, methacrolein, methyl vinyl ketone, and organic acids, have been covered by a review article on heterogeneous reactions of VOCs (Shen et al., 2013). The NASA-JPL data evaluation panel has compiled and evaluated kinetic data for heterogeneous reactions with alumina (Burkholder et al., 2015). In a very recent paper, Ge et al. (2015) summarized previous studies on heterogeneous reactions of mineral dust with NO_2, SO_2, and monocarboxylic acids, with work conducted by scientists in China emphasized. In his monograph entitled Atmospheric Reaction Chemistry, Akimoto (2015) briefly discussed some heterogeneous reactions of mineral dust particles in the troposphere. Roles heterogeneous chemistry of aerosol particles (including mineral dust) play in haze formation in China were outlined (Zhu et al., 2011), and effects of surface adsorbed water and thus relative humidity (RH) on heterogeneous reactions of mineral dust have also been discussed by a recent feature article (Rubasinghege and Grassian, 2013).

After the publication of the two benchmark review articles (Usher et al., 2003a; Crowley et al., 2010a), much advancement has been made in this field. For example, heterogeneous uptake of HO_2 radicals by mineral dust particles had not been explored at the time when Crowley et al. (2010a) published the IUPAC evaluation, and in the last few years this reaction has been investigated by two groups (Bedjanian et al., 2013a; Matthews et al., 2014). A large number of new studies on the heterogeneous reactions of mineral dust with H_2O_2 (Wang et al., 2011; Zhao et al., 2011b; Romanias et al., 2012a; Yi et al., 2012; Zhou et al.,

2012; Romanias et al., 2013; Zhao et al., 2013; El Zein et al., 2014; Zhou et al., 2016) and N_2O_5 (Tang et al., 2012; Tang et al., 2014a; Tang et al., 2014c; Tang et al., 2014d) have emerged. Therefore, a review on atmospheric heterogeneous reaction of mineral dust is both timely and necessary.

Furthermore, the novelty of our current review, which distinguishes it from previous reviews in the same/similar fields (Usher et al., 2003a; Cwiertny et al., 2008; Crowley et al., 2010a; Zhu et al., 2011; Chen et al., 2012; Shen et al., 2013; Ge et al., 2015; George et al., 2015), is the fact that atmospheric relevance and significance of laboratory studies are illustrated, discussed, and emphasized. We hope that this paper will be useful not only for those whose expertise is laboratory work but also for experts in field measurements and atmospheric modelling. The following approaches are used to achieve this goal: 1) lifetimes of reactive trace gases with respect to heterogeneous uptake by mineral dust, calculated using preferred uptake coefficients and typical mineral dust mass concentrations, are compared to their lifetimes in the troposphere (discussed in Section 2.1) in order to discuss the significance of heterogeneous reactions as atmospheric sinks for these trace gases; 2) atmospheric importance of these heterogeneous reactions are further discussed by referring to representative box, regional, and global modelling studies reported previously; 3) we also describe two of the largest challenges in the laboratory studies of heterogeneous reactions of mineral dust particles (Section 2.2), and explain why reported uptake coefficients show large variability and how we interpret and use these kinetic data. In fact, the major expertise of a few coauthors of this review paper is field measurements and/or modelling studies, and their contribution should largely increase the readability of this paper for the entire atmospheric chemistry community regardless of the academic background of individual readers.

OH, NO_3, and O_3 are the most important gas phase oxidants in the troposphere, and their contribution to tropospheric oxidation capacity has been well recognized (Brown and

Stutz, 2012; Stone et al., 2012). HO_2 radicals are closely linked with OH radicals (Stone et al., 2012). H_2O_2, HCHO and HONO are important precursors for OH radicals in the troposphere (Stone et al., 2012), and they may also be important oxidants in the aqueous phase (Seinfeld and Pandis, 2006). Tropospheric N_2O_5 is found to be in dynamic equilibrium with NO_3 radicals (Brown and Stutz, 2012). Therefore, in order to provide a comprehensive view of implications of heterogeneous reactions of mineral dust particles for tropospheric oxidation capacity, not only heterogeneous uptake of OH, NO_3, and O_3 but also heterogeneous reactions of HO_2, H_2O_2, HCHO, HONO, and N_2O_5 are included. Cl atoms (Spicer et al., 1998; Osthoff et al., 2008; Thornton et al., 2010; Phillips et al., 2012; Liao et al., 2014; Wang et al., 2016) and stable Criegee radicals (Mauldin III et al., 2012; Welz et al., 2012; Percival et al., 2013; Taatjes et al., 2013) are proposed to be potentially important oxidants in the troposphere, thought their atmospheric significance is to be systematically assessed (Percival et al., 2013; Taatjes et al., 2014; Simpson et al., 2015). In addition, their heterogeneous reactions with mineral dust have seldom been explored. Therefore, heterogeneous uptake of Cl atoms (and their precursors such as $ClNO_2$) and stable Criegee radicals by mineral dust is not included here.

In Section 2, a brief introduction to tropospheric chemistry of OH, HO_2, H_2O_2, O_3, HCHO, HONO, NO_3, and N_2O_5 (eight species in total) is provided first. After that, we describe two major challenges in laboratory studies of heterogeneous reactions of mineral dust particles, and then discuss their implications in reporting and interpreting kinetic data. Following this in Section 3, we review previous laboratory studies of heterogeneous reactions of mineral dust particles with these eight reactive trace gases, and we have tried our best to cover all the journal articles (limited to those in English) published in this field. Uncertainties for each individual reactions are discussed, and future work required to reduce these uncertainties is suggested. In addition, atmospheric importance of these reactions is discussed by 1) comparing their lifetimes with respect to heterogeneous uptake to typical lifetimes in the troposphere and 2) discussing

representative modelling studies at various spatial and temporal scales. Finally in Section 4 we outline key challenges which preclude better understanding of impacts of heterogeneous reactions of mineral dust on tropospheric oxidation capacity and discuss how they can be addressed by future work.

2 Background

In first part of this section we provide a brief introduction of production and removal pathways, chemistry, and lifetimes of OH, HO_2, H_2O_2, O_3, HCHO, HONO, NO_3, and N_2O_5 in the troposphere. In the second part we describe two of the largest challenges in laboratory investigation of heterogeneous reactions of mineral dust particles and discuss their implications for reporting, interpreting, and using uptake coefficients.

2.1 Sources and sinks of tropospheric oxidants

Figure 1 shows a simplified schematic diagram of atmospheric chemistry of major free radicals in the troposphere. Sources, sinks, and atmospheric lifetimes of these radicals and their important precursors are discussed below.

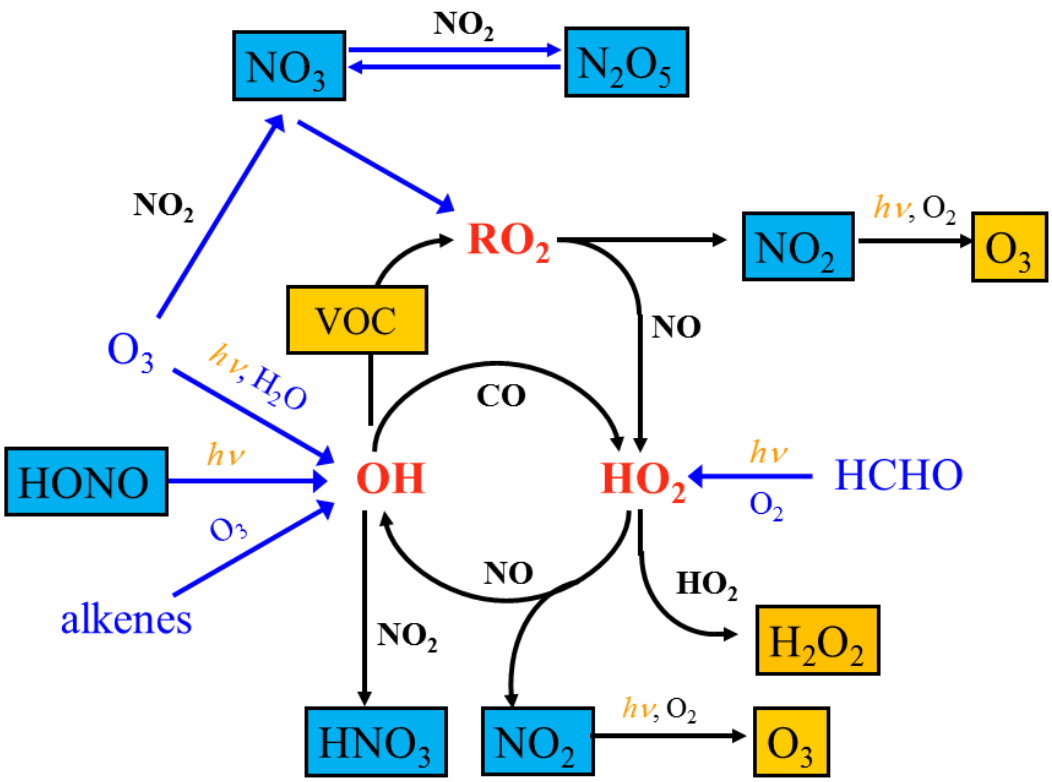

Figure 1. Simplified schematic diagram of chemistry of major free radicals in the troposphere.

2.1.1 OH, HO_2, and H_2O_2

Large amounts of OH (10^6 - 10^7 molecule cm^{-3}) and HO_2 radicals (10^8 - 10^9 cm^{-3}) have been observed and predicted for the lower troposphere (Stone et al., 2012). The first major primary source of OH radicals in the troposphere is the reaction of water vapor with $O(^1D)$ (R1), which is produced from photolysis of O_3 by UV radiation with wavelengths smaller than 325 nm (R2) (Atkinson et al., 2004; Burkholder et al., 2015):

$$O(^1D) + H_2O \rightarrow OH + OH \quad (R1)$$

$$O_3 + h\nu\ (\lambda < 325\ nm) \rightarrow O_2 + O(^1D) \quad (R2)$$

In polluted urban areas, another two primary sources of OH and HO_2 radicals, i.e. photolysis of HONO and HCHO, become significant (Seinfeld and Pandis, 2006) and sometimes even dominate the primary production of OH (Su et al., 2008):

$$HONO + h\nu\ (\lambda < 400\ nm) \rightarrow NO + OH \quad (R3)$$

$$HCHO + h\nu\ (\lambda < 340\ nm) \rightarrow H + HCO \quad (R4a)$$

$$H + O_2 + M \rightarrow HO_2 + M \quad (R4b)$$

$$HCO + O_2 \rightarrow HO_2 + CO \quad (R4c)$$

Photolysis of higher oxygenated volatile organic compounds (OVOCs) such as di-carbonyl compounds has also been suggested as important primary sources for HOx radicals in megacities in China (Lu et al., 2012; Lu et al., 2013) and Mexico (Dusanter et al., 2009). Under twilight conditions as well as during winter time, ozonolysis of alkenes and photolysis of OVOCs have been found to be dominant primary sources of OH and HO_2 (Geyer et al., 2003; Heard et al., 2004; Kanaya et al., 2007b; Edwards et al., 2014; Lu et al., 2014).

After initiated by primary production channels described above, OH radicals further react with volatile organic compounds (VOCs) to generate organic peroxy radicals (RO_2). RO_2

radicals are then converted to HO_2 radicals by reacting with NO (R5) and the produced HO_2 radicals are finally recycled back to OH via reaction with NO (R6).

$$RO_2 + NO \rightarrow HO_2 + NO_2 \quad (R5)$$

$$HO_2 + NO \rightarrow OH + NO_2 \quad (R6)$$

Due to these chain reactions, ambient OH levels are sustained and emitted reductive trace gas compounds (e.g., VOCs and NO) are catalytically oxidized (Seinfeld and Pandis, 2006). These chain reactions are terminated by reaction of OH with NO_2 (R7, in which M is the third-body molecule) at high NOx conditions and by cross reaction of HO_2 with RO_2 and self-reaction of HO_2 radicals (R8) at low NOx conditions.

$$OH + NO_2 + M \rightarrow HNO_3 + M \quad (R7)$$

$$HO_2 + HO_2 \rightarrow H_2O_2 + O_2 \quad (R8)$$

In recent years, a new OH regeneration mechanism, which has not been completely elucidated so far, has been identified for low NOx environments including both forested (Lelieveld et al., 2008) and rural areas (Hofzumahaus et al., 2009; Lu et al., 2012). This new mechanism is found to stabilize the observed OH-$j(O^1D)$ relationships and enables a type of maximum efficiency of OH sustainment under low NOx conditions (Rohrer et al., 2014). Nevertheless, in a recent study (Mao et al., 2012), the proposed new OH regeneration mechanism is thought to be at least partly caused by unrecognized instrumental interference in OH measurements (Mao et al., 2012). A community effort is now started to assure the data quality of the OH measurement under different conditions especially for the chemical complex areas (http://www.fz-juelich.de/iek/iek8/EN/AboutUs/Projects/HOxROxWorkingGroup/HOxWorkshop2015_node.html).

Table 1 summarizes representative lifetimes of OH and HO_2 radicals in the troposphere as determined by previous field campaigns. The OH lifetime is an important parameter to characterize HOx chemistry as well as VOC reactivity in the troposphere. As a result, it has

been widely measured at different locations using a variety of experimental methods (Sinha et al., 2008; Ingham et al., 2009), as discussed by a very recent paper (Yang et al., 2016b). OH lifetimes in clean environments, like open ocean and remote continental areas, are dominated by reactions with CO, CH_4, and HCHO, summed up to values of about 0.5-1 s (Ehhalt, 1999; Brauers et al., 2001). OH lifetimes in forested areas, mainly contributed by oxidation of biogenic VOCs, are typically in the range of 0.01-0.05 s (Ingham et al., 2009; Nölscher et al., 2012). In urban areas, OH lifetimes are determined by anthropogenically emitted hydrocarbons, NOx, CO, and biogenic VOCs as well, and they are typically smaller than 0.1 s (Ren et al., 2003; Mao et al., 2010b; Lu et al., 2013).

Compared to OH radicals, lifetimes of HO_2 radicals have been much less investigated and are mainly determined by ambient NO concentrations when NO is larger than 10 pptv (parts per trillion by volume). Therefore, the lower limit of HO_2 lifetimes, on the order of 0.1 s, often appear in polluted urban areas (Ren et al., 2003; Kanaya et al., 2007a; Lu et al., 2012). The upper limit of HO_2 lifetimes, up to 1000-2000 s, is often observed in clean regions and sometimes also in urban areas during nighttime (Holland et al., 2003; Lelieveld et al., 2008; Whalley et al., 2011). In addition, heterogeneous uptake of HO_2 radicals have been frequently considered in the budget analysis of HOx radicals for marine and polluted urban regions (Abbatt et al., 2012).

Table 1. Summary of typical lifetimes of OH, HO_2, NO_3 and N_2O_5 in the troposphere reported by field measurements.

Time	Location	Lifetimes	Reference
	OH radicals		
OCT-NOV 1996	Tropical Atlantic Ocean	1 s	(Brauers et al., 2001)
AUG 1994	Mecklenburg Vorpommern, Germany	0.5 s	(Ehhalt, 1999)

JUL-AUG 1998	Pabstthum (rural Berlin), Germany	0.15-0.5 s	(Mihelcic et al., 2003)
AUG-SEP 2000	Houston, US	0.08-0.15 s	(Mao et al., 2010b)
JUN-AUG 2001	New York, US	0.04-0.06 s	(Ren et al., 2003)
AUG 2007	Tokyo, Japan	0.01-0.1 s	(Chatani et al., 2009)
JUL 2006	Backgarden (rural Guangzhou), China	0.008-0.1 s	(Lou et al., 2010)
AUG 2006	Yufa (rural Beijing), China	0.01-0.1s	(Lu et al., 2013)
APR-MAY 2008	Borneo, Malaysia	0.015-0.1 s	(Ingham et al., 2009)
JUL-AUG 2010	Hyytiala, Finland	0.01-0.5 s	(Nölscher et al., 2012)
	HO_2 radicals		
JUL-AUG 1998	Pabstthum (rural Berlin), Germany	3-500 s	(Holland et al., 2003)
JUN-AUG 2001	New York, US	0.1-1.5 s	(Ren et al., 2003)
JUL-AUG 2004	Tokyo, Japan	0.05-1000 s	(Kanaya et al., 2007a)
JUL 2006	Backgarden (rural Guangzhou), China	0.1-500 s	(Lu et al., 2012)
AUG 2006	Yufa (rural Beijing), China	0.06-500 s	(Lu et al., 2013)
OCT 2005	Suriname	500-1000 s	(Lelieveld et al., 2008)
APR-MAY 2008	Borneo, Malaysia	20-2000 s	(Whalley et al., 2011)
	NO_3 radicals		
OCT 1996	Helgoland, Germany	10-1000 s	(Martinez et al., 2000)
JUL-AUG 1998	Berlin, Germany	10-500 s	(Geyer et al., 2001)
JUL-AUG 2002	US east coast	typically a few min, up to 20 min	(Aldener et al., 2006)
MAY 2008	Klein Feldberg, Germany	up to ~1500 s	(Crowley et al., 2010b)
AUG-SEP 2011	Klein Feldberg, Germany	up to 1 h, with an average value of ~200 s	(Sobanski et al., 2016)
	N_2O_5		
OCT 1996	Helgoland, Germany	hundred to thousand seconds	(Martinez et al., 2000)
JAN 2004	Contra Costa, California, US	600-1800 s	(Wood et al., 2005)

JUL-AUG 2002	US east coast	up to 60 min	(Aldener et al., 2006)
NOV 2009	Fairbank, Alaska, US	~6 min on average	(Huff et al., 2011)
NOV-DEC 2013	Hong Kong, China	from <0.1 h to 13 h	(Brown et al., 2016)

Formation and removal of gas phase H_2O_2 in the troposphere is closely linked with the HOx radical chemistry. Tropospheric H_2O_2 is mainly produced from self-reaction of HO_2 radicals (R8) and this process is further enhanced by the presence of water vapor (Stockwell, 1995). In addition to dry and wet deposition, another two pathways, i.e. photolysis (R9) and the reaction with OH (R10), dominate the removal of H_2O_2 in the troposphere:

$$H_2O_2 + h\nu\ (\lambda < 360\ \text{nm}) \rightarrow OH + OH \quad (R9)$$

$$H_2O_2 + OH \rightarrow H_2O + HO_2 \quad (R10)$$

Typical $J(H_2O_2)$ daily maximum values are ~7.7×10^{-6} s^{-1} for solar zenith angle of 0° and ~6.0×10^{-6} s^{-1} in the northern mid-latitude (Stockwell et al., 1997), corresponding to $\tau_{phot}(H_2O_2)$ (H_2O_2 lifetimes with respect to photolysis) of 33-56 h (or 1.5-2 days). The rate constant for the bimolecular reaction of H_2O_2 with OH radicals is 1.7×10^{-12} cm^3 $molecule^{-1}$ s^{-1} at room temperature, and its temperature dependence is quite small (Atkinson et al., 2004). Concentrations of OH radicals in the troposphere are usually in the range of $(1\text{-}10)\times10^6$ molecule cm^{-3}, and thus $\tau_{OH}(H_2O_2)$ (H_2O_2 lifetimes with respect to reaction with OH radicals) are estimated to be around 16-160 h. Dry deposition rates of H_2O_2 were determined to be ~5 cm s^{-1} (Hall and Claiborn, 1997), and an assumed boundary height of 1 km gives $\tau_{dry}(H_2O_2)$ (H_2O_2 lifetimes with respect to dry deposition) of 5-6 h. Therefore, dry deposition is a major sink for near surface H_2O_2. We do not estimate H_2O_2 lifetimes with respect to wet deposition because wet deposition rates depend on amount of precipitation which shows large spatial and temporal variation. Heterogeneous uptake of H_2O_2 by ambient aerosols as well as fog and rain droplets is also considered to be a significant sink for H_2O_2, especially when the ambient SO_2 concentrations are high (de Reus et al., 2005; Hua et al., 2008).

As mentioned previously, HONO and HCHO are two important precursors for OH radicals, and therefore their removal (as well as production) significantly affects tropospheric oxidation capacity. The typical J(HONO) daily maximum value for the northern mid-latitude is ~1.63×10^{-3} s^{-1} (Stockwell et al., 1997), corresponding to τ_{phot}(HONO) of about 10 min. This is supported by field measurements which suggest that lifetimes of HONO due to photolysis during the daytime are typically in the range of 10-20 min (Alicke et al., 2003; Li et al., 2012). The second order rate constant for the reaction of HONO with OH radicals is 6.0×10^{-12} cm^3 $molecule^{-1}$ s^{-1} at 298 K (Atkinson et al., 2004), giving τ_{OH}(HONO) of ~280 min (~4.6 h) if OH concentration is assumed to be 1×10^7 molecule cm^{-3}. Dry deposition velocities of HONO reported by previous work show large variability, ranging from 0.077 to 3 cm s^{-1} (Harrison and Kitto, 1994; Harrison et al., 1996; Stutz et al., 2002), and thus τ_{dry}(HONO) are estimated to be in the range of ~9 h to several days if a boundary height of 1 km is assumed. Therefore, photolysis is the main sink for HONO in the troposphere and the contribution from dry deposition and reaction with OH is quite minor.

The second order rate constant for the reaction of HCHO with OH radicals is 8.5×10^{12} cm^3 $molecule^{-1}$ s^{-1} at 298 K (Atkinson et al., 2006), and τ_{OH}(HCHO) is calculated to be ~200 min (~3.3 h) if OH concentration is assumed to be 1×10^7 molecule cm^{-3}. The typical J(HCHO) daily maximum value for the northern mid-latitude is ~5.67×10^{-5} s^{-1} (Stockwell et al., 1997), giving τ_{phot}(HCHO) of about 300 min (~5 h). The dry deposition velocity for HCHO was measured to be 1.4 cm s^{-1} (Seyfioglu et al., 2006), corresponding to τ_{dry}(HCHO) of ~20 h if the boundary layer height is assumed to be 1 km. To summarize, lifetimes of HCHO in the troposphere are estimated to be a few hours, with photolysis and reaction with OH radicals being major sinks.

2.1.2 O_3

After being emitted, NO is converted to NO_2 in the troposphere through its reactions with O_3 (R11) and peroxy radicals (R5, R6). NO_2 is further photolyzed to generate O_3 (R12), and NO oxidation processes through R5 and R6 are the reason for O_3 increase in the troposphere (Wang and Jacob, 1998).

$$O_3 + NO \rightarrow NO_2 + O_2 \quad (R11)$$

$$NO_2 + O_2 + hv\ (\lambda < 420\ nm) \rightarrow O_3 + NO \quad (R12)$$

Tropospheric O_3 is mainly destroyed via its photolysis (R1) and the subsequent reaction of O^1D with H_2O (R2). Other important removal pathways include dry deposition, reaction with NO_2 (to produce NO_3 radicals) (R13), and ozonolysis of alkenes, etc.

$$NO_2 + O_3 \rightarrow NO_3 + O_2 \quad (R13)$$

In addition, the loss of NO_2 through reaction with OH (R7) and the loss of peroxy radicals through their self-reactions (R8) would be a significant term of O_3 losses in large scales. Therefore, it is anticipated that both the formation and destruction of O_3 is closely related with gas phase HOx and NOx radical chemistry.

Several processes remove O_3 from the troposphere. The first one is the photolysis of O_3 to produce O^1D (R1) and the subsequent reaction of O^1D with H_2O (R2); therefore, the removal rate of O_3 through this pathway depends on solar radiation and RH. $\tau_{pho}(O_3)$ is typically in the range of 1.8-10 days in the troposphere (Stockwell et al., 1997). Ozonolysis of alkenes is another significant sink for O_3 under high VOCs conditions, and $\tau_{alkene}(O_3)$ with respect to reaction with alkenes are estimated to be 3-8 h for urban and forested areas (Shirley et al., 2006; Kanaya et al., 2007b; Whalley et al., 2011; Lu et al., 2013; Lu et al., 2014). O_3 lifetimes in the remote troposphere are primarily determined by O_3 photolysis (and the subsequent reaction of O^1D with H_2O) and reactions of O_3 with HO_2 and OH. For typical conditions ($j(O^1D)$, H_2O, HO_2, OH, temperature, and pressure) over northern mid-latitude oceans, O_3 lifetimes are

calculated to be a few days in summer, 1-2 weeks in spring/autumn, and about a month for in winter, using the GEOS-Chem model (to be published). O_3 dry deposition has been extensively studied and as a rule of thumb, 1 cm s^{-1} is taken as its dry deposition rate (Wesely and Hicks, 2000). Consequently, $\tau_{dry}(O_3)$ is calculate to be ~28 h, assuming a boundary height of 1 km. Reactions with NO and NO_2 will further contribute to the removal of O_3 in the troposphere at night. The second-order rate constants are 1.9×10^{-14} cm^3 $molecule^{-1}$ s^{-1} for the reaction of O_3 with NO and 3.5×10^{-17} cm^3 $molecule^{-1}$ s^{-1} for its reaction with NO_2 at 298 K (Atkinson et al., 2004), and O_3 lifetimes are calculated to be ~29 h and ~32 h in the presence of 20 pptv NO and 10 ppbv (parts per billion by volume) NO_2, respectively.

Moreover, heterogeneous processes may also strongly influence the budget of O_3 through impacts on sources and sinks of HOx and NOx (Dentener et al., 1996; Jacob, 2000; Zhu et al., 2010), the production of halogen radicals (Thornton et al., 2010; Phillips et al., 2012; Wang et al., 2016), and possibly also direct removal of O_3 due to heterogeneous uptake (de Reus et al., 2000).

2.1.3 NO_3 radicals (and N_2O_5)

Oxidation of NO_2 by O_3 (R13) is the dominant source for NO_3 radicals in the troposphere. NO_3 radicals further react with NO_2 to form N_2O_5 (R14), which can thermally dissociate back to NO_3 and NO_2 (R15) (Wayne et al., 1991; Brown and Stutz, 2012).

$$NO_2 + O_3 \rightarrow NO_3 + O_2 \quad \text{(R13)}$$

$$NO_2 + NO_3 + M \rightarrow N_2O_5 + M \quad \text{(R14)}$$

$$N_2O_5 + M \rightarrow NO_2 + NO_3 + M \quad \text{(R15)}$$

The equilibrium between NO_3 and N_2O_5 is usually reached within several seconds under typical tropospheric conditions. Therefore, NO_3 radicals are considered to be in dynamic equilibrium with N_2O_5, as confirmed by a number of field measurements (Brown and Stutz, 2012, and references therein). As a results, NO_3 and N_2O_5 are discussed together here. Recently reactions

of Criegee radicals with NO_2 are proposed as another source for NO_3 radicals (Ouyang et al., 2013), though atmospheric significance of this source has not been systematically assessed yet (Sobanski et al., 2016).

Photolysis of NO_3 (R17) and its reaction with NO (R16) are both very fast (Wayne et al., 1991), and atmospheric chemistry of NO_3 (and thus N_2O_5) is only important during nighttime, though the daytime presence of NO_3 and N_2O_5 in the troposphere has also been reported (Brown and Stutz, 2012). Therefore, for a sink to be important for NO_3 or N_2O_5, the lifetime with respect to this sink should be comparable to or shorter than half one day.

$$NO_3 + NO \rightarrow NO_2 + NO_2 \text{ (R16)}$$

$$NO_3 + (\lambda < 11080 \text{ nm}) \rightarrow NO + O_2 \text{ (R17a)}$$

$$NO_3 + (\lambda < 587 \text{ nm}) \rightarrow NO_2 + O \text{ (R17b)}$$

The predominant sinks for tropospheric NO_3 and N_2O_5 include reactions with unsaturated volatile organic compounds (VOCs), reaction with dimethyl sulfite in the marine and coastal troposphere, and heterogeneous uptake by aerosol particles and cloud droplets (Brown and Stutz, 2012). The gas phase reaction of N_2O_5 with water vapor was investigated by a laboratory study (Wahner et al., 1998), and several field measurements have suggested that this reaction is unlikely to be significant in the troposphere (Brown et al., 2009; Crowley et al., 2010b; Brown and Stutz, 2012). Lifetimes of NO_3 and N_2O_5 during nighttime depend on a variety of atmospheric conditions (including concentrations of VOCs and aerosols, aerosol composition and mixing state, and RH etc.) (Brown and Stutz, 2012), exhibiting large spatial and temporal variations. As shown in Table 1, NO_3 lifetimes typically range from tens of seconds to 1 h, while N_2O_5 lifetimes are usually longer, spanning from <10 min to several hours.

2.2 Laboratory studies of atmospheric heterogeneous reactions of mineral dust particles

Kinetics of heterogeneous reactions can be determined by measuring the decay and/or production rates of trace gases in the gas phase (Hanisch and Crowley, 2001; Usher et al., 2003b; Liu et al., 2008a; Vlasenko et al., 2009; Pradhan et al., 2010a; Tang et al., 2012; Zhou et al., 2014). Alternatively, reaction rates can also be measured by detecting changes in particle composition (Goodman et al., 2000; Sullivan et al., 2009a; Li et al., 2010; Tong et al., 2010; Ma et al., 2012; Kong et al., 2014). A number of experimental techniques have been developed and utilized to investigate heterogeneous reactions of mineral dust particles, as summarized in Table 1. It should be emphasized that this list is far from being complete and only techniques mentioned in this review paper are included. These techniques can be classified into three groups according to the way particles under investigation exist: 1) particle ensembles deposited on a substrate, 2) an ensemble of particles as an aerosol, and 3) single particles, either levitated or deposited on a substrate. Detailed description of these techniques can be found in several previous review articles and monographies (Usher et al., 2003a; Cwiertny et al., 2008; Crowley et al., 2010a; Kolb et al., 2010; Akimoto, 2016) and thus is not repeated here. Instead, in this paper we intend to discuss two critical issues in determining and reporting uptake coefficients for heterogeneous reactions of mineral dust particles, i.e. 1) surface area available for heterogeneous uptake and 2) time dependence of heterogeneous kinetics. In addition to these two important issues, it should also be mentioned that single minerals (e.g., illite, calcite, and quartz) and authentic dust samples (e.g., Saharan dust and Arizona test dust) may not necessarily reflect mineral dust particles found in the troposphere. After emitted into the troposphere, mineral dust particle will undergo heterogeneous reactions and cloud processing (Usher et al., 2003a; Tang et al., 2016a), forming soluble inorganic and organic materials coated on dust particles (Sullivan et al., 2007; Sullivan and Prather, 2007; Formenti et al., 2011;

Fitzgerald et al., 2015). Therefore, heterogeneous reactivity of ambient mineral dust particles can be largely different from those used in laboratory studies.

For experiments in which single particles are used, usually surface techniques, including Raman spectroscopy (Liu et al., 2008b; Zhao et al., 2011a), scanning electron microscopy (SEM) (Krueger et al., 2003a; Laskin et al., 2005b), and secondary ion mass spectroscopy (SIMS) (Harris et al., 2012), can be utilized to characterize their compositional and morphological changes simultaneously. Nevertheless, it is still non-trivial to derive quantitative information for most of surface techniques. In addition to being deposited on a substrate, single particles can also be levitated by an electrodynamic balance (Lee and Chan, 2007; Pope et al., 2010) or optical levitation (Tong et al., 2011; Krieger et al., 2012; Rkiouak et al., 2014), and Raman spectroscopy can be used to measure the compositional changes of levitated particles (Lee et al., 2008; Tang et al., 2014a).

Table 2: Abbreviations of experimental techniques used by previous laboratory studies to investigate heterogeneous reactions of mineral dust. Only techniques mentioned in this review paper are included.

abbreviation	full name
AFT	aerosol flow tube
CIMS	chemical ionization mass spectrometry
CLD	chemiluminescence detector
CRDS	cavity ring-down spectroscopy
CRFT	coated rod flow tube
CWFT	coated wall flow tube
DRIFTS	diffuse reflectance infrared Fourier transform spectroscopy
EC	environmental chamber
KC	Knudsen cell reactor
IC	ion chromatography
LIF	laser induced fluorescence
MS	mass spectrometry

T-FTIR	transmission FTIR

2.2.1 Surface area available for heterogeneous uptake

As described by Eq. (1), surface area concentration is required to derive uptake coefficients from measured pseudo first order reaction rates. However, it can be a difficult task to obtain surface area concentrations for particles. In fact, variation in estimated surface area available for heterogeneous uptake is one of the main reasons why large differences in uptake coefficients have been reported by different groups for the same reaction system of interest.

For experiments in which aerosol particles are used, surface area concentrations are typically derived from size distribution measured using an aerodynamic particle sizer (APS) or scanning mobility particle sizer (SMPS). Because of the non-sphericity of mineral dust particles, it is not straightforward to convert aerodynamic and mobility diameters to surface area. It has been reported that the median aspect ratios are in the range of 1.6-17 for Saharan dust particles (Chou et al., 2008; Kandler et al., 2009) and 1.4-1.5 for Asian dust particles (Okada et al., 2001). In some aerosol chamber studies, surface areas available for heterogeneous uptake are assumed to be equal to the BET surface areas of dust particles introduced into the chamber (Mogili et al., 2006b; Mogili et al., 2006a; Chen et al., 2011b). Some dust particles are porous, making their BET surface areas much larger than the corresponding geometrical surface areas. $\gamma(N_2O_5)$ for airborne SiO_2 particles reported by two previous studies (Mogili et al., 2006b; Wagner et al., 2009) differed by almost two orders of magnitude. Tang et al. (2014a) suggested that such a large difference is mainly due to the fact that different methods were used to calculate surface area available for heterogeneous uptake. Specifically, Mogili et al. (2006a) used the BET surface area, while Wagner et al. (2009) used Stoke diameters derived from APS measurements to calculate the surface area. Tang et al. (2014a) further found that if the same method is used to calculate surface area concentrations,

$\gamma(N_2O_5)$ reported by the two studies (Mogili et al., 2006b; Wagner et al., 2009) agree fairly well.

This issue becomes even more severe for experiments using mineral dust particles deposited on a substrate. In these experiments the surface area available for heterogeneous uptake is assumed to be either the projected area of dust particles (usually also referred to the geometrical area of dust particles, equal to the geometrical surface area of the sample holder) or the BET surface area of the dust sample. Description of methods used in measuring BET surface area of solid particles can be found elsewhere (Sing, 2014; Naderi, 2015). Multiple layers of powdered dust samples are typically deposited on a substrate. Consequently, it is not uncommon that the BET surface area is several orders of magnitude larger than the projected area (Nicolas et al., 2009; Liu et al., 2010; Tong et al., 2010). The surface area actually available for heterogeneous uptake falls between the two extreme cases and varies for different studies. When gas molecules are transported towards the top layer of the powdered sample, they may collide with the surface of particles on the top layer, be adsorbed, and undergo heterogeneous reaction; they may also be transported within the interior space and then collide and react with particles in the underlying layers. The depth gas molecules can reach depends on the microstructure of the powdered sample (e.g., how compactly particles are stacked) as well as their reactivity towards the surface. For a very fast heterogeneous reaction it is likely that only the topmost few layers of a powdered sample are accessible for the reactive trace gases, whereas more underlying layers become available for slower uptake processes. Therefore, uptake coefficients reported by experiments using aerosol samples, if available, are preferred and used in this study to estimate the atmospheric importance of heterogeneous reactions. We note that a similar strategy has also been adopted by the IUPAC task group (Crowley et al., 2010a).

In theory, transport of gaseous molecules within the interior space of the powdered sample coupled to reaction with particle surface can be described by mathematical models. The KML (Keyser-Moore-Leu) model initially developed to describe diffusion and reaction of gaseous molecules in porous ice (Keyser et al., 1991; Keyser et al., 1993) has been used to derive uptake coefficients for heterogeneous reactions of mineral dust particles. An "effectiveness factor" was determined and used in the KML model to account for the contribution of underlying layers to the observed heterogeneous uptake. One major drawback of the KML model (and other models with similar principles but different complexities) is that it can be difficult to measure or accurately calculate diffusion constants of reactive trace gases through powdered samples (Underwood et al., 2000).

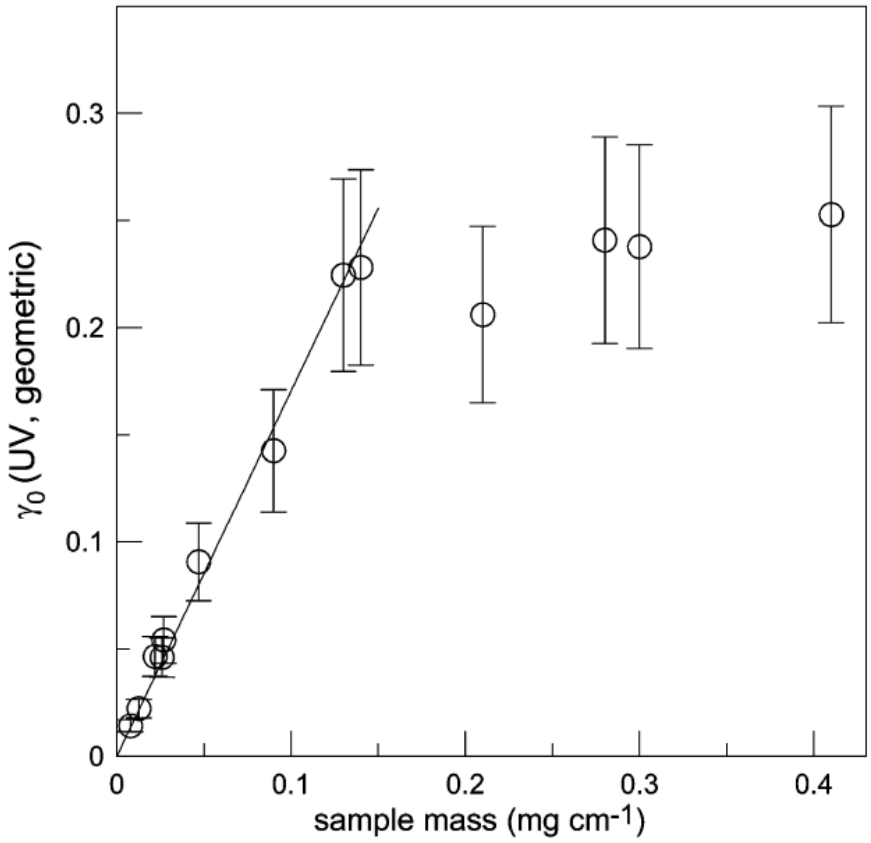

Figure 2. Projected area based uptake coefficients of H_2O_2 on irradiated TiO_2 particles as a function of TiO_2 sample mass (per cm length of the support tube onto which TiO_2 particles

were deposited). Reprinted with permission from (Romanias et al., 2012a). Copyright 2012 American Chemical Society.

Grassian and coworkers developed a simple method to calculate surface area available for heterogeneous uptake (Underwood et al., 2000; Li et al., 2002). If the thickness of a powdered sample is smaller than the interrogation depth of the reactive trace gas (i.e. depth of the sample which can actually be reached by the reactive trace gas), all the particles should be accessible for heterogeneous uptake. In this case, uptake coefficients calculated using the projected area should exhibit a linear mass dependence. The linear mass dependent (LMD) regime can be experimentally determined, with an example shown in Figure 2. Figure 2 suggests that when the TiO_2 sample mass is <0.15 mg cm^{-1}, the projected area based uptake coefficients depend linearly on the sample mass. If measurements are carried out within the LMD regime, surfaces of all the particles are available for heterogeneous uptake and the BET surface area should be used to calculate uptake coefficients (Underwood et al., 2000; Romanias et al., 2012a; Bedjanian et al., 2013a).

Another way to circumvent the problem due to diffusion within interior space of powdered samples is to use particles less than one layer (Hoffman et al., 2003a; Hoffman et al., 2003b). This experimental strategy was used to investigate heterogeneous reactions of NaCl with HNO_3, N_2O_5, and $ClONO_2$, and a mathematical model was developed to calculate the effective surface area exposed to reactive trace gases (Hoffman et al., 2003a; Hoffman et al., 2003b). Nevertheless, to our knowledge this method has not yet be used by laboratory studies of heterogeneous reaction of mineral dust particles.

2.2.2 Time dependence of heterogeneous kinetics

When exposed to reactive trace gases, mineral dust surface may become deactivated and thus gradually lose its heterogeneous reactivity. Figure 3 shows three representative

examples of changes in the measured concentration of a reactive trace gas, X, after exposure to mineral dust particles. For the case shown in Figure 3a, no surface active sites are consumed and the uptake rate is independent of reaction time. Figure 3b displays another case in which surface reactive sites may be consumed and heterogeneous uptake will cease after some exposure. In addition, as shown in Figure 3c, an initial large uptake rate gradually decreases with time to a non-zero constant value for longer exposure (i.e. the heterogeneous reaction reaches a "steady state").

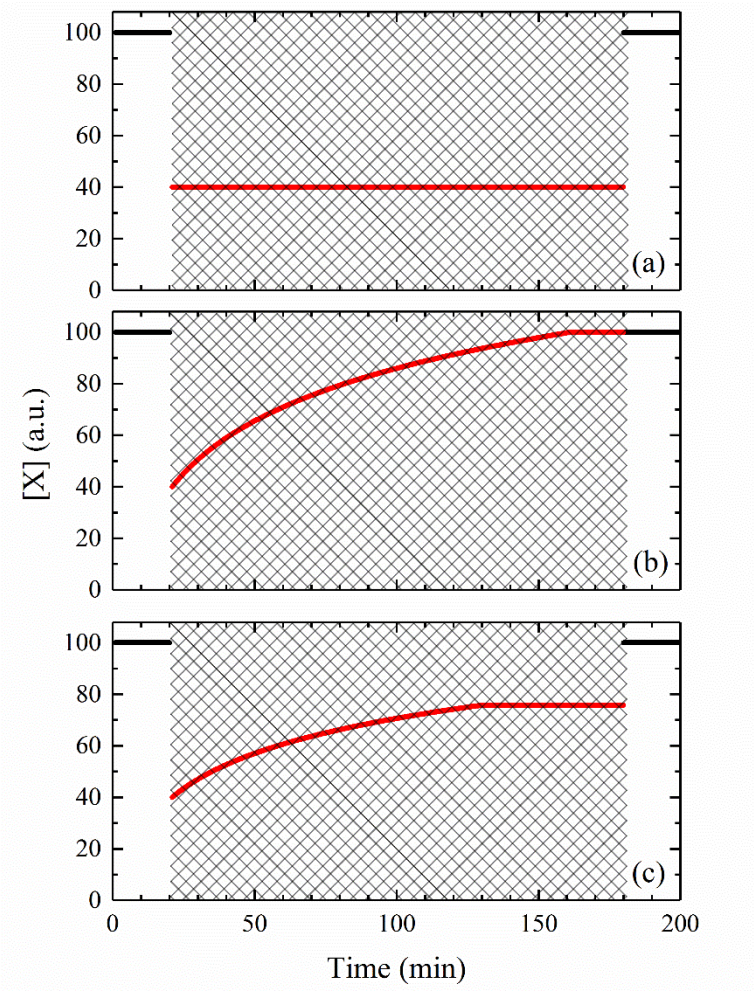

Figure 3. Synthetic data of changes in the measured concentration of a trace gas, X, due to heterogeneous reaction when it is exposed to mineral dust particles. The heterogeneous reaction starts at 20 min and ceases at 180 min (the shadowed area). Black curves represent the measured concentration of X without exposure to mineral dust particles (i.e. initial [X]), and

red curves represent the evolution of measured [X] during exposure of X to mineral dust particles. a) No surface deactivation; b) complete surface deactivation; c) partial surface deactivation. Surface deactivation would result in reduced loss of X due to heterogeneous uptake and thus increase in measured [X].

In atmospheric chemistry community, heterogeneous reactions are usually treated as pseudo-first-order processes (with respect to reactive trace gases), as implied by Eq. (1). However, deactivation of mineral dust surfaces has been reported for a variety of trace gases by experiments using particle ensembles deposited on a substrate (Underwood et al., 2001; Hanisch and Crowley, 2003a; Ndour et al., 2009; Tang et al., 2010; Zhou et al., 2012; Romanias et al., 2013; Liu et al., 2015). Therefore, uptake coefficients are normally set to be time dependent (instead of assuming to be a constant), such that Eq. (1) is still valid for time dependent heterogeneous kinetics. Many studies (Michel et al., 2003; Seisel et al., 2005; Karagulian et al., 2006; Wang et al., 2011; El Zein et al., 2014) have reported initial and/or steady-state uptake coefficients (γ_0 and γ_{ss}, respectively). What makes interpreting reported uptake coefficients more difficult is that even for the same heterogeneous reaction, γ_0 and γ_{ss} may exhibit dependence on experimental conditions (e.g., dust sample mass, trace gas concentration, temperature, and etc.). For example, it takes less time for a reaction to reach steady-state when higher concentrations are used for the same reactive trace gas. In many cases, surface may be completely deactivated given sufficient reaction time. Furthermore, γ_0 is usually reported as the first measurable uptake coefficient, which largely depends on the response time (and time resolution) of the instrument used to detect the trace gas.

In aerosol flow tube experiments, on the other hand, exposure time of mineral dust aerosol particles to trace gases are very short (typically <1 min). Therefore, significant surface deactivation is not observed and decays of trace gases can usually be well described by pseudo-

first-order kinetics with time independent uptake coefficients (Vlasenko et al., 2006; Pradhan et al., 2010a; Tang et al., 2012; Matthews et al., 2014).

Ideally laboratory studies of heterogeneous reactions should be carried out at or at least close to atmospherically relevant conditions, such that experimental results can be directly used. However, due to experimental challenges, laboratory studies are usually performed at much shorter time scales (from <1 min to a few hours, compared to average residence time of several days for mineral dust aerosol) and with much higher trace gas concentrations. Alternatively, measurements can be conducted over a wide range of experimental conditions in order that fundamental physical and chemical processes can be deconvoluted and corresponding rate constants can be determined (Kolb et al., 2010; Davidovits et al., 2011; Pöschl, 2011). With more accurate kinetic data, kinetic models which integrate these fundamental processes can be constructed and applied to predict uptake coefficients for atmospherically relevant condition (Ammann and Poschl, 2007; Pöschl et al., 2007; Shiraiwa et al., 2012; Berkemeier et al., 2013). Unfortunately, measurements of this type are resource-demanding. In practice laboratory studies of heterogeneous kinetics are usually carried out under very limited experimental conditions. Therefore, there is a great need to invest more resource in fundamental laboratory research.

3 Heterogeneous reactions of mineral dust particles with tropospheric oxidants and their direct precursors

The importance of a heterogeneous reaction for removal of a trace gas, X, is determined by the uptake coefficient and the aerosol surface area concentration, as suggested by Eq. (1). It also depends on the rates of other removal processes in competition, although it is not uncommon that this aspect has not been fully taken into account. In this section, previous laboratory studies of heterogeneous reactions of mineral dust particles with OH, HO_2, H_2O_2, O_3, HCHO, HONO, NO_3, and N_2O_5 are summarized, analyzed, and discussed. After that,

lifetimes of each trace gases with respect to their heterogeneous reactions with mineral dust are calculated, using uptake coefficients listed in Table 2, followed by discussion of relative importance of heterogeneous reactions for their removal in the troposphere. In addition, we also discuss representative modeling studies to further demonstrate and illustrate the importance of these heterogeneous reactions.

Uptake coefficients which are used in this paper to calculate lifetimes with respect to heterogeneous reactions with mineral dust particles are shown in Table 2. The IUPAC Task Group on Atmospheric Chemical Kinetic Data Evaluation has been compiling and evaluating kinetic data for atmospheric heterogeneous reactions (Crowley et al., 2010a), and preferred uptake coefficients are also recommended. It should be noted that uptake coefficients listed in Table 2 do not intend to compete with those recommended by the IUPAC task group. Instead, some of our values are largely based on their recommended values if available and proper. We also acknowledge that a single uptake coefficient may not always be enough to describe the kinetics of a heterogeneous reaction of mineral dust, because 1) uptake kinetics may change with reaction time, as discussed in Section 2.2; 2) uptake kinetics are also affected by particle mineralogy and composition, RH, temperature, the co-presence of other reactive trace gases, and etc.; and 3) for some reactive trace gases, such as O_3, the uptake coefficients may strongly depend on their concentrations.

Table 3: Uptake coefficients used in this work to calculate lifetimes of OH, HO_2, H_2O_2, O_3, HCHO, HONO, NO_3, and N_2O_5 with respect to heterogeneous reactions with mineral dust aerosol.

species	uptake coefficient	species	uptake coefficient
OH	0.2	HCHO	1×10^{-5}
HO_2	0.038	HONO	1×10^{-6}
H_2O_2	1×10^{-3}	NO_3	0.018

O_3	4.5×10^{-6}	N_2O_5	0.020

The pseudo-first-order loss rate depends on the aerosol surface area concentration, which depends on aerosol number concentration and its size distribution. Although particle sizing instruments such as aerodynamic particle sizer (APS) and scanning particle mobility sizer (SMPS) are commercially available, particle mass concentrations are still more widely measured and reported. Therefore, it is convenient to calculate lifetimes based on mass concentration instead of surface area concentration. This calculation requires information of particle size and density. For simplicity dust aerosol particles are assumed to have an average particles diameter of 1 μm and a density of 2.7 g cm^{-3}. Consequently, the lifetime of X with respect to its heterogeneous reaction with mineral dust, $\tau_{het}(X)$, can be described by Eq. (6) (Wagner et al., 2008; Tang et al., 2010; Tang et al., 2012):

$$\tau_{het}(X) = \frac{1.8\times10^{8}}{\gamma_{eff}(X)\cdot c(X)\cdot L} \quad (6)$$

where $\gamma_{eff}(X)$ is the effective uptake coefficient of X, $c(X)$ is the average molecular speed of X (cm s^{-1}), and L is the mineral dust loading (i.e. mass concentration) in μg m^{-3}. Mass concentrations of mineral dust aerosol particles in the troposphere show high variability, ranging from a few μg m^{-3} in background regions such as north Atlantic to >1000 μg m^{-3} during extreme dust storms (Prospero, 1979; Zhang et al., 1994; de Reus et al., 2000; Gobbi et al., 2000; Alfaro et al., 2003). To take into account this spatial and temporal variation, mass concentrations of 10, 100, and 1000 μg m^{-3} are used in this paper to assess atmospheric significance of heterogeneous reactions with mineral dust for the removal of trace gases.

3.1 OH and HO_2 radicals

3.1.1 OH radicals

Heterogeneous uptake of OH radicals by mineral dust particles was first investigated using a coated wall flow tube with detection of OH radicals by electron paramagnetic resonance

(EPR) (Gershenzon et al., 1986). The uptake coefficient was reported to be 0.04±0.02 for Al_2O_3 and 0.0056±0.0020 for SiO_2, independent of temperature in the range of 253-348 K (Gershenzon et al., 1986). Using laser induced fluorescence (LIF), Suh et al. (2000) measured concentration changes of OH radicals after the gas flow was passed through a wire screen loaded with TiO_2 (anatase or rutile), α-Al_2O_3, or SiO_2 under dry conditions. It is shown that the uptake coefficients, γ(OH), increased with temperature from ~310 K to ~350 K for all the three oxides, being (2-4)×10^{-4} for TiO_2, (2-4)×10^{-3} for SiO_2, and (5-6)×10^{-3} for α-Al_2O_3 (Suh et al., 2000). Unfortunately, most of the results reported by Suh et al. (2000) are only presented graphically. In an earlier study (Bogart et al., 1997), γ(OH) was reported to be 0.41±0.04 at 300 K on deposited SiO_2 films, decreasing with temperature. OH(X^2II) radicals used by Bogart et al. were generated in a 20:80 tetraethoxysilane/O_2 plasmas and their atmospheric relevance is not very clear; therefore, this study is not included in Table 1 or further discussed.

The average γ(OH) was determined to be 0.20 for Al_2O_3 at room temperature under dry conditions (Bertram et al., 2001), using a coated wall flow tube coupled to chemical ionization mass spectrometry (CIMS). In a following study, the RH dependence of γ(OH) on SiO_2 and Al_2O_3 at room temperature was investigated (Park et al., 2008). It is found that γ(OH) increased from 0.032±0.007 at 0% RH to 0.098±0.022 at 33% RH for SiO_2 and from 0.045±0.005 at 0% RH to 0.084±0.012 at 38% RH for Al_2O_3 (Park et al., 2008).

Table 4: Summary of previous laboratory studies on heterogeneous reactions of mineral dust with OH and HO_2 radicals

Trace gases	Dust	Reference	*T* (K)	Concentration (molecule cm^{-3})	Uptake coefficients	Techniques
OH	TiO_2	Suh et al., 2000	308 to 350	~4×10^{12}	$(2\text{-}4)\times10^{-4}$, increasing with temperature	LIF
	SiO_2	Gershenzon et al., 1986	253-343	<2×10^{12}	0.0056±0.002, independent of temperature	CWFT-EPR
		Suh et al., 2000	308 to 350	~4×10^{12}	$(2\text{-}4)\times10^{-3}$, increasing with temperature	LIF
		Park et al, 2008	room temperature	~4×10^{11}	0.032±0.007 at 0% RH and 0.098±0.022 at 33% RH	CWFT-CIMS
	Al_2O_3	Gershenzon et al., 1986	253-343	<2×10^{12}	0.04±0.02, independent of temperature	CWFT-EPR
		Suh et al., 2000	308 to 350	~4×10^{12}	$(5\text{-}6)\times10^{-3}$, increasing with temperature	LIF
		Bertram et al, 2001	room temperature	$(1\text{-}100)\times10^{9}$	0.20	CWFT-CIMS
		Park et al, 2008	room temperature	~4×10^{11}	0.045±0.005 at 0%RH and 0.084±0.012 at 38% RH	CWFT-CIMS
	ATD	Bedjanian et al., 2013a	275-320	$(0.4\text{-}5.2)\times10^{12}$	0.20 at 0% RH, showing a negative RH dependence but no dependence on temperatures	CRFT-MS
HO_2	ATD	Bedjanian et al., 2013b	275-320	$(0.35\text{-}3.3)\times10^{12}$	0.067±0.004 at 0% RH, showing a negative RH dependence (0.02-94%) but no dependence on temperature.	CRFT-MS
		Matthews et al., 2014	291±2	$(3\text{-}10)\times10^{8}$	0.018±0.006 when HO_2 concentration was 3×10^{8} molecule cm^{-3} and 0.031±0.008 when HO_2 concentration was 3×10^{8} molecule cm^{-3}. No RH (5-76%) dependence was observed.	AFT-FAGE
	forsterite	James et al., 2017	293	1.6×10^{9}	$(4.3\pm0.4)\times10^{-3}$ at 12% RH	AFT-FAGE
	olivine	James et al., 2017	293	1.6×10^{9}	$(6.9\pm1.2)\times10^{-2}$ at 10% RH	AFT-FAGE
	fayalite	James et al., 2017	293	1.6×10^{9}	$(7.3\pm0.4)\times10^{-2}$ at 10% RH	AFT-FAGE

TiO_2	Moon et al., 2017	293	1.6×10^{9}	0.021±0.001 at ~11% RH, 0.029±0.005 at ~45%, and 0.037±0.007 at ~66%, showing a positive dependence on RH.	AFT-FAGE

Recently a coated rod flow tube was used to investigate uptake of OH radicals by Arizona test dust (ATD) particles (Bedjanian et al., 2013b) as a function of temperature (275-320 K) and RH (0.03-25.9%). Gradual surface deactivation was observed, and the initial uptake coefficient was found to be independent of temperature and decrease with increasing RH, given by Eq. (7):

$$\gamma_0 = 0.2/(1 + RH^{0.36}) \quad (7)$$

with an estimated uncertainty of ±30%. Please note that uptake coefficients reported by Bedjanian et al. (2013a) are based on the geometrical area of the rod coated with ATD particles and thus should be considered as the upper limit. No effect of UV radiation, with $J(NO_2)$ up to 0.012 s^{-1}, was observed (Bedjanian et al., 2013b). In addition, H_2O and H_2O_2 were found to be the major and minor products in the gas phase respectively (Bedjanian et al., 2013b), as shown in Figure 4.

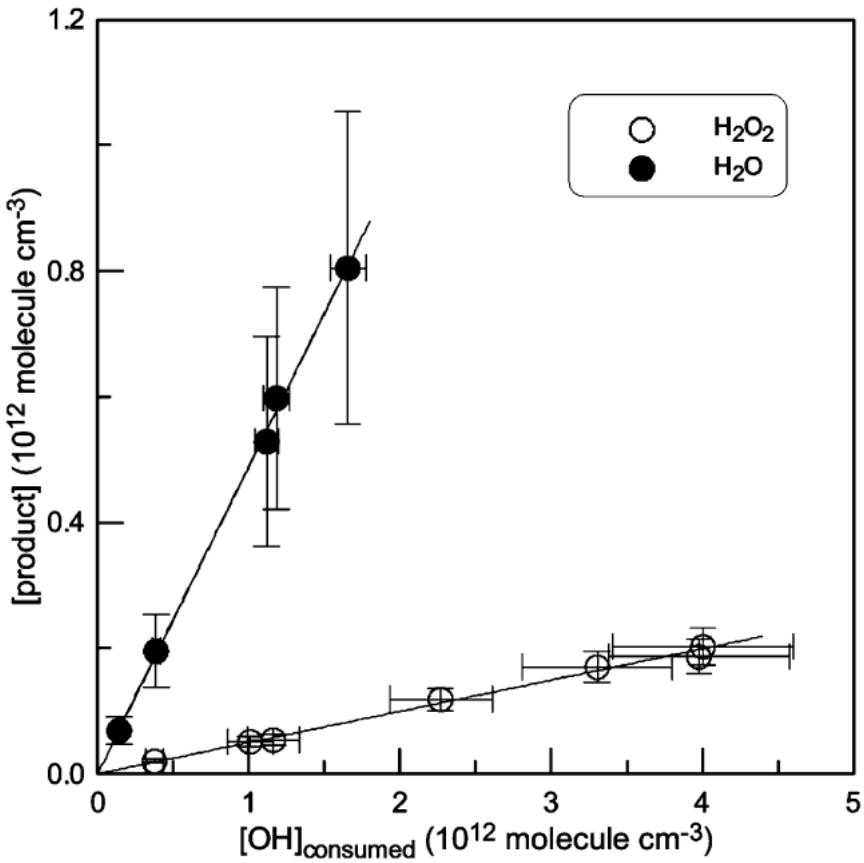

Figure 4. Concentrations of H_2O (solid circles) and H_2O_2 (open circles) produced in the gas phase due to heterogeneous reaction of OH radicals with ATD particles. Reprinted with permission from Bedjanian et al. (2013a). Copyright 2013 American Chemical Society.

As shown in Figure 5, γ(OH) reported by previous flow tube studies, except that onto SiO_2 particles reported by Gershenzon et al. (1986), show reasonably good agreement, considering that different minerals were used. Reported γ(OH) are larger than 0.02 in general, suggesting that mineral dust exhibits relatively large reactivity towards OH radicals. Discrepancies are also identified from data presented in Figure 5, with the most evident one being the effect of RH. Park et al. (2008) found that γ(OH) increased significantly with RH for both SiO_2 and Al_2O_3, while Bedjanian et al. (2013b) suggested that γ(OH) showed a negative dependence on RH. It is not clear yet whether different minerals used by these two studies can fully account for the different RH dependence observed. Furthermore, a positive dependence of γ(OH) on temperature was found by Suh et al. (2000) for TiO_2, α-Al_2O_2, and SiO_2, while Bogart et al. (1997) reported a negative temperature effect for deposited SiO_2 film and no significant dependence on temperature was found for ATD (Bedjanian et al., 2013b).

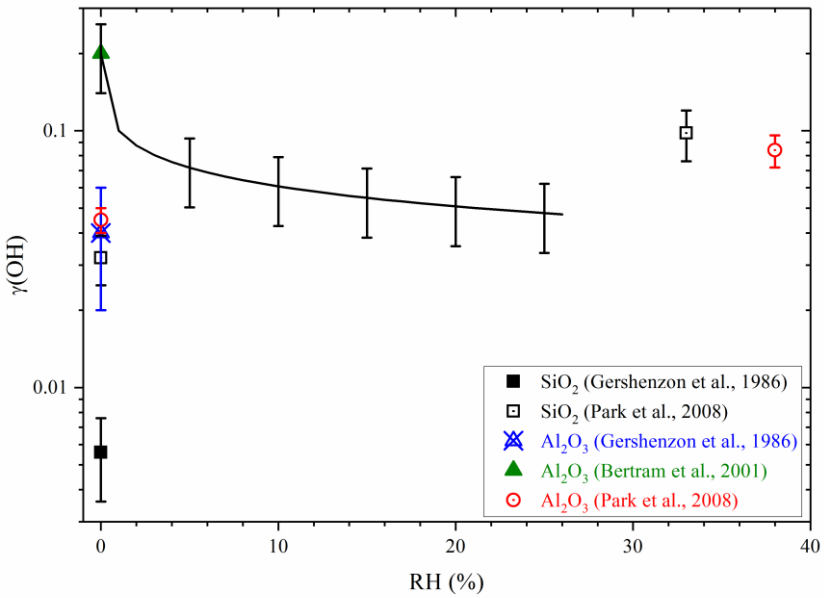

Figure 5. Uptake coefficients of OH radicals for different minerals at room temperature, as reported by different studies. The plotted RH dependence of γ(OH) for ATD (solid curve) is based on the parameterization reported by Bedjanian et al. (2013a), i.e. Eq. (7).

A γ(OH) value of 0.2, reported by Bedjanian et al. (2013a) for ATD, is used in our present work to evaluate the importance of heterogeneous uptake of OH radicals by mineral dust aerosol. According to Eq. (6), dust mass loadings of 10, 100, and 1000 μg m^{-3} correspond to τ_{het}(OH) of ~25 min, 150 s, and 15 s with respect to heterogeneous uptake by mineral dust. As discussed in Section 2.1.1, lifetimes of tropospheric OH are in the range of 1 s or less in very clean regions and <0.1 s in polluted and forested areas, much shorter than τ_{het}(OH). Even if γ(OH) is assumed to be 1, for uptake by 1 μm particles γ_{eff}(OH) is calculated to be 0.23, which is only 15% larger than what we use to calculate τ_{het}(OH). Therefore, it can be concluded that heterogeneous reaction with mineral dust aerosol is not a significant sink for OH radicals in the troposphere.

3.1.2 HO_2 radicals

A few laboratory studies have investigated heterogeneous uptake of HO_2 radicals by mineral dust particles. Bedjanian et al. (2013b) used a coated rod flow tube to study the interaction of HO_2 radicals with ATD film as a function of temperature and RH. Surface deactivation was observed, and γ_0, based on the geometrical area of dust films, was determined to be 0.067±0.004 under dry conditions (Bedjanian et al., 2013a). The initial uptake coefficient, independent of temperature, was found to decrease with RH, given by Eq. (8):

$$\gamma_0 = 1.2/(18.7 + RH^{1.1}) \quad (8)$$

with an estimated uncertainty of ±30%. UV radiation, with $J(NO_2)$ ranging from 0 to 0.012 s^{-1}, did not affect uptake kinetics significantly. In addition, the yield of H_2O_2(g), defined as the ratio of formed H_2O_2(g) molecules to consumed HO_2 radicals, was determined to be <5% (Bedjanian et al., 2013a). In the second study (Matthews et al., 2014), an aerosol flow tube was deployed to measure $\gamma(HO_2)$ onto ATD aerosol particles at 291±2 K, with HO_2 detection via the fluorescence assay by gas expansion technique. No significant effect of RH in the range of 5-76% was observed, and $\gamma(HO_2)$ was reported to be 0.031±0.008 for $[HO_2]$ of 3×10^8 molecule cm^{-3} and 0.018±0.006 for $[HO_2]$ of 1×10^9 molecule cm^{-3} (Matthews et al., 2014). In addition, $\gamma(HO_2)$ was found to decrease with increasing reaction time. The negative dependence of $\gamma(HO_2)$ on $[HO_2]$ and reaction time implies that ATD surface is gradually deactivated upon exposure to HO_2 radicals, as directly observed by Bedjanian et al. (2013a).

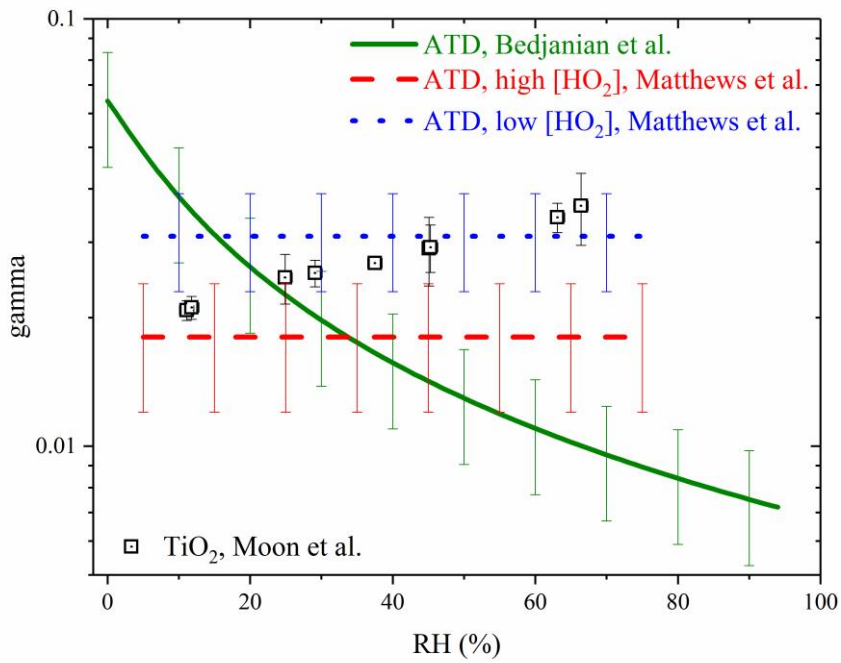

Figure 6. RH dependence of $\gamma(HO_2)$ for ATD reported by two previous studies. Solid curve, reported by Bedjanian et al. (2013b) with initial $[HO_2]$ in the range of $(0.35\text{-}3)\times10^{12}$ molecule cm^{-3}; dashed and dotted curve, reported by Matthews et al. (2014) with initial $[HO_2]$ of 1×10^{9} and 3×10^{8} molecule cm^{-3}, respectively. Numerical data for $\gamma(HO_2)$ at different RH were not provided by Matthews et al. (2014), and thus in this figure we plot their reported average $\gamma(HO_2)$ together with their estimated uncertainties. The plotted RH dependence of $\gamma(HO_2)$ reported by Bedjanian et al. (2013b) is based on their proposed parameterization, i.e. Eq. (8).

Figure 6 shows the effect of RH on $\gamma(HO_2)$ for ATD particles. A quick look at Figure 6 could lead to the impression that $\gamma(HO_2)$ reported by two previous studies (Bedjanian et al., 2013a; Matthews et al., 2014) agree relatively well, especially considering that two very different experimental techniques were used. Nevertheless, Matthews et al. (2014), who conducted their measurements with initial $[HO_2]$ which are 3-4 orders of magnitude lower than those used by Bedjanian et al. (2013a), found a significant negative dependence of $\gamma(HO_2)$ on initial $[HO_2]$. If this trend can be further extrapolated to higher initial $[HO_2]$, one may expect

that if carried out with initial [HO_2] similar to those used by Bedjanian et al. (2013a), Matthews et al. (2014) may find much smaller $\gamma(HO_2)$. In addition, these two studies also suggest very different RH effects, as evident from Figure 6. We also note that ATD is the only one type of mineral dust onto which heterogeneous uptake of HO_2 radicals was investigated, and the effect of mineralogy is not clear at all yet. Therefore, our understanding of heterogeneous reactions of HO_2 radicals with mineral dust particles is very limited.

In a very recent study (Moon et al., 2017), heterogeneous reaction of HO_2 with TiO_2 aerosol particles was examined as a function of RH at room temperature. As shown in Figure 6, $\gamma(HO_2)$ was observed to depend on RH, increasing from 0.021±0.001 at ~11% RH to 0.029±0.005 at ~45% and 0.037±0.007 at ~66%. More specifically, it has been shown that for the RH range covered (11-66%), $\gamma(HO_2)$ depends linearly on the amount of water adsorbed on TiO_2 particles, revealing the critical role adsorbed water plays in heterogeneous uptake of HO_2 radicals by TiO_2. Apart from these displayed in Figure 6, the uptake of HO_2 by analogues of meteoric smoke particles was also examined at room temperature (James et al., 2017), using an aerosol flow tube. At (10±1)% RH, the uptake coefficient was determined to be 0.069±0.012 for olivine ($MgFeSiO_4$), 0.073±0.004 for fayalite (Fe_2SiO_4), and 0.0043±0.0004 for forsterite (Mg_2SiO_4), respectively. It appears that compared to meteoric smoke particles which do not contain Fe, Fe-containing meteoric smoke particles show much larger heterogeneous reactivity towards HO_2 radicals. The experimental result indicates a catalytic role of Fe in HO_2 uptake, as supported by electronic structure calculations (James et al., 2017). Though its tropospheric relevance is limited, this study provides valuable mechanistic insights into heterogeneous reaction of mineral dust with HO_2 radicals.

For reasons discussed in Section 2.2.1, $\gamma(HO_2)$ reported by Matthews et al. (2014) using ATD aerosol samples are used to calculate $\tau_{het}(HO_2)$ with respect to uptake onto mineral dust. Another reason that the data reported by Matthews et al. (2014) are preferred is that [HO_2] used

in this study were low enough to be of direct atmospheric relevance. As a result, $\gamma(HO_2)$ measured at lower initial $[HO_2]$ (3×10^8 molecule cm^{-3}), equal to 0.031±0.008, is adopted in our current work to assess the significance of HO_2 uptake by mineral dust. Using Eq. (6), $\tau_{het}(HO_2)$ is estimated to be 2.2, 22, and 222 min for dust mass concentrations of 1000, 100, and 10 μg m^{-3}, respectively. Typical HO_2 lifetimes in the troposphere, as summarized in Table 1, show large variability, ranging from <1 s (Ren et al., 2003) to >30 min (Whalley et al., 2011). Therefore, dust aerosol with moderate mass concentrations could be a significant tropospheric HO_2 sink except regions with very high NO levels.

The importance of heterogeneous uptake as a HO_2 sink in the troposphere has also been demonstrated by several more sophisticated modelling studies. For example, it is found that while standard gas phase chemical mechanism used by the GEOS-Chem model would overestimate HO_2 and H_2O_2 concentrations observed in the Arctic troposphere in the spring, including heterogeneous reaction of HO_2 with an average $\gamma(HO_2)$ of >0.1 in the model could better reproduce the measured concentrations and vertical profiles of HO_2 and H_2O_2 (Mao et al., 2010a). Though not directly relevant for mineral dust aerosol, this study provided strong evidence that heterogeneous uptake can be an important but yet not fully recognized sink for tropospheric HO_2 radicals (Mao et al., 2010a). Using a global tropospheric model, Macintyre and Evans (2011) analyzed the sensitivity of model output to $\gamma(HO_2)$ values used in the model. A global average $\gamma(HO_2)$ of 0.028 was derived from available laboratory studies (Macintyre and Evans, 2011), and large regional differences in modelled O_3 were observed between simulations using $\gamma(HO_2)$ parameterization developed by Macintyre and Evans (2011) and those using a constant $\gamma(HO_2)$ of 0.2. This results highlights the importance of accurate determination of $\gamma(HO_2)$ under different tropospheric conditions (e.g., aerosol composition, RH, and temperature).

The impact of HO_2 uptake by mineral dust has also been investigated by several modelling studies. For example, an observation constrained box model study (Matthews et al., 2014) suggested that heterogeneous reaction with mineral dust could result in >10% reduction in HO_2 concentrations in Cape Verde, using a $\gamma(HO_2)$ of 0.038. A WRF-Chem simulation, using $\gamma(HO_2)$ reported by Bedjanian et al. (2013a), showed that heterogeneous uptake by mineral dust could reduce HO_2 concentrations by up to 40% over northern India during a pre-monsoon dust storm (Kumar et al., 2014).

One may assume that heterogeneous reaction of HO_2 with aerosol particles leads to the formation of H_2O_2 (Graedel et al., 1986; Thornton and Abbatt, 2005). A second channel without H_2O_2 formation, i.e. simple decomposition of HO_2 radicals to H_2O and O_2, may also be important (Bedjanian et al., 2013a; Mao et al., 2013a). Atmospheric impacts can be very different for these two mechanisms. While the second pathway represents a net sink for HO_2 in the troposphere, the first channel only converts HO_2 to H_2O_2 via heterogeneous reaction and is thus of limited efficacy as a net sink for HOx because H_2O_2 can undergo photolysis to generate OH radicals.

The relative importance of these two mechanisms has been explored by modelling studies. In the modeling work carried out by de Reus et al. (2005), $\gamma(HO_2)$ was assumed to be 0.2 for heterogeneous uptake onto Saharan dust particles. If no H_2O_2 is formed in heterogeneous reaction of HO_2 with Saharan dust, modeled H_2O_2 concentrations would agree well with measurements; in contrast, if heterogeneous uptake of HO_2 radicals were assumed to produce H_2O_2, modeled H_2O_2 concentrations would be much larger than measured values. In a more recent study, Mao et al. (2010a) found that only including the first reaction channel (with H_2O_2 production) will overestimate H_2O_2 in the Arctic, while only considering the second channel (without H_2O_2 production) would cause underestimation of H_2O_2. Consequently, it seems that both channels have non-negligible contributions in the troposphere (Mao et al.,

2010a). Significant differences in modelled OH, HO_2, O_3, and sulfate concentrations have been found by a global model study when including two mechanisms separately (Macintyre and Evans, 2011). One experimental study (Bedjanian et al., 2013a) measured gas phase products for heterogeneous reaction of HO_2 radicals with ATD particles and found that gaseous H_2O_2 formed in this reaction is minor but probably non-negligible. Considering the importance of mechanisms of heterogeneous reaction of HO_2 with mineral dust, further experimental work is required. Furthermore, mineralogy and RH may also impact the yield of H_2O_2(g), but these effects are not clear yet.

3.2 H_2O_2

Pradhan et al. (2012a, 2012b) utilized an aerosol flow tube to investigate heterogeneous interaction of H_2O_2 with airborne TiO_2, Gobi dust, and Saharan dust particles at 295±2 K, and H_2O_2 was detected by CIMS. A negative dependence of $\gamma(H_2O_2)$ on RH was observed for TiO_2, with $\gamma(H_2O_2)$ decreasing from $(1.53\pm0.11)\times10^{-3}$ at 15% RH to $(6.47\pm0.74)\times10^{-4}$ at 40% RH and $(5.04\pm0.58)\times10^{-4}$ at 70% RH (Pradhan et al., 2010a). In contrast, H_2O_2 uptake kinetics displayed positive dependence on RH for Gobi and Saharan dust, with $\gamma(H_2O_2)$ increasing from $(3.33\pm0.26)\times10^{-4}$ at 15% RH to $(6.03\pm0.42)\times10^{-4}$ at 70% RH for Gobi dust and from $(6.20\pm0.22)\times10^{-4}$ at 15% RH to $(9.42\pm0.41)\times10^{-4}$ at 70% RH for Saharan dust (Pradhan et al., 2010b). It appears that heterogeneous reactivity of Saharan dust towards H_2O_2 is significantly higher than Gobi dust.

Heterogeneous interaction of gaseous H_2O_2 with SiO_2 and α-Al_2O_3 particles was investigated at 298±1 K, using transmission FTIR to probe particle surfaces and a HPLC-based offline technique to measure gaseous H_2O_2 (Zhao et al., 2011b). It is found that most of H_2O_2 molecules were physisorbed on SiO_2 surface and a small amount of molecularly adsorbed H_2O_2 underwent thermal decomposition. In contrast, catalytic decomposition occurred to a large fraction of H_2O_2 uptaken by α-Al_2O_3, though some H_2O_2 molecules were also physisorbed on

the surface (Zhao et al., 2011b). The uptake coefficient, based on the BET surface area, was found to be independent of initial H_2O_2 concentrations (1.27-13.8 ppmv) while largely affected by RH (Zhao et al., 2011b). $\gamma(H_2O_2)$ decreased from $(1.55\pm0.14)\times10^{-8}$ at 2% RH to $(0.81\pm0.11)\times10^{-8}$ at 21% RH for SiO_2 particles, and further increase in RH (up to 76%) did not affect the uptake kinetics (Zhao et al., 2011b). A similar dependence of $\gamma(H_2O_2)$ on RH was also observed for α-Al_2O_3: $\gamma(H_2O_2)$ decreased from $(1.21\pm0.04)\times10^{-7}$ at 2% RH to $(0.84\pm0.07)\times10^{-7}$ at 21% RH, and the effect of RH was not significant for RH in the range of 21-76% (Zhao et al., 2011b). Compared to SiO_2, α-Al_2O_3 appears to be much more reactive towards H_2O_2.

In a following study, using the same experimental setup, Zhao et al. (2013) explored heterogeneous interaction of H_2O_2 with fresh, HNO_3-processed, and SO_2-processed $CaCO_3$ particles. The uptake of H_2O_2 on fresh $CaCO_3$ particles was drastically reduced with increasing RH, indicating that H_2O_2 and H_2O compete for surface reactive sites. In addition, about 85-90% of H_2O_2 molecules uptaken by fresh $CaCO_3$ particles undergo decomposition (Zhao et al., 2013). Unfortunately no uptake coefficients were reported (Zhao et al., 2013). Pretreatment of $CaCO_3$ particles with HNO_3 or SO_2 can significantly affect their heterogeneous reactivity towards H_2O_2. The effect of HNO_3 pretreatment increases with surface coverage of nitrate (formed on $CaCO_3$ particles), showing an interesting dependence on RH. Pretreatment of $CaCO_3$ with HNO_3 reduced its heterogeneous reactivity by 30-85% at 3% RH, while it led to enhancement of reactivity towards H_2O_2 by 20-60% at 25% RH, a factor of 1-3 at 45% RH, and a factor of 3-8 at 75% RH (Zhao et al., 2013). At low RH, formation of $Ca(NO_3)_2$ on the surface could deactivate $CaCO_3$; however, $Ca(NO_3)_2$ may exit as an aqueous film at higher RH (Krueger et al., 2003b; Liu et al., 2008b), consequently leading to large enhancement of H_2O_2 uptake. Compared to fresh $CaCO_3$, SO_2-processed particles always exhibit much higher

reactivity towards H_2O_2, and enhancement factors, increasing with RH, were observed to fall into the range of 3-10 (Zhao et al., 2013).

Heterogeneous uptake of H_2O_2 by several oxides was investigated at 298 K using a Knudsen cell reactor with H_2O_2 measured by a quadrupole mass spectrometer (Wang et al., 2011). $\gamma_0(H_2O_2)$, based on the BET surface area of sample powders, was determined to be $(1.00\pm0.11)\times10^{-4}$ for α-Al_2O_3, $(1.66\pm0.23)\times10^{-4}$ for MgO, $(9.70\pm1.95)\times10^{-5}$ for Fe_2O_3, and $(5.22\pm0.90)\times10^{-5}$ for SiO_2, respectively (Wang et al., 2011). Surface deactivation occurred for all the surfaces, though complete surface saturation was only observed for SiO_2 after extended H_2O_2 exposure. This may indicate that the uptake of H_2O_2 by α-Al_2O_3, MgO, and Fe_2O_3 are of catalytic nature to some extent (Wang et al., 2011).

Continuous wave CRDS was employed to detect the depletion of H_2O_2 and formation of HO_2 radicals in the gas phase above TiO_2 films which were exposed to gaseous H_2O_2 and illuminated by a light-emitting diode at 375 nm (Yi et al., 2012). Three different TiO_2 samples were investigated, including Degussa P25 TiO_2, Aldrich anatase, and Aldrich rutile. H_2O_2 decays did not occur in the absence of TiO_2. In addition, production of HO_2 radicals was only observed in the presence of H_2O_2, and the presence of O_2 did not have a significant effect. Therefore, Yi et al. (2012) suggested that the production of HO_2 radicals is due to the photodecomposition of H_2O_2 on TiO_2 surfaces. Decays of H_2O_2 and formation of HO_2 are found to vary with TiO_2 samples (Yi et al., 2012). Photo-degradation of H_2O_2 is fast for P25 TiO_2 samples and much slower for anatase and rutile; furthermore, significant production of HO_2 radicals in the gas phase was observed for anatase and rutile but not for P25 TiO_2. However, no uptake coefficients were reported by Yi et al. (2012).

Zhou et al. (2012) first explored the temperature dependence of heterogeneous reactivity of mineral dust towards H_2O_2, using a Knudsen cell reactor coupled to a quadrupole mass spectrometer. The uptake kinetics show negative temperature dependence, with $\gamma_0(H_2O_2)$

(BET surface area based) decreasing from $(12.6\pm2.52)\times10^{-5}$ at 253 K to $(6.08\pm1.22)\times10^{-5}$ at 313 K for SiO_2 and from $(7.11\pm1.42)\times10^{-5}$ at 253 K to $(3.00\pm0.60)\times10^{-5}$ at 313 K for $CaCO_3$ (Zhou et al., 2012). Complete surface deactivation was observed for both dust samples after long exposure to H_2O_2 (Zhou et al., 2012). In a following study, the effects of temperature on the uptake of H_2O_2 by ATD and two Chinese dust samples were also investigated (Zhou et al., 2016). $\gamma_0(H_2O_2)$, based on the BET surface area, was observed to decrease with temperature, from $(2.71\pm0.54)\times10^{-4}$ at 253 K to $(1.47\pm0.29)\times10^{-4}$ at 313 K for ATD, and from $(3.56\pm0.71)\times10^{-4}$ at 253 K to $(2.19\pm0.44)\times10^{-4}$ at 313 K for Inner Mongolia desert dust, and from $(7.34\pm1.47)\times10^{-5}$ at 268 K to $(4.46\pm0.889)\times10^{-4}$ at 313 K for Xinjiang sierozem (Zhou et al., 2016). In addition, loss of heterogeneous reactivity towards H_2O_2 was observed for all the three dust samples (Zhou et al., 2016).

Table 5: Summary of previous laboratory studies on heterogeneous reactions of mineral dust with H_2O_2

Dust	Reference	*T* (K)	Concentration (molecule cm^{-3})	Uptake coefficient	Techniques
TiO_2	Pradhan et al., 2010a	295±2	~4.1×10^{12}	$(1.53\pm0.11)\times10^{-3}$ at 15% RH, $(6.47\pm0.74)\times10^{-4}$ at 40% RH, and $(5.04\pm0.58)\times10^{-4}$ at 70% RH	AFT-CIMS
	Romanias et al., 2012a	275-320	$(0.17\text{-}120)\times10^{12}$	Under dark conditions at 275 K, γ_0 was determined to be $(4.1\pm1.2)\times10^{-3}$ at 0% RH, $(5.1\pm1.5)\times10^{-4}$ at 20% RH, $(3.4\pm1.0)\times10^{-4}$ at 40% RH, $(2.7\pm0.8)\times10^{-4}$ at 60% RH, and $(2.3\pm0.7)\times10^{-4}$ at 80% RH. Surface deactivation was observed under dark conditions, and UV illumination could enhance the steady state uptake of H_2O_2.	CRFT-MS
	Yi et al., 2012	not stated	$(3\pm1)\times10^{13}$	No uptake coefficients were not reported.	CRDS
SiO_2	Zhao et al., 2011	298±1	$(3.2\text{-}34.5)\times10^{13}$	$\gamma(H_2O_2)$ decreased from $(1.55\pm0.14)\times10^{-8}$ at 2% RH to $(0.81\pm0.11)\times10^{-8}$ at 21% RH, and further increase in RH (up to 76%) did not affect uptake kinetics.	T-FTIR, HPLC
	Wang et al., 2011	298	$(1\text{-}25)\times10^{11}$	γ_0: $(5.22\pm0.90)\times10^{-5}$	KC-MS
	Zhou et al., 2012	253-313	$(0.37\text{-}3.7)\times10^{12}$	Under dry conditions, γ_0 decreased from $(12.6\pm2.52)\times10^{-5}$ at 253 K to $(6.08\pm1.22)\times10^{-5}$ at 313 K.	KC-MS
Al_2O_3	Zhao et al., 2011	298±1	$(3.2\text{-}34.5)\times10^{13}$	$\gamma(H_2O_2)$ decreased from $(1.21\pm0.04)\times10^{-7}$ at 2% RH to $(0.84\pm0.07)\times10^{-7}$ at 21% RH, and the effect of RH was not significant for RH in the range of 21-76%.	T-FTIR, HPLC
	Wang et al., 2011	298	$(1\text{-}25)\times10^{11}$	γ_0: $(1.00\pm0.11)\times10^{-4}$; γ_{ss}: 1.1×10^{-5}	KC-MS
	Romanias et al., 2013	268-320	$(0.16\text{-}12.6)\times10^{12}$	At 280 K, γ_0 was determined to be $(1.1\pm0.3)\times10^{-3}$ at 0% RH, $(1.2\pm0.3)\times10^{-4}$ at 10% RH, $(3.5\pm1.0)\times10^{-5}$ at 40% RH, and $(2.1\pm0.6)\times10^{-5}$ at 70% RH, showing a negative dependence on RH. No significant effect was observed for UV illumination.	CRFT-MS

Fe_2O_3	Wang et al., 2011	298	$(1\text{-}25)\times10^{11}$	γ_0: $(9.70\pm1.95)\times10^{-4}$; γ_{ss}: 5.5×10^{-5}	KC-MS
	Romanias et al., 2013	268-320	$(0.16\text{-}12.6)\times10^{12}$	At 280 K, γ_0 was determined to be $(1.1\pm0.3)\times10^{-3}$ at 0% RH, $(1.7\pm0.5)\times10^{-4}$ at 10% RH, $(6.7\pm2.0)\times10^{-5}$ at 40% RH, and $(4.5\pm1.4)\times10^{-5}$ at 70% RH, showing a negative dependence on RH. No significant effect was observed for UV illumination.	CRFT-MS
$CaCO_3$	Zhou et al., 2012	253-313	$(0.37\text{-}3.7)\times10^{12}$	Under dry conditions, γ_0 decreased from $(7.11\pm1.42)\times10^{-5}$ at 253 K to $(3.00\pm0.60)\times10^{-5}$ at 313 K.	KC-MS
	Zhao et al., 2013	298±1	1.3×10^{14}	The uptake of H_2O_2 on fresh $CaCO_3$ particles decreased drastically with RH. Pretreatment with SO_2 always enhances its reactivity towards H_2O_2, whereas exposure to HNO_3 could either enhance or suppress H_2O_2 uptake, depending on RH. Numerical values for uptake coefficients were reported.	T-FTIR, HPLC
ATD	El Zein et al., 2014	268-320	$(0.18\text{-}5.1)\times10^{12}$	Under dark conditions at 275 K, γ_0 was determined to be $(4.8\pm1.4)\times10^{-4}$ at 0% RH, $(5.8\pm1.8)\times10^{-5}$ at 20% RH, $(3.9\pm1.2)\times10^{-5}$ at 40% RH, and $(3.0\pm0.9)\times10^{-5}$ at 60% RH. Surface deactivation was observed under dark conditions, and UV illumination could enhance the steady state uptake of H_2O_2.	CRFT-MS
	Zhou et al., 2016	253-313	$(0.26\text{-}1.2)\times10^{12}$	Under dry conditions, γ_0 decreased with temperature, from $(2.71\pm0.54)\times10^{-4}$ at 253 K to $(1.47\pm0.29)\times10^{-4}$ at 313 K.	KC-MS
Saharan dust	Pradhan et al., 2012b	295±2	$\sim4.2\times10^{12}$	$\gamma(H_2O_2)$ increased from $(6.20\pm0.22)\times10^{-4}$ at 15% RH to $(9.42\pm0.41)\times10^{-4}$ at 70% RH.	AFT-CIMS
Gobi dust	Pradhan et al., 2012b	295±2	$\sim4.2\times10^{12}$	$\gamma(H_2O_2)$ increased from $(3.33\pm0.26)\times10^{-4}$ at 15% RH to $(6.03\pm0.42)\times10^{-4}$ at 70% RH.	AFT-CIMS
Chinese dust	Zhou et al., 2016	253-313	$(0.26\text{-}1.2)\times10^{12}$	Under dry conditions, γ_0 decreased with temperature, from $(3.56\pm0.71)\times10^{-4}$ at 253 K to $(2.19\pm0.44)\times10^{-4}$ at 313 K for Inner Mongolia desert dust and	KC-MS

				from (7.34±1.47)×10^{-4} at 268 K to (4.46±0.89)×10^{-4} at 313 K for Xinjiang sierozem.	
MgO	Wang et al., 2011	298	(1-25)×10^{11}	γ_0: (1.66±0.23)×10^{-4}; γ_{ss}: 1.6×10^{-5}.	KC-MS

A coated rod flow tube was coupled to a quadrupole mass spectrometer to investigate heterogeneous reactions of H_2O_2 with a variety of mineral dust particles as a function of initial H_2O_2 concentrations, irradiance intensity, RH, and temperature (Romanias et al., 2012a; Romanias et al., 2013; El Zein et al., 2014). Under dark conditions, quick surface deactivation was observed for TiO_2. When $[H_2O_2]_0$ was $<1\times10^{12}$ molecule cm^{-3}, γ_0 was found to be independent of $[H_2O_2]_0$; however, when $[H_2O_2]_0$ was above this threshold, a negative dependence of γ_0 on $[H_2O_2]_0$ occurred. At 275 K, γ_0 (based on BET surface area) depended on RH (up to 82%), given by (Romanias et al., 2012a):

$$\gamma_0(dark) = 4.1 \times 10^{-3}/(1 + RH^{0.65}) \quad (9)$$

The uncertainty was estimated to be ±30%.

UV illumination (315-400 nm) could lead to photocatalytic decomposition of H_2O_2 on TiO_2 surface. The steady state uptake coefficient, γ_{ss}(UV), increasing linearly with illumination intensity, was found to be independent of RH and depended inversely on $[H_2O_2]_0$ (Romanias et al., 2012a). When $[H_2O_2]_0$ is ~5×10^{11} molecule cm^{-3} and $J(NO_2)$ for UV illumination is 0.012 s^{-1}, the dependence of γ_{ss}(UV) on temperature (275-320 K) at 0.3% RH can be described by (Romanias et al., 2012a):

$$\gamma_{ss}(UV) = (7.2 \pm 1.9) \times 10^{-4} \times \exp[(460 \pm 80)/T] \quad (10)$$

It has also been found that NO added into the gas flow was converted to NO_2 during heterogeneous reaction of H_2O_2 with TiO_2. As shown in Figure 7, the ratio of consumed NO to formed NO_2 is close to 1. This indirect evidence suggests that HO_2 radicals (which could convert NO to NO_2) were found in the gas phase due to photocatalytic reaction of H_2O_2 with TiO_2 particles (Romanias et al., 2012a).

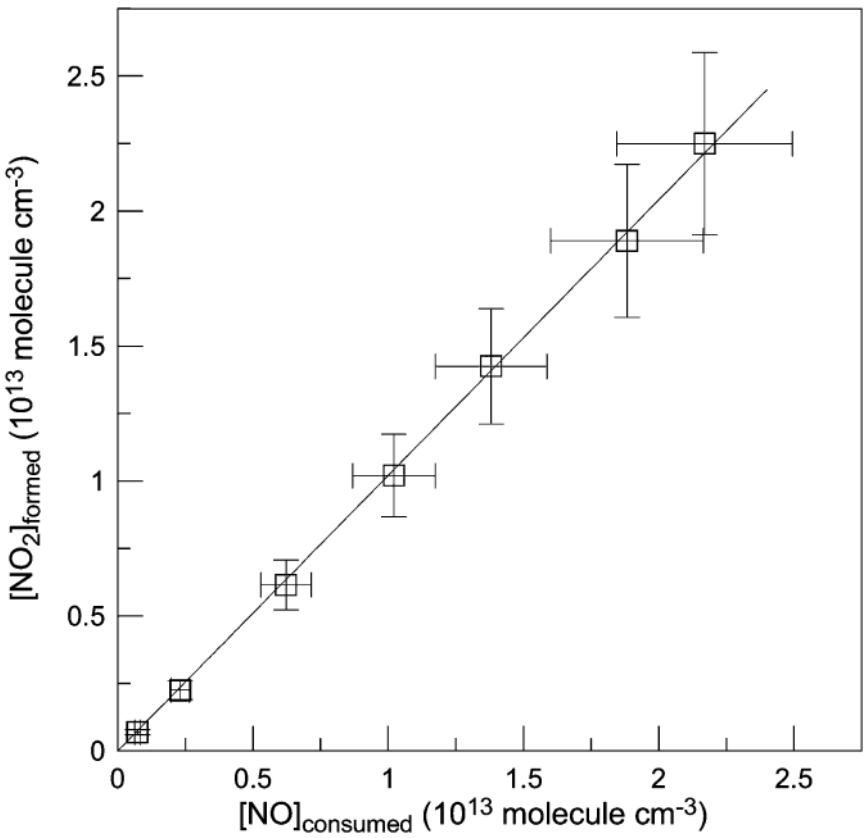

Figure 7. Consumed NO versus formed NO_2 in the heterogeneous reaction of H_2O_2 with TiO_2 particles under illumination. Reprinted with permission from Romanias et al. (2012a). Copyright 2012 American Chemical Society.

Gradual surface deactivation was also observed for uptake of H_2O_2 by ATD particles. γ_0, independent of $[H_2O_2]_0$ in the range of (0.18-5.1)×10^{12} molecule cm^{-3} and irradiation for $J(NO_2)$ up to 0.012 s^{-1}, was observed to decrease with RH and temperature (El Zein et al., 2014). At 275 K, the dependence of γ_0 on RH (up to 69%) can be described by (El Zein et al., 2014):

$$\gamma_0 = 4.8 \times 10^{-4}/(1 + RH^{0.66}) \quad (11)$$

At 0.35% RH, the effect of temperature on γ_0 is given by (El Zein et al., 2014):

$$\gamma_0 = 3.2 \times 10^{-4}/[1 + 2.5 \times 10^{10} \times \exp\left(-\frac{7360}{T}\right)] \quad (12)$$

It has also been found that γ_{ss}, independent of RH and T, decreased with $[H_2O_2]_0$ under dark and irradiated conditions, given by (El Zein et al., 2014):

$$\gamma_{ss}(dark) = 3.8 \times 10^{-5} \times ([H_2O_2]_0)^{-0.6} \quad (13)$$

UV irradiation could enhance heterogeneous reactivity of ATD towards H_2O_2. For example, when $J(NO_2)$ was equal to 0.012 s^{-1}, γ_{ss}(dark) and γ_{ss}(UV) were determined to be $(0.95\pm0.30)\times10^{-5}$ and $(1.85\pm0.55)\times10^{-5}$, respectively (El Zein et al., 2014).

Romanias et al. (2013) examined heterogeneous interactions of H_2O_2 with γ-Al_2O_3 and Fe_2O_3, and found that both surfaces were gradually deactivated after exposure to H_2O_2. γ_0, independent of $[H_2O_2]_0$ in the range of $(0.15\text{-}16.6)\times10^{12}$ molecule cm^{-3}, was found to vary with RH and temperature (Romanias et al., 2013). At 280 K, the dependence of γ_0 on RH (up to 73%) can be given by

$$\gamma_0(Al_2O_3) = 1.10 \times 10^{-3}/(1 + RH^{0.93}) \quad (14)$$

$$\gamma_0(Fe_2O_3) = 1.05 \times 10^{-3}/(1 + RH^{0.73}) \quad (15)$$

At 0.3% RH, the dependence of γ_0 on temperature (T) in the range of 268-320 K can be described by:

$$\gamma_0(Al_2O_3) = 8.7 \times 10^{-4}/[1 + 5.0 \times 10^{13} \times \exp(-9700/T)] \quad (16)$$

$$\gamma_0(Fe_2O_3) = 9.3 \times 10^{-4}/[1 + 3.6 \times 10^{14} \times \exp(-10300/T)] \quad (17)$$

In contract to TiO_2 and ATD, no significant effects of UV irradiation with $J(NO_2)$ up to 0.012 s^{-1} were observed for γ-Al_2O_3 and Fe_2O_3 (Romanias et al., 2013).

3.2.1 Discussion of previous laboratory studies

The dependence of $\gamma(H_2O_2)$ on RH, measured at room temperature, is plotted in Figure 8 for different dust particles. Uptake coefficients reported by Zhao et al. (2011b) are several orders of magnitude smaller than those reported by other studies, and therefore they are not included in Figure 8. For studies using dust particles supported on substrates, $\gamma_0(H_2O_2)$ are plotted.

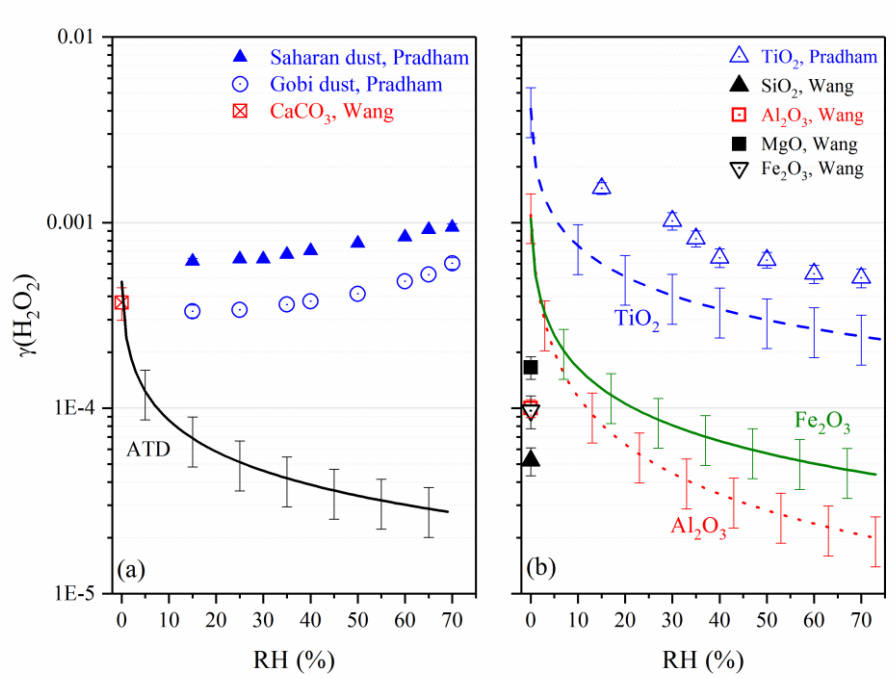

Figure 8. RH dependence of $\gamma(H_2O_2)$ for mineral dust particles as reported by previous studies (Pradhan et al., 2010a; Pradhan et al., 2010b; Wang et al., 2011; Romanias et al., 2012a; Romanias et al., 2013; El Zein et al., 2014).

Figure 8 suggests that different minerals show various heterogeneous reactivity towards H_2O_2, and the effects of RH also appear to be different. Two previous studies have investigated heterogeneous uptake of H_2O_2 by TiO_2 at different RH under dark conditions, one using an aerosol flow tube (Pradhan et al., 2010a) and the other using coated rod flow tube (Romanias et al., 2012a). For TiO_2, $\gamma(H_2O_2)$ reported by Romanias et al. (2012a) are around 40-50% of those determined by Pradhan et al. (2010a) over 10-75% RH. The agreement is quite good considering the fact that two very different techniques were used. Wang et al. (2011) and Romanias (2013) examined heterogeneous reactions of H_2O_2 with Fe_2O_3 and Al_2O_3. Their reported $\gamma_0(H_2O_2)$ differ significantly, though BET surface area was used by both studies to calculate uptake coefficients. This may be largely explained by the variation of interrogation depth of H_2O_2 molecules under investigation in different studies, as discussed in Section 2.2.1.

Experiments in which aerosol samples are used can largely overcome the difficulty in estimating surface area available for heterogeneous uptake. Up to now only two studies (Pradhan et al., 2010a; Pradhan et al., 2010b) used aerosol flow tubes, and more aerosol flow tube studies will help better constrain $\gamma(H_2O_2)$ onto mineral dust particles.

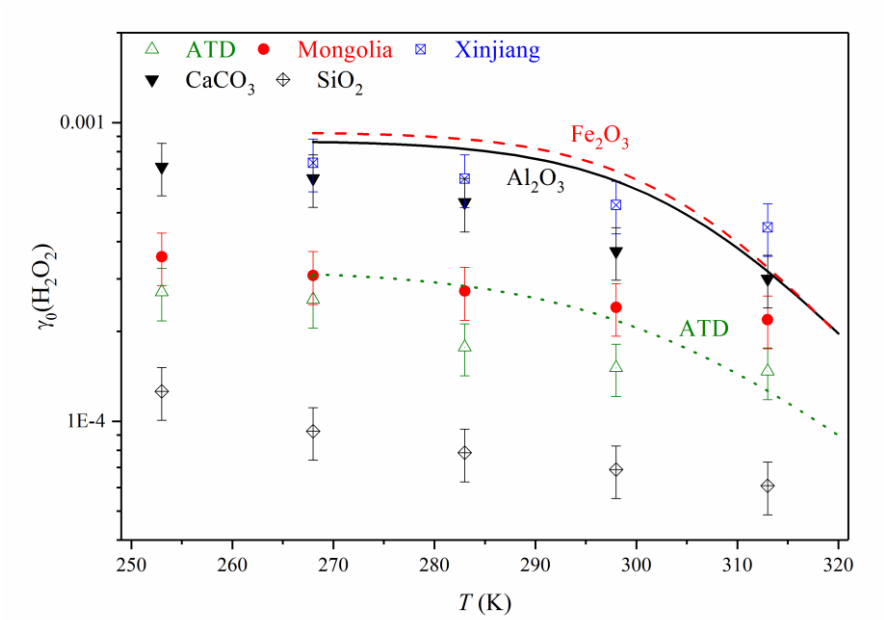

Figure 9. Temperature dependence of $\gamma_0(H_2O_2)$ for mineral dust particles under dark conditions as reported by previous studies. Upward triangles: ATD (Zhou et al., 2016); circles: Inner Mongolia desert dust (Zhou et al., 2016); squares: Xinjiang sierozem (Zhou et al., 2016); downward triangles: $CaCO_3$ (Zhou et al., 2012); diamonds: SiO_2 (Zhou et al., 2012); olive circle: ATD (El Zein et al., 2014); solid black curve: Al_2O_3 (Romanias et al., 2013); dashed red curve: Fe_2O_3 (Romanias et al., 2013).

The effects of temperature on heterogeneous reactions of H_2O_2 with mineral dust have also been explored. As shown in Figure 9, $\gamma_0(H_2O_2)$ decrease with increasing temperature. Zhou et al. (2012, 2016) suggest that $\gamma_0(H_2O_2)$ are reduced by a factor of ~2 for all the five minerals they investigated when temperature increases from 253 K to 313 K. Romanias et al. (2013) and El Zein et al. (2014) reported larger temperature impacts, with $\gamma_0(H_2O_2)$ reduced by a factor of

~4 when temperature increases from 268 to 320 K. These studies show that the temperature effect is significant and should be taken into account when assessing the importance of heterogeneous uptake of H_2O_2 by mineral dust in the troposphere. It should also be pointed out that the effect of temperature on heterogeneous reactions of H_2O_2 with airborne mineral dust particles has never been investigated.

In addition, it has been suggested that uptake of H_2O_2 by mineral dust can affect heterogeneous oxidation of other trace gases (Zhao et al., 2011b; Zhao et al., 2013; Huang et al., 2015a). For examples, heterogeneous uptake of H_2O_2 could convert sulfite formed by the adsorption of SO_2 on $CaCO_3$ particles to sulfate, and this conversion is enhanced by adsorbed water (Zhao et al., 2013). Similarly, Huang et al. (2015a) found that the presence of H_2O_2 could enhance the uptake of SO_2 on Asian mineral dust, Tengger desert dust, and ATD, and the enhancement factors, varying with dust mineralogy and RH, can be as large as a factor of ~6. Heterogeneous oxidation of methacrolein on kaolinite, α-Al_2O_3, α-Fe_2O_3, and TiO_2 (but not on $CaCO_3$) is largely accelerated by the presence of H_2O_2, which also changes the oxidation products (Zhao et al., 2014).

3.2.2 Atmospheric implication

For reasons we have discussed in Section 2.2.1, $\gamma(H_2O_2)$ reported by studies using aerosol samples (Pradhan et al., 2010a; Pradhan et al., 2010b) are preferred. Since Saharan dust is the most abundant mineral dust particles in the troposphere, in our work we use $\gamma(H_2O_2)$ reported by Pradhan et al. (2010b) for Saharan dust to assess the atmospheric importance of heterogeneous uptake of H_2O_2. $\gamma(H_2O_2)$ onto Saharan dust depends on RH, increasing from 6.2×10^{-4} at 15% to 9.4×10^{-4} at 70% RH. For simplicity, a $\gamma(H_2O_2)$ value of 1×10^{-3}, very close to that at 70%, is used here to calculate $\tau_{het}(H_2O_2)$. When dust mass concentrations are 10, 100, and 1000 μg m^{-3}, $\tau_{het}(H_2O_2)$ are calculated to be 120, 12, and 1.2 h, using Eq. (6). Typical $\tau(H_2O_2)$ are estimated to be 33-56 h with respect to photolysis and 16-160 h with respect to

reaction with OH radicals. Therefore, heterogeneous uptake by mineral dust particles can be a significant sink for H_2O_2 when dust mass concertation is as low as 10 μg m^{-3}.

Several modelling studies have also discussed and evaluated the contribution of heterogeneous uptake by mineral dust to the removal of H_2O_2 in the troposphere. Pradhan et al. (2010b) determined $\gamma(H_2O_2)$ for Saharan dust as a function of RH experimentally and then included this reaction in a box model based on the MCM. It has been found that heterogeneous uptake by mineral dust could reduce simulated H_2O_2 concentrations by up to ~40%, and its impacts on total peroxy organic radicals, OH, O_3, and NOx are small but non-negligible (Pradhan et al., 2010b). In another box model study, $\gamma(H_2O_2)$ onto Saharan dust was varied in order to reproduce H_2O_2 concentrations measured in July/August 2002 at Tenerife (de Reus et al., 2005). It is found that using $\gamma(H_2O_2)$ of 5×10^{-4}, which agrees very well with these measured by Pradhan et al. (2010b), could reach the best agreement between measured and simulated H_2O_2 concentrations (de Reus et al., 2005).

In addition to the uncertainties in $\gamma(H_2O_2)$ related to the effects of mineralogy, RH, and temperature, products formed in heterogeneous reactions of H_2O_2 with mineral dust are not entirely clear. Three pathways have been proposed, including i) simple partitioning of H_2O_2 onto dust particles (Zhao et al., 2011b; Zhao et al., 2013), ii) surface decomposition of H_2O_2 to H_2O and O_2, and iii) heterogeneous conversion of H_2O_2 to HO_2 radicals (Romanias et al., 2012a; Yi et al., 2012). Branching ratios seem to depend on mineralogy, RH, and probably also UV illumination (Zhao et al., 2011b; Yi et al., 2012; Zhao et al., 2013); however, our knowledge in this aspect is very limited. Since these three different pathways may have very different impacts on tropospheric oxidation capacity, product distribution in heterogeneous reactions of H_2O_2 with mineral dust deserves further investigation.

3.3 O_3

Heterogeneous reactions of O_3 with Al_2O_3, $CaCO_3$, and Saharan dust were explored using a fluidized bed reactor more than two decades ago, and substantial O_3 decays were observed after interactions with dust power in the reactor (Alebić-Juretić et al., 1992). This study did not report uptake coefficients and thus is not included in Table 4. Uptake coefficients in the range of $(1\text{-}100)\times10^{-11}$ were reported for Al_2O_3 (Hanning-Lee et al., 1996). Since their experiments were carried out with O_3 concentrations in the range of $(5\text{-}200)\times10^{15}$ molecule cm^{-3} which are several orders of magnitude higher than typical O_3 levels in the troposphere, this work is also not included in Table 4.

A Knudsen cell reactor was used by Grassian and co-workers (Michel et al., 2002; Michel et al., 2003; Usher et al., 2003b) to study heterogeneous reactions of O_3 with fresh and aged mineral dust particles. Measurements were carried out in the linear mass dependent regime (see Section 2.2.1 for more explanations of the linear mass dependent regime), and thus the BET surface areas of dust samples were used to calculate uptake coefficients. In the first study (Michel et al., 2002), $\gamma_0(O_3)$ was determined to be $(1.8\pm0.7)\times10^{-4}$ for α-Fe_2O_3, $(8\pm5)\times10^{-5}$ for α-Al_2O_3, $(5\pm3)\times10^{-5}$ for SiO_2, $(2.7\pm0.9)\times10^{-5}$ for China loess, $(6\pm3)\times10^{-5}$ for ground Saharan dust, and $(4\pm2)\times10^{-6}$ for sieved Saharan dust at 296 K when $[O_3]_0$ was 1.9×10^{11} molecule cm^{-3}. In a following study, Michal et al. (2003) systematically investigated heterogeneous reactions of O_3 with several mineral dust particles, and progressive surface deactivation was observed for all the dust samples. At 295±1 K and $[O_3]_0$ of $(1.9\pm0.6)\times10^{11}$ molecule cm^{-3}, $\gamma_0(O_3)$ were reported to be $(2.0\pm0.3)\times10^{-4}$ for α-Fe_2O_3, $(1.2\pm0.4)\times10^{-4}$ for 25 μm α-Al_2O_3, $(6.3\pm0.9)\times10^{-5}$ for SiO_2, $(3\pm1)\times10^{-5}$ for kaolinite, $(2.7\pm0.8)\times10^{-5}$ for China loess, $(6\pm2)\times10^{-5}$ for ground Saharan dust, and $(2.7\pm0.9)\times10^{-6}$ for ground Saharan dust, respectively. $\gamma_0(O_3)$ was also measured for 1 μm α-Al_2O_3, and with the experimental uncertainties it shows no difference with that for 25 μm α-Al_2O_3. The steady-state uptake coefficients, γ_{ss}, were

determined to be 2.2×10^{-5} for α-Fe_2O_3, 7.6×10^{-6} for α-Al_2O_3, and 6×10^{-6} for ground Saharan dust. The effect of initial O_3 concentration in the range of $(1\text{-}10)\times10^{11}$ molecule cm^{-3} on $\gamma_0(O_3)$ is insignificant for either α-Al_2O_3 or α-Fe_2O_3. In addition, $\gamma_0(O_3)$ was found to have a very weak dependence on temperature (250-330 K) for α-Al_2O_3, with an activation energy of 7±4 kJ mol^{-1} (Michel et al., 2003).

Heterogeneous processing of mineral dust particles by other trace gases could affect O_3 uptake. It has been observed that $\gamma_0(O_3)$ was reduced by ~70% after pretreatment of α-Al_2O_3 with HNO_3 and increased by 33% after pretreatment with SO_2 (Usher et al., 2003b). Similarly, functionalization of SiO_2 with a C8 alkene would increase its heterogeneous reactivity towards O_3 by 40% whereas its heterogeneous reactivity was reduced by about 40% if functionalized by a C8 alkane (Usher et al., 2003b). The presence of O_3 can also promote heterogeneous oxidation of other trace gases on mineral dust surface (Ullerstam et al., 2002; Hanisch and Crowley, 2003b; Li et al., 2006; Chen et al., 2008; Wu et al., 2011), including NO, SO_2, methacrolein, methyl vinyl ketone, and etc.

Table 6: Summary of previous laboratory studies on heterogeneous reactions of mineral dust with O_3

Dust	Reference	T (K)	Concentration (molecule cm^{-3})	Uptake coefficient	Techniques
Al_2O_3	Michel et al., 2002	296	1.9×10^{11}	γ_0: $(8\pm5)\times10^{-5}$	KC-MS
	Michel et al., 2003	250-330	$(1\text{-}10)\times10^{11}$	At 296 K, γ_0 was determined to be $(1.2\pm0.4)\times10^{-4}$ and γ_{ss} was determined to be 7.6×10^{-6}. A very weak temperature dependence was observed.	KC-MS
	Usher et al., 2003b	295±1	1.9×10^{11}	Compared to fresh particles, γ_0 were reduced by 72% to $(3.4\pm0.6)\times10^{-5}$ when the surface coverage of HNO_3 was $(6\pm3)\times10^{14}$ molecule cm^{-2} and increased by 33% to $(1.6\pm0.2)\times10^{-4}$ when the surface coverage of SO_2 was $(1.5\pm0.3)\times10^{14}$ molecule cm^{-2}.	KC-MS
	Sullivan et al., 2004	room temperature	$(1\text{-}10)\times10^{13}$	$\gamma(O_3)$ decreased from $\sim1\times10^{-5}$ to $\sim1\times10^{-6}$ when initial O_3 concentration increased from 1×10^{13} to 1×10^{14} molecule cm^{-3}.	static reactor
	Mogili et al., 2006a	room temperature	1×10^{15}	$\gamma(O_3)$ decreased from $(3.5\pm0.9)\times10^{-8}$ at <1% RH to $(4.5\pm1.1)\times10^{-9}$ at 19% RH.	EC
	Chen et al., 2011a	room temperature	$\sim1.9\times10^{15}$	Irradiation from a solar simulation could enhance O_3 uptake by α-Al_2O_3, but no uptake coefficient was reported.	EC
	Chen et al., 2011b	room temperature	$(2\text{-}3)\times10^{15}$	Uptake of O_3 by α-Al_2O_3 was insignificant under both dark and irradiated conditions.	EC

Saharan dust	Michel et al., 2002	296	1.9×10^{11}	γ_0 was determined to be $(6\pm3)\times10^{-5}$ for ground Saharan dust and $(4\pm2)\times10^{-6}$ for sieved Saharan dust.	KC-MS
	Hanisch and Crowley, 2003	296	$(0.54\text{-}84)\times10^{11}$	$\gamma_0 = 3.5\times10^{-4}$ and $\gamma_{ss} = 4.8\times10^{-5}$ when $[O_3]_0 = 5.4\times10^{10}$ molecule cm^{-3}; $\gamma_0 = 5.8\times10^{-5}$ and $\gamma_{ss} = 1.3\times10^{-5}$ when $[O_3]_0 = 2.8\times10^{11}$ molecule cm^{-3}; $\gamma_0 = 5.5\times10^{-6}$ and $\gamma_{ss} = 2.2\times10^{-6}$ when $[O_3]_0 = 8.4\times10^{12}$ molecule cm^{-3}.	KC-MS
	Michel et al., 2003	295±1	$(1.9\pm0.6)\times10^{11}$	For ground Saharan dust, γ_0: $(6\pm2)\times10^{-5}$ and γ_{ss}: 6×10^{-6}. For sieved Saharan dust, γ_0: $(2.7\pm0.9)\times10^{-6}$.	KC-MS
	Chang et al., 2005	room temperature	$(0.2\text{-}10)\times10^{13}$	$\gamma(O_3)$ decreased from 6×10^{-6} to ~2×10^{-7} when $[O_3]$ increased from 2×10^{12} to 1×10^{14} molecule cm^{-3}.	static reactor
	Karagulian and Rossi, 2006	298±2	$(3.5\text{-}10)\times10^{12}$	$\gamma_0 = (9.3\pm2.6)\times10^{-2}$ and $\gamma_{ss} = (6.7\pm1.3)\times10^{-3}$ when $[O_3]_0 = 3.5\times10^{12}$ molecule cm^{-3}; $\gamma_0 = (3.7\pm1.8)\times10^{-3}$ and $\gamma_{ss} = (3.3\pm2.5)\times10^{-3}$ when $[O_3]_0 = 1.0\times10^{13}$ molecule cm^{-3}. Reported uptake coefficients were based on the projected surface area.	KC-MS
Fe_2O_3	Michel et al., 2002	296	1.9×10^{11}	γ_0: $(1.8\pm0.7)\times10^{-4}$	KC-MS
	Michel et al., 2003	295±1	$(1\text{-}10)\times10^{11}$	γ_0: $(2.0\pm0.3)\times10^{-4}$; γ_{ss}: 2.2×10^{-5}	KC-MS
	Mogili et al., 2006a	room temperature	$(1.8\text{-}8.5)\times10^{14}$	When $[O_3]_0$ was 7.9×10^{14} molecule cm^{-3}, $\gamma(O_3)$ decreased from $(1.0\pm0.3)\times10^{-7}$ at <1% RH to $(1.2\pm0.3)\times10^{-8}$ at 23% RH and to $(2.5\pm0.6)\times10^{-9}$ at 58% RH. When $[O_3]_0$ was 2.1×10^{14} molecule cm^{-3},	EC

				$\gamma(O_3)$ decreased from $(5.0\pm1.2)\times10^{-8}$ at <1% RH to $(2.0\pm0.5)\times10^{-8}$ at 21% RH and to $(9.0\pm2.3)\times10^{-9}$ at 43% RH.	
	Chen et al., 2011a	room temperature	$\sim1.9\times10^{15}$	Irradiation from a solar simulation could enhance the O_3 uptake by α-Fe_2O_3, but no uptake coefficient was reported.	EC
	Chen et al., 2011b	room temperature	$(2\text{-}3)\times10^{15}$	Under dark conditions, $\gamma(O_3)$ decreased from $(4.1\pm0.2)\times10^{-7}$ at <2% RH to $(2.7\pm0.1)\times10^{-7}$ at 21% RH. When irradiated, $\gamma(O_3)$ decreased from $(6.6\pm0.3)\times10^{-7}$ at <2% RH to $(5.5\pm0.3)\times10^{-7}$ at 12% RH and to $(1.1\pm0.1)\times10^{-7}$ at 25% RH.	EC
SiO_2	Michel et al., 2002	296	1.9×10^{11}	γ_0: $(5\pm3)\times10^{-5}$	KC-MS
	Michel et al., 2003	295±1	$(1.9\pm0.6)\times10^{11}$	γ_0: $(6.3\pm0.9)\times10^{-5}$	KC-MS
	Usher et al., 2003b	295±1	1.9×10^{11}	Compared to fresh particles, γ_0 was increased by 40% to $(7\pm2)\times10^{-5}$ when the surface coverage of a C8 alkene was $(2\pm1)\times10^{14}$ molecule cm^{-2} and reduced by 40% to $(3\pm1)\times10^{-5}$ when the surface coverage of a C8 alkane was $(2\pm1)\times10^{14}$ molecule cm^{-2}.	KC-MS
	Nicolas et al., 2009	298	$(1.3\text{-}7.3)\times10^{12}$	$\gamma(O_3)$ was found to be $<1\times10^{-8}$, showing negative dependence on $[O_3]_0$ and RH. No difference in $\gamma(O_3)$ under dark and illuminated conditions was reported.	CWFT
China loess	Michel et al., 2002	296	1.9×10^{11}	γ_0: $(2.7\pm0.9)\times10^{-5}$	KC-MS
	Michel et al., 2003	295±1	$(1.9\pm0.6)\times10^{11}$	γ_0: $(2.7\pm0.8)\times10^{-5}$	KC-MS

kaolinite	Michel et al., 2003	295±1	$(1.9\pm0.6)\times10^{11}$	γ_0: $(3\pm1)\times10^{-5}$	KC-MS
	Karagulian and Rossi, 2006	298±2	$(2.4\pm0.7)\times10^{12}$	Projected surface area based: γ_0 = $(6.3\pm0.2)\times10^{-2}$ and γ_{ss} = $(1.0\pm0.2)\times10^{-2}$; pore diffusion corrected γ_{ss}: $(2.7\pm0.3)\times10^{-6}$.	KC-MS
$CaCO_3$	Karagulian and Rossi, 2006	298±2	$(5.3\pm0.7)\times10^{12}$	Projected surface area based: γ_0 = $(1.2\pm0.3)\times10^{-2}$ and γ_{ss} = $(3.6\pm0.2)\times10^{-3}$; pore diffusion corrected γ_{ss}: $(7.8\pm0.7)\times10^{-7}$.	KC-MS
TiO_2	Nicolas et al., 2009	298	$(1.3\text{-}7.3)\times10^{12}$	$\gamma(O_3)$ on TiO_2/SiO_2 decreased with $[O_3]_0$ and RH under both dark and illuminated conditions. Under illuminated conditions it increased with TiO_2 mass fraction in TiO_2/SiO_2 and depended almost linearly on irradiance intensity. At 24% RH and $[O_3]_0$ of 51 ppbv, $\gamma(O_3)$ on 1 wt% TiO_2/SiO_2 was reported to be $(2.8\pm0.4)\times10^{-9}$ under dark conditions and $(4.7\pm0.7)\times10^{-8}$ under a near UV irradiance of 3.2×10^{-8} mW cm^{-2}.	CWFT
	Chen et al., 2011b	room temperature	$(2\text{-}3)\times10^{15}$	Uptake of O_3 was negligible under dark conditions. Under the irradiation of a solar simulator, $\gamma(O_3)$ was determined to be $(2.0\pm0.1)\times10^{-7}$ at <2% RH, $(2.2\pm0.1)\times10^{-7}$ at 12% RH, $(2.4\pm0.1)\times10^{-7}$ at 22% RH, and $(1.9\pm0.1)\times10^{-7}$ at 39% RH, respectively.	EC
ATD	Karagulian and Rossi, 2006	298±2	$(3.3\text{-}8.0)\times10^{12}$	γ_0 = $(1.3\pm0.6)\times10^{-2}$ and γ_{ss} = $(2.2\pm1.2)\times10^{-3}$ when $[O_3]_0$= 3.3×10^{12} molecule cm^{-3}; γ_0 = $(1.3\pm0.7)\times10^{-2}$ and γ_{ss} = $(2.5\pm1.2)\times10^{-3}$ when $[O_3]_0$= 8×10^{12} molecule cm^{-3}. Reported uptake coefficients were based on the projected surface area.	KC-MS

limestone	Karagulian and Rossi, 2006	298±2	(3-20)×10^{12}	γ_0 = (1.3±0.2)×10^{-2} and γ_{ss} = (1.6±0.5)×10^{-3} when $[O_3]_0$= 3×10^{12} molecule cm^{-3}; γ_0 = (2.1±0.3)×10^{-3} and γ_{ss} = (2.4±0.7)×10^{-4} when $[O_3]_0$= 2×10^{13} molecule cm^{-3}. Reported uptake coefficients were based on the projected surface area.	KC-MS

Another two groups also utilized Knudsen cell reactors to investigate O_3 uptake by mineral dust (Hanisch and Crowley, 2003a; Karagulian and Rossi, 2006). The uptake of O_3 by Saharan dust was investigated over a broad range of $[O_3]_0$ by Hanisch and Crowley (2003), and $\gamma_0(O_3)$ and $\gamma_{ss}(O_3)$ were determined to be 3.5×10^{-4} and 4.8×10^{-5} when $[O_3]_0$ was $(5.4\pm0.8)\times10^{10}$ molecule cm^{-3}, 5.8×10^{-5} and 1.3×10^{-5} when $[O_3]_0$ was 2.8×10^{11} molecule cm^{-3}, and 5.5×10^{-6} and 2.2×10^{-4} when $[O_3]_0$ was $(8.4\pm3.4)\times10^{12}$ molecule cm^{-3}, showing a negative dependence on $[O_3]_0$. It should be noted that the KML model (Keyser et al., 1991; Keyser et al., 1993) was applied by Hanisch and Crowley (2003) to derive the uptake coefficients. Furthermore, they found that O_3 was converted to O_2 after reaction with Saharan dust and physisorption was negligible (Hanisch and Crowley, 2003a).

Karagulian and Rossi et al. (2006) investigated heterogeneous interactions of O_3 with kaolinite, $CaCO_3$, natural limestone, Saharan dust, and ATD. Based on the projected surface areas of dust samples, their reported γ_0 are in the range of $(2.3\pm0.4)\times10^{-2}$ to $(9.3\pm2.6)\times10^{-2}$ and γ_{ss} are in the range of $(3.5\pm1.6)\times10^{-5}$ to $(1.0\pm0.2)\times10^{-2}$. These values, summarized in Table 4 together with corresponding $[O_3]_0$, are not repeated here. Pore diffusion corrected γ_{ss} were reported to be $(2.7\pm0.3)\times10^{-6}$ for kaolinite when $[O_3]_0$ was 2.4×10^{12} molecule cm^{-3} and $(7.8\pm0.7)\times10^{-7}$ for $CaCO_3$ when $[O_3]_0$ was 5.3×10^{12} molecule cm^{-3}, more than three orders of magnitude smaller than those based on the projected surface area (Karagulian and Rossi, 2006).

The uptake of O_3 on α-Al_2O_3 (Sullivan et al., 2004) and Saharan dust (Chang et al., 2005) was investigated using a static reactor, in which a dust-coated Pyrex tube was exposed to O_3 at room temperature. In the first few tens of seconds after exposure to dust particles, O_3 decays followed an exponential manner, and the average decay rates were used to derive uptake coefficients. $\gamma(O_3)$, based on the BET surface area, was found to decrease with increasing initial $[O_3]$. For α-Al_2O_3, $\gamma(O_3)$ decreased from $\sim1\times10^{-5}$ to $\sim1\times10^{-6}$ when $[O_3]$ increased from 1×10^{13} to 1×10^{14} molecule cm^{-3} (Sullivan et al., 2004). For Saharan dust, $\gamma(O_3)$ decreased from 2×10^{-7}

to 2×10^{-6} for Saharan dust when $[O_3]$ increased from 2×10^{12} to 1×10^{14} molecule cm^{-3}, and the dependence of $\gamma(O_3)$ on $[O_3]$ can be described by Eq. (18) (Chang et al., 2005):

$$\gamma(O_3) = 7.5 \times 10^5 \times [O_3]^{-0.90} \quad (18)$$

where $[O_3]$ is the O_3 concentration in molecule cm^{-3}. No significant effect of RH (0-75%) on uptake kinetics was observed for α-Al_2O_3 and Saharan dust (Sullivan et al., 2004; Chang et al., 2005).

An environmental chamber in which O_3 was exposed to suspended particles was deployed to investigate heterogeneous reactions of airborne mineral dust with O_3 under dark and illuminated conditions (Mogili et al., 2006a; Chen et al., 2011a; Chen et al., 2011b). O_3 concentrations in the chamber, detected using FTIR or UV/Vis absorption spectroscopy, were found to decay exponentially with reaction time. As shown in Figure 10, uptake of O_3 by α-Fe_2O_3 was significantly suppressed at increasing RH, and a negative effect of RH was also observed for uptake of O_3 by α-Al_2O_3 (Mogili et al., 2006a). In addition, increasing $[O_3]_0$ resulted in reduction in $\gamma(O_3)$ for both minerals. Heterogeneous reactivity towards O_3 under similar conditions is higher for α-Fe_2O_3 when compared to α-Al_2O_3 (Mogili et al., 2006a). For α-Fe_2O_3, when $[O_3]_0$ was 7.9×10^{14} molecule cm^{-3}, $\gamma(O_3)$ decreased from $(1.0\pm0.3)\times10^{-7}$ at <1% RH to $(1.2\pm0.3)\times10^{-8}$ at 23% RH and to $(2.5\pm0.6)\times10^{-9}$ at 58% RH; when $[O_3]_0$ was 2.1×10^{14} molecule cm^{-3}, $\gamma(O_3)$ was reduced from $(5.0\pm1.2)\times10^{-8}$ at <1% RH to $(2.0\pm0.5)\times10^{-8}$ at 21% RH and to $(9.0\pm2.3)\times10^{-9}$ at 43% RH. Meanwhile, $\gamma(O_3)$ was observed to decrease from $(3.5\pm0.9)\times10^{-8}$ at <1% RH to $(4.5\pm1.1)\times10^{-9}$ at 19% RH for α-Al_2O_3 when $[O_3]_0$ was 1×10^{15} molecule cm^{-3}.

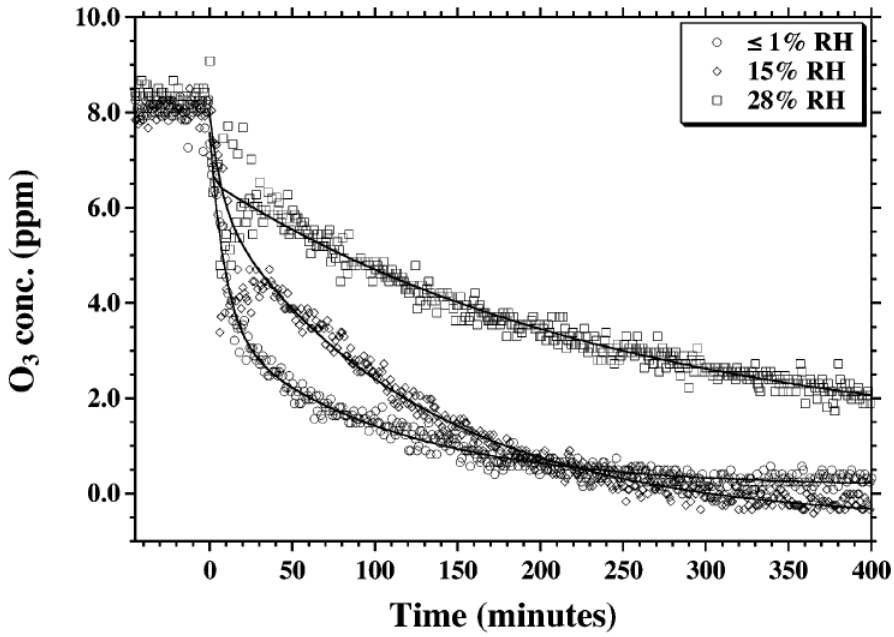

Figure 10. Measured O_3 decays in an aerosol chamber due to interaction with airborne α-Fe_2O_3 particles (starting at 0 min). The solid curves represent exponential fits to the measured O_3 concentrations as a function of reaction time. Reprinted with permission from Mogili et al. (2006b). Copyright 2006 American Chemical Society.

A solar simulator was coupled to the environmental chamber by Chen et al. (2011a), and irradiation from the solar simulator was found to enhance heterogeneous uptake of O_3 by α-Fe_2O_3 and α-Al_2O_3; however, no uptake coefficient was reported. In a following study, Chen et al. (2011b) found that heterogeneous uptake of O_3 by α-Al_2O_3 was insignificant under both dark and irradiated conditions. In contract, while the uptake of O_3 by TiO_2 was negligible under dark conditions, when irradiated $\gamma(O_3)$ was determined to be $(2.0\pm0.1)\times10^{-7}$ at <2% RH, $(2.2\pm0.1)\times10^{-7}$ at 12% RH, $(2.4\pm0.1)\times10^{-7}$ at 22% RH, and $(1.9\pm0.1)\times10^{-7}$ at 39% RH, respectively (Chen et al., 2011b). Photo-enhanced O_3 uptake was also observed for α-Fe_2O_3 (Chen et al., 2011b). Under dark conditions $\gamma(O_3)$ decreased from $(4.1\pm0.2)\times10^{-7}$ at <2% RH to $(2.7\pm0.1)\times10^{-7}$ at 21% RH, while when irradiated $\gamma(O_3)$ was reported to be $(6.6\pm0.3)\times10^{-7}$ at <2% RH, $(5.5\pm0.3)\times10^{-7}$ at 12% RH, and $(1.1\pm0.1)\times10^{-7}$ at 25% RH, respectively.

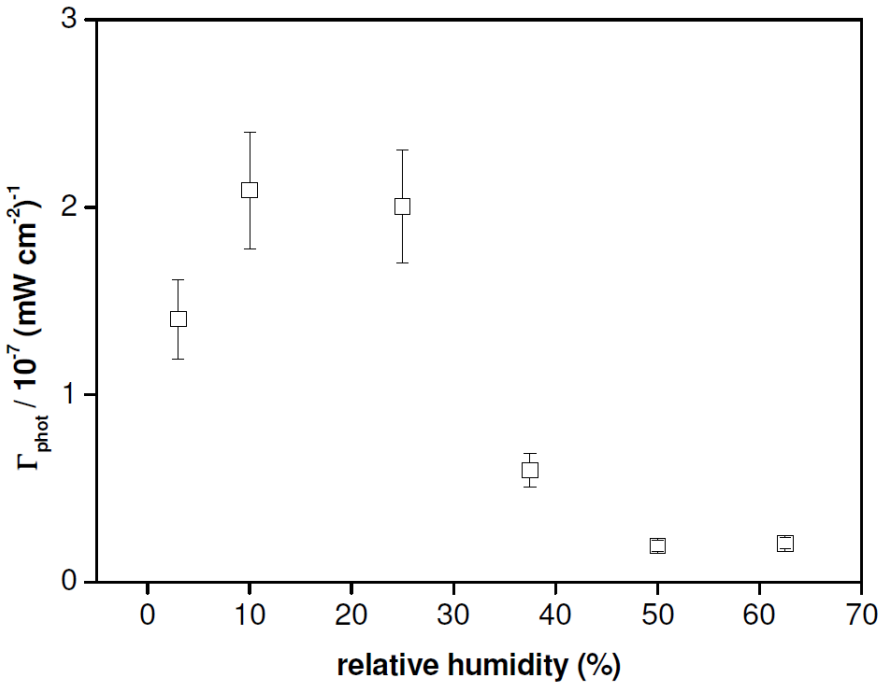

Figure 11. Effects of RH on the irradiance-normalized O_3 uptake coefficients. The TiO_2/SiO_2 films which contained 1 wt% TiO_2 were exposed to 37 ppbv O_3 at 298 K under irradiance of 2.7×10^{14} photons cm^{-2} s^{-1}. Reprinted with permission from Nicolas et al. (2009). Copyright 2009 American Chemical Society.

Photo-enhanced catalytic decomposition of O_3 on mineral dust was in fact first reported by a coated wall flow tube study at 298 K (Nicolas et al., 2009). Under their experimental conditions ($[O_3]_0$: 50-290 ppbv; RH: 3-60%), the BET surface area based $\gamma_{ss}(O_3)$, was found to be $<1\times10^{-8}$ for SiO_2 and TiO_2/SiO_2 mixture with TiO_2 mass fraction up to 5% under dark conditions. Near UV irradiation could largely increase the uptake of O_3 by TiO_2/SiO_2 mixture, and the effect increased with the TiO_2 mass fraction (the effect is insignificant for pure SiO_2) and almost depended linearly on the intensity of UV irradiance (Nicolas et al., 2009). When RH was 24% and $[O_3]_0$ was 51 ppbv, $\gamma(O_3)$ for TiO_2/SiO_2 mixture with a TiO_2 mass fraction of 1% was measured to be $(2.8\pm0.4)\times10^{-9}$ under dark conditions and $(4.7\pm0.7)\times10^{-8}$ under near UV irradiation of 3.0×10^{-8} mW cm^{-2}. RH was found to play a profound role in heterogeneous

photochemical reaction of O_3 with TiO_2/SiO_2. Figure 11 shows that the irradiance-normalized uptake coefficient, defined as the uptake coefficient divided by the irradiance intensity, increased with RH for RH <20% and then decreased significantly with RH when RH was further increased. This phenomenon was also observed by Chen et al. (2011b), who found that under illuminated conditions $\gamma(O_3)$ first increased and then decreased with RH for TiO_2 aerosol particles.

Heterogeneous uptake of O_3 may lead to oxidation of organic materials coated on mineral dust particles. Gligorovski and coworkers extensively investigated heterogeneous ozonation of aromatic compounds adsorbed on silica particles used as a proxy of mineral dust particles in the atmosphere (Net et al., 2009; Net et al., 2010a; Net et al., 2010b; Net et al., 2010c; Net et al., 2010d; Net et al., 2011). For example, compared to dark conditions, loss of veratraldehyde coated on silica particles due to heterogeneous ozonolysis was increased under exposure to light (Net et al., 2010b). Heterogeneous reactivity of 4-phenoxyphenol towards ozone was significantly enhanced in the presence of aromatic ketones (4-carboxybenzophenone) under light irradiation as compared to dark ozone reaction (Net et al., 2010d). This photosensitized reaction proceeds through the electron transfer reaction to ozone with formation of an ozonide anion (O_3^-) which can further react to produce OH radicals (De Laurentiis et al., 2013), and the formation of OH radicals was confirmed during such photochemical processing on the silica particles. The same group (Net et al., 2009) proposed a comprehensive reaction mechanism based on identified products arising from the OH-addition to 4-phenoxyphenol. The phenoxyl radicals were proposed as a key intermediate which may react with OH radicals, producing hydroquinone, catechol or other polyhydroxylated benzenes. The phenoxyl radicals are also responsible for the formation of oligomers by adding to another 4-phenoxyphenol molecule. Heterogeneous ozonolysis of phenols and methoxyphenols adsorbed on mineral oxide surface is substantially impacted by sunlight irradiation. These

photosensitized processes may play important roles in many issues, such as adverse health effects of inhaled particles and formation of secondary organic aerosols.

3.3.1 Discussion

All the initial $\gamma(O_3)$ reported by previous studies for different minerals are summarized in Figure 12 as a function of $[O_3]$. Karagulian and Rossi (2006) reported projected area based $\gamma_0(O_3)$, which are several orders of magnitude larger than values reported by other work. This is because O_3 uptake by mineral dust is relatively slow and some underlying dust layers, if not all, must be accessible by O_3 molecules. Therefore, results reported by Karagulian and Rossi (2006) are not included in Figure 12. Sullivan et al. (2004) and Chang et al. (2005) measured O_3 decay rates in the first tens of seconds due to interaction with dust particles deposited onto the inner wall of a Pyrex tube to derive $\gamma(O_3)$. Their reported $\gamma(O_3)$ are in fact the average uptake coefficients in the first tens of seconds, and can be classified as either $\gamma_0(O_3)$ and $\gamma_{ss}(O_3)$. Therefore, $\gamma(O_3)$ reported by Sullivan et al. (2004) and Chang et al. (2005) are included in Figure 12 which summarizes $\gamma_0(O_3)$ and also in Figure 13 which summarizes $\gamma_{ss}(O_3)$.

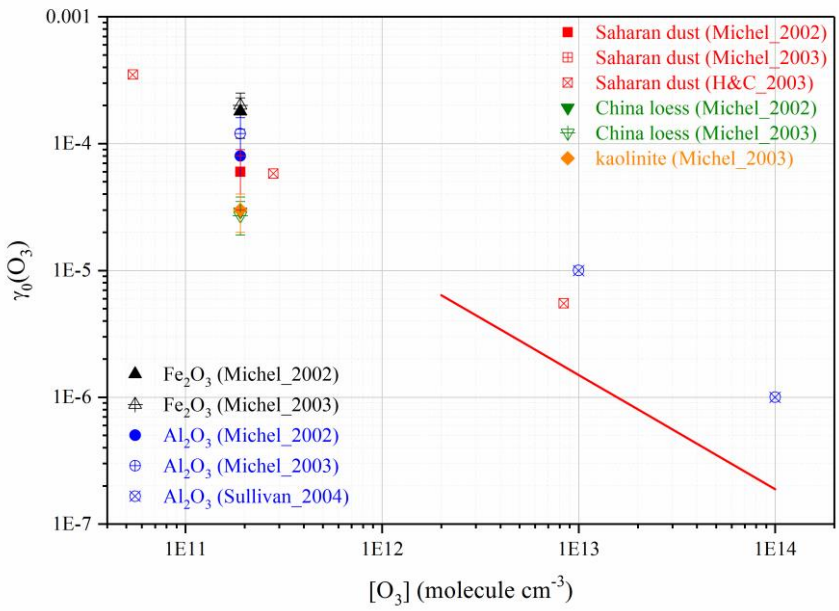

Figure 12. Dependence of $\gamma_0(O_3)$ on initial O_3 concentrations under dry conditions for different mineral dust particles as reported by previous studies: Michel_2002 (Michel et al., 2002),

Michel_2003 (Michel et al., 2003), H&C_2003 (Hanisch and Crowley, 2003a), Sullivan_2004 (Sullivan et al., 2004). The red curve represents the dependence of $\gamma(O_3)$ on $[O_3]$ for Saharan dust reported by Chang et al. (2005). Both O_3 concentrations and $\gamma(O_3)$ are plotted on the logarithm scale because their values span over a few orders of magnitude.

It should be noted that all the studies included in Figure 12 used dust powder samples supported on substrates. Significant variation in reported $\gamma_0(O_3)$ is evident from Figure 12. For examples, $\gamma_0(O_3)$ determined at $[O_3]$ of ~2×10^{11} molecule cm^{-3} are differed by a factor of ~10. The observed difference in $\gamma_0(O_3)$ may be caused by 1) variability in heterogeneous reactivity of different minerals and 2) that different experimental methods can lead to different results. For example, it has been suggested that pretreatment of mineral dust particles (e.g., heating, grounding, and evacuation) could modify their initial heterogeneous reactivity towards O_3 (Hanisch and Crowley, 2003a; Michel et al., 2003). Furthermore, as discussed in Section 2.2, time resolution in different studies is also different, making interpretation of γ_0 difficult.

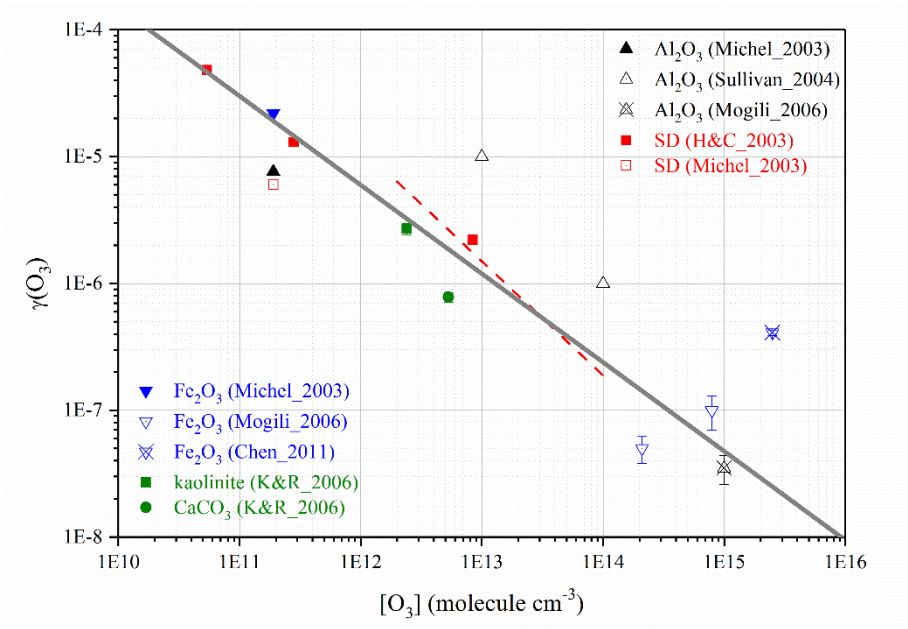

Figure 13. Dependence of $\gamma_{ss}(O_3)$ on initial O_3 concentrations under dry conditions for different mineral dust particles: Michel_2003 (Michel et al., 2003), H&C_2003 (Hanisch and Crowley,

2003a), Sullivan_2004 (Sullivan et al., 2004), Mogili_2006 (Mogili et al., 2006a), K&R_2006 (Karagulian and Rossi, 2006), and Chen_2011 (Chen et al., 2011b). The red dashed curve represents the dependence of $\gamma(O_3)$ on $[O_3]$ for Saharan dust reported by Chang et al. (2005), and the grey solid curve represents the dependence of $\gamma(O_3)$ on $[O_3]$ for mineral dust particles recommended by the IUPAC Task Group on Atmospheric Chemical Kinetic Data Evaluation. Reprinted (with modification) with permission from the IUPAC Task Group on Atmospheric Chemical Kinetic Data Evaluation ((http://iupac.pole-ether.fr).

In contrast, $\gamma_{ss}(O_3)$ reported by previous studies under dry conditions show fairly good agreement (as displayed in Figure 13), considering the fact that very different experimental techniques have been used (for example, aerosol samples were used by Mogili et al. (2006b) and Chen et al. (2011b) while all the other studies used dust powder samples supported on substrates). In addition, a rather strong dependence of $\gamma_{ss}(O_3)$ on initial O_3 concentration can be observed. Eq. (19) has been recommended by the IUPAC task group on Atmospheric Chemical Kinetic Data Evaluation to parameterize the dependence of $\gamma_{ss}(O_3)$ on $[O_3]$ (Crowley et al., 2010a):

$$\gamma(O_3) = 1500 \times [O_3]^{-0.7} \quad (19)$$

where $[O_3]$ is O_3 concentration in molecule cm^{-3}. It is quite surprising that $\gamma_{ss}(O_3)$ under dry conditions are very similar for all the minerals investigated. It can also been observed from Figure 13 that $\gamma_{ss}(O_3)$ for α-Al_2O_3 reported by Sullivan et al. (2004) and for α-Fe_2O_3 reported by Chen et al. (2011b) may be significantly larger than those recommended by Crowley et al. (2010), and the reason is not very clear yet. It should be pointed out that the work by Sullivan et al. (2005), though published, was not included in the original figure prepared by the IUPAC Task Group. In addition, the work by Chen et al. (2011b) was published after the IUACP report was released online.

Only three previous studies have explored effects of RH on heterogeneous reactions of O_3 with mineral dust, and different results have been reported. While a strong negative effect of RH on O_3 uptake kinetics was observed for α-Al_2O_3 and α-Fe_2O_3 by Mogili et al. (2006b), the other two studies (Sullivan et al., 2004; Chang et al., 2005) suggested that the influence of RH on heterogeneous uptake of O_3 by α-Al_2O_3 and Saharan dust was insignificant. Further experimental and theoretical work is required to better understand the effect of RH on O_3 uptake by mineral dust. As discussed below, surface adsorbed water may play different roles in heterogeneous reaction of minerals with O_3.

A few other studies (Li et al., 1998; Li and Oyama, 1998; Roscoe and Abbatt, 2005; Lampimaki et al., 2013) used different surface techniques to monitor mineral dust surfaces during exposure to O_3. These studies did not report uptake coefficients and hence are not included in Table 4. Nevertheless, they have provided valuable insights into reaction mechanisms at the molecular level and are worthy of further discussion. A new Raman peak at 884 cm^{-1} was observed after exposure MnO_2 to O_3, and it is attributed to peroxide species (i.e. SS-O_2) by combining Raman spectroscopy, ^{18}O isotope substitution measurements, and ab initio calculation (Li et al., 1998). Consequently, the following reaction mechanism has been proposed for heterogeneous reaction of O_3 with metal oxides (Li et al., 1998):

$$O_3(g) + SS \rightarrow SS\text{-}O + O_2(g) \qquad \text{(R18a)}$$

$$SS\text{-}O + O_3(g) \rightarrow SS\text{-}O_2 + O_2(g) \qquad \text{(R18b)}$$

where SS represents reactive surface sites towards O_3. The intensity of the SS-O_2 peak was found to decrease gradually with time after O_3 exposure was terminated, suggesting that SS-O_2 would slowly decompose to O_2 (Li et al., 1998):

$$SS\text{-}O_2 \rightarrow SS + O_2(g) \qquad \text{(R18c)}$$

A following study by the same group (Li and Oyama, 1998) suggested that the steady-state and transient kinetics of heterogeneous decomposition of O_3 on MnO_2 could be well described by

the aforementioned reaction mechanism (R18a, R18b, and R18c). Reaction R18a is expected to be of the Eley-Rideal type, because desorption of O_3 from mineral surfaces has never been observed (Hanisch and Crowley, 2003a; Michel et al., 2003; Karagulian and Rossi, 2006) and thus the Langmuir-Hinshelwood mechanism is unlikely. It is also suggested that reaction R18a is much faster than the other two steps and the reactivation step (R18c) is slowest (Li et al., 1998; Li and Oyama, 1998).

The reaction mechanism proposed by Li et al. was supported by several following studies. For examples, gradual surface passivation was observed for a variety of minerals (Hanisch and Crowley, 2003a; Michel et al., 2003), suggesting that the number of reactive surface sites towards O_3 is limited, as implied by reactions R18a and R18b. On the other hand, two previous studies (Hanisch and Crowley, 2003a; Sullivan et al., 2004) observed that surface reactivation would slowly occur after O_3 exposure was stopped, and Michel et al. (2003) found that heterogeneous uptake of O_3 by minerals is of catalytic nature to some extent. These studies (Hanisch and Crowley, 2003a; Michel et al., 2003; Sullivan et al., 2004) clearly demonstrate that a slow surface reactivation step exists, consistent with the reaction mechanism (more precisely, reaction R18c) proposed by Li and coworkers (Li et al., 1998; Li and Oyama, 1998).

Using DRIFTS, Roscoe and Abbatt (2005) monitored the change of alumina during its heterogeneous interaction with O_3 and water vapor. A new IR peak at 1380 cm^{-1}, attributed to SS-O, appeared after alumina was exposed to O_3. Because alumina is opaque below 1100 cm^{-1}, the SS-O_2 peak, expected to appear at around 884 cm^{-1} (Li et al., 1998), could not be detected by IR. When alumina was simultaneously exposed O_3 and water vapor, the intensity of the SS-O peak was substantially decreased, compared to the case when exposure to O_3 alone. This suggests that water molecules can be adsorbed strongly to sites which would otherwise react with O_3, thus suppressing the formation of SS-O on the surface (Roscoe and Abbatt, 2005). In this aspect, increasing RH will reduce heterogeneous reactivity of alumina towards O_3. It was

further found that if O_3-reacted alumina was exposed to water vapor, the intensity of the SS-O IR peak would gradually decrease while the amount of surface adsorbed water would increase. This indicates that SS-O would react with adsorbed water to regenerate reactive surface sites (i.e. SS as shown in reaction R18a), implying that the presence of water vapor may also promote O_3 uptake by alumina. As we discussed before, previous studies which examined the effects of RH on heterogeneous reactions of O_3 with minerals (Sullivan et al., 2004; Chang et al., 2005; Mogili et al., 2006a) do not agree with each other. This inconsistence may be (at least partly) be caused by complex roles which adsorbed water plays in heterogeneous uptake of O_3 by mineral dust. Further work is required to elucidate the effect of RH, especially considering that heterogeneous reaction of O_3 with minerals is of interest not only for atmospheric chemistry but also for indoor air quality and industrial application (Dhandapani and Oyama, 1997).

3.3.2 Atmospheric implications

Using the dependence of $\gamma(O_3)$ on $[O_3]$ recommended by Crowley et al. (2010) and assuming an typical O_3 concentration of 1.5×10^{12} molecule cm^{-3} (~60 ppbv) in the troposphere, $\gamma(O_3)$ is calculated to be 4.5×10^{-6}. Consequently, lifetimes of O_3 with respect to heterogeneous reaction with mineral dust, $\tau_{het}(O_3)$, are estimated to be about 1280, 128, 13 days for dust mass concentrations of 10, 100, and 1000 μg m^{-3}, respectively. As discussed in Section 2.1.2, in polluted and forested areas where alkenes are abundant, O_3 lifetimes are around several hours; in these regions, O_3 removal due to direct heterogeneous uptake by mineral dust is unlikely to be significant. On the other hand, O_3 lifetimes in remote free troposphere are in the range of several days to a few weeks; therefore, direct removal of O_3 by heterogeneous reaction with mineral dust could play a minor but non-negligible role for some regions in the remote free troposphere heavily impact by mineral dust.

3.4 HCHO

The photocatalytic oxidation of HCHO on P25 TiO_2 surface was investigated as a function of HCHO concentration and RH (Obee and Brown, 1995). It has been shown that at a given HCHO concentration, oxidation rates of HCHO first increased and then decreased with RH. Noguchi et al. (1998) found that under dark conditions, P25 TiO_2 particles showed higher HCHO adsorption capacity (after normalized to surface area) than activated carbon. Under UV illumination, TiO_2 thin films could convert HCHO completely to CO_2 and H_2O, with formic acid (HCOOH) being an intermediate product; furthermore, the dependence of photo-degradation rates on $[HCHO]_0$ could be described by the Langmuir-Hinshelwood model (Noguchi et al., 1998). In another study (Liu et al., 2005), it has also been suggested that kinetics of photocatalytic oxidation of HCHO on TiO_2 surface could be described by the Langmuir-Hinshelwood model, and CO was identified as one of the products.

Ao et al. (2004) explored effects of NO, SO_2, and VOCs (including benzene, toluene, ethylbenzene, and o-xylene) on the photo-degradation of HCHO on P25 TiO_2 particles. Formic acid was identified as a major reaction intermediate, and HCHO degradation rates and HCOOH yields both decreased with increasing RH (Ao et al., 2004). In addition, NO could accelerate HCHO oxidation rates and HCOOH yields, whereas co-presence of SO_2 and VOCs used in this study was found to inhibit photo-oxidation of HCHO (Ao et al., 2004). DRIFTS was used by Sun et al. (2010) to investigate adsorption and photo-oxidation of HCHO on TiO_2. It has been shown that adsorbed HCHO molecules can be rapidly converted to formate on the surface under UV irradiation, and the presence of water vapor could significantly accelerate oxidation of HCHO on TiO_2 (Sun et al., 2010).

All the aforementioned studies (Obee and Brown, 1995; Noguchi et al., 1998; Ao et al., 2004; Liu et al., 2005; Sun et al., 2010) clearly showed that UV illumination could largely enhance heterogeneous uptake of HCHO by TiO_2 particles, and HCOOH/$HCOO^-$, CO_2, CO,

and H_2O were identified as reaction intermediates and/or products. Though these studies provide useful insights into mechanisms of heterogeneous reaction of HCHO with TiO_2 surface, they are not listed in Table 5 because no uptake coefficients have been reported. Heterogeneous reaction of HCHO (10-40 ppbv) with soil samples was investigated using a coated wall flow tube (Li et al., 2016). At 0% RH, the initial uptake coefficient was determined to be $(1.1\pm0.05)\times10^{-4}$, gradually decreasing to $(5.5\pm0.4)\times10^{-5}$ within 8 h. Increasing RH would suppress the uptake of HCHO, and around two thirds of HCHO molecules uptaken by the soil was reversible (Li et al., 2016). The soil sample used by Li et al. were collected from a cultivated field site (Mainz, Germany) and may not resemble the composition and mineralogy of mineral dust aerosol; therefore, this study is not included in Table 7.

Table 7: Summary of previous laboratory studies on heterogeneous reactions of mineral dust with HCHO

Dust	Reference	T (K)	Concentration (molecule cm^{-3})	Uptake coefficient	Techniques
TiO_2	Xu et al., 2010	163-673	$(1\text{-}20)\times10^{13}$	At 295±2 K, γ_0 (based on the BET surface area) were determined to be in the range of 0.5×10^{-8} to 5×10^{-8}, increasing linearly with HCHO concentration (1×10^{13} to 2×10^{14} molecule cm^{-3}). UV irradiation and increasing temperature could both accelerate this reaction.	DRIFTS, IC
	Sassine et al., 2010	278-303	$(9\text{-}82)\times10^{10}$	γ_{ss} were determined to range from $(3.00\pm0.45)\times10^{-9}$ to $(2.26\pm0.34)\times10^{-6}$, depending on UV irradiation, HCHO concentration, RH, and temperature.	CWFT
Al_2O_3	Carlos-Cuellar et al., 2003	295	room temperature	γ_0: $(7.7\pm0.3)\times10^{-5}$	KC-MS
	Xu et al., 2006	273-333	$(1\text{-}10)\times10^{13}$	At 296 K, γ_0 was determined to be $(9.4\pm1.7)\times10^{-9}$ based on the BET surface area and $(2.3\pm0.5)\times10^{-5}$ based on the geometrical area for α-Al_2O_3. UV irradiation and increasing temperature could both accelerate this reaction.	DRIFTS, IC
	Xu et al., 2011	84-573	$(1.3\text{-}3.6)\times10^{13}$	At 295±2 K, γ_0 was determined to be $(3.6\pm0.8)\times10^{-4}$ based on the geometrical area and $(1.4\pm0.31)\times10^{-8}$ based on the BET surface area for γ-Al_2O_3. UV irradiation and increasing temperature could both accelerate this reaction.	DRIFTS, IC
SiO_2	Carlos-Cuellar et al., 2003	295	room temperature	γ_0: $(2.6\pm0.9)\times10^{-7}$	KC-MS
	Sassine et al., 2010	278-303	$(9\text{-}82)\times10^{10}$	γ_{ss} under dark conditions: $\sim3\times10^{-9}$	CWFT
Fe_2O_3	Carlos-Cuellar et al., 2003	295	room temperature	γ_0: $(1.1\pm0.5)\times10^{-5}$	KC-MS

Carlos-Cuellar et al. (2003) first determined uptake coefficients of HCHO on several mineral dust particles at room temperature, using a Knudsen cell reactor. Gradual surface deactivation was observed for all three types of particles, and initial uptake coefficients (γ_0), based on the BET surface area, were reported to be $(1.1\pm0.5)\times10^{-4}$ for α-Fe_2O_3, $(7.7\pm0.3)\times10^{-5}$ for α-Al_2O_3, and $(2.6\pm0.9)\times10^{-7}$ for SiO_2, respectively (Carlos-Cuellar et al., 2003).

Using DRIFTs and ion chromatography, Xu and co-workers systematically investigated heterogeneous reactions of HCHO with α-Al_2O_3 (Xu et al., 2006), γ-Al_2O_3 (Xu et al., 2011), and TiO_2 particles (Xu et al., 2010) as a function of temperature, UV irradiation, and HCHO concentration. It has been found that HCHO was first converted to dioxymethylene which was then oxidized to formate on the surface, and UV irradiation and increasing temperature both could enhance heterogeneous reactivity of all three types of particles towards HCHO (Xu et al., 2006; Xu et al., 2010; Xu et al., 2011). γ_0(HCHO) on α-Al_2O_3 at 293 K was determined to be $(9.4\pm1.7)\times10^{-9}$ based on the BET surface area of the sample and $(2.3\pm0.5)\times10^{-5}$ based on the geometrical area of the sample holder (Xu et al., 2006). At room temperature (295±2 K) and under dark conditions, γ_0(HCHO), based on the BET surface area, were determined to be in the range of 0.5×10^{-8} to 5×10^{-8} for TiO_2 (Xu et al., 2010), increasing linearly with HCHO concentration (1×10^{13} to 2×10^{14} molecule cm^{-3}). Under the same condition, γ_0(HCHO) was determined to be $(3.6\pm0.8)\times10^{-4}$ based on the geometrical area and $(1.4\pm0.31)\times10^{-8}$ based on the BET surface area for γ-Al_2O_3 (Xu et al., 2011). The effect of RH was further studied for γ-Al_2O_3 at 295±2 K, and the dependence of BET surface area based γ_0(HCHO) on RH is given by (Xu et al., 2011):

$$\ln[\gamma_0(BET)] = -17.5 - 0.0127 \times RH \quad (20)$$

where RH is in the unit of %.

A coated wall flow tube was deployed to investigate heterogeneous reactions of HCHO with TiO_2 and SiO_2 particles, and the effects of UV irradiation, temperature (278-303 K), RH

(6-70 %), and HCHO concentration (3.5-32.5 ppbv) were systematically examined (Sassine et al., 2010). Under dark conditions, the uptake of HCHO onto SiO_2 and TiO_2 was very slow, with BET surface area based γ_{ss} being $(3.00\pm0.45)\times10^{-9}$. Nevertheless, its uptake on TiO_2 and TiO_2/SiO_2 mixture was largely enhanced by near-UV irradiation (340-420 nm) (Sassine et al., 2010). For pure TiO_2 under the condition of 293 K, 30% RH and 2 ppbv HCHO, γ_{ss} depended linearly on irradiation intensity (1.9×10^{15} to 2.7×10^{15} photons cm^{-2} s^{-1}). The uptake kinetics can be described by the Langmuir-Hinshelwood model: under the condition of 293 K, 6% RH, and 2.7×10^{15} photons cm^{-2} s^{-1}, γ_{ss} decreased from $(6.0\pm0.9)\times10^{-7}$ to $(2.0\pm0.3)\times10^{-7}$ for TiO_2 when [HCHO] increased from 3.5 to 32.5 ppbv (Sassine et al., 2010).

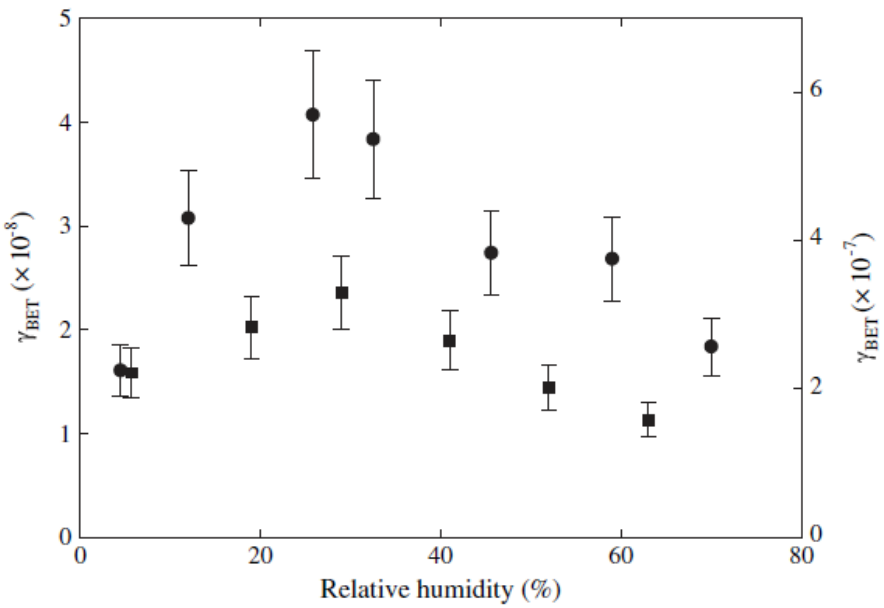

Figure 14. Effects of RH on heterogeneous uptake of HCHO by pure TiO_2 (circles, right y-axis) and TiO_2/SiO_2 mixture (squares, left y-axis) which contains 5%wt TiO_2. Experimental conditions: 293 K, 11 ppbv HCHO, 2.7×10^{15} photons cm^{-2} s^{-1} illumination. Reprinted with permission from Sassine et al. (2010). Copyright Elsevier 2010.

In addition, the effects of RH and temperature were also explored. As shown in Figure 14, γ_{ss} was found to first increase with RH for TiO_2 (and TiO_2/SiO_2 mixture as well), reaching

a maximum at ~30%, and then decrease with RH. Under conditions of 30% RH, 11 ppbv HCHO, and 2.7×10^{15} photons cm^{-2} s^{-1}, γ_{ss} increased from $(1.8\pm0.3)\times10^{-7}$ at 298 K to $(3.2\pm0.5)\times10^{-7}$ at 303 K (Sassine et al., 2010).

3.4.1 Discussion and atmospheric implication

Two previous studies determined BET surface area based γ_0(HCHO) for α-Al_2O_3 particles under dry conditions at room temperature, and γ_0(HCHO) reported by Carlos-Cuellar et al. (2003) is >3 orders of magnitude larger than that reported by Xu et al. (2006). It is not very clear yet why such a large difference was found between these two studies. Two studies (Sassine et al., 2010; Xu et al., 2010) measured γ(HCHO) for TiO_2 particles; however, it is difficult to make comparison because one study reported γ_0 (Xu et al., 2010) and the other one reported γ_{ss} (Sassine et al., 2010).

What we can conclude from previous studies as summarized in Table 7 is that our understanding of atmospheric heterogeneous reaction of HCHO with mineral dust is very limited. For example, all the previous studies only examined its reactions with oxides, while clay minerals and authentic dust samples have never been investigated. Second, as discussed above, large discrepancies are found for uptake coefficients reported by previous studies. Furthermore, roles of RH in heterogeneous uptake of HCHO by mineral dust are not fully understood. Last but not least, though several studies have observed that UV illumination could largely enhance heterogeneous reaction of HCHO with mineral particles, it is non-trivial to know that compared to dark conditions, to which extent this reaction is accelerated under irradiation conditions relevant to the troposphere. Therefore, it is difficult to assess the significance of heterogeneous uptake by mineral dust aerosol particles as a sink for HCHO in a reliable manner.

An uptake coefficient of $(9.7\pm1.4)\times10^{-6}$ was used by Sassine et al. (2010) to evaluate the significance of heterogeneous reaction of HCHO with pure TiO_2 particles as a sink for

HCHO. This value was linearly extrapolated from their experimental measurements (2 ppbv HCHO, 293 K, and 30% RH) to realistic solar conditions in the troposphere (1.21×10^{16} photons cm^{-2} s^{-1}). The value used by Sassine et al. (2010) is also adopted here to preliminarily assess the impact of heterogeneous reaction of HCHO with mineral dust. For simplicity in our work γ(HCHO) is set to 1×10^{-5} which is only 3% larger than that used by Sassine et al. (2010). Consequently, τ_{het}(HCHO) are calculated to be about 456, 46, and 4.6 days for mineral dust mass concentrations of 10, 100, and 1000 μg m^{-3}, respectively. For comparison, as we have discussed in Section 2.1, typical lifetimes of HCHO are a few hours in the troposphere, with photolysis and reaction with OH radicals being the two major removal processes. It is quite clear that τ_{het}(HCHO) are much larger than typical lifetimes of HCHO, and thus heterogeneous reaction with mineral dust is unlikely to be significant for the removal of HCHO in the troposphere.

3.5 HONO

Bedjanian and coworkers utilized a coated rod flow tube coupled to a mass spectrometer to investigate heterogeneous reaction of HONO with TiO_2, γ-Al_2O_3, Fe_2O_3, and ATD particles under dark and illuminated conditions (El Zein and Bedjanian, 2012; Romanias et al., 2012b; El Zein et al., 2013a; El Zein et al., 2013b). All these measurements were carried out with dust mass in the linear mass dependent regime, and thus BET surface area was used to calculate uptake coefficients. We note that several previous studies have explored heterogeneous interactions of HONO with Pyrex (Kaiser and Wu, 1977; Ten Brink and Spoelstra, 1998), borosilicate glass (Syomin and Finlayson-Pitts, 2003), and TiO_2-doped commercial paints (Laufs et al., 2010). However, these studies are not further discussed here because they are not of direct atmospheric relevance. Uptake of HONO by soil samples was investigated using a coated-wall flow tube (Donaldson et al., 2014), and uptake coefficients were found to decrease with RH, from $(2.5\pm0.4)\times10^{-4}$ at 0% RH to $(1.1\pm0.4)\times10^{-5}$ at 80% RH. Soil used by Donaldson

et al. were collected from an agricultural field in Indiana and its mineralogical composition may be quite different from mineral dust aerosol; as a result, this study is not included in Table 8.

Table 8: Summary of previous laboratory studies on heterogeneous reactions of mineral dust with HONO

Dust	Reference	*T* (K)	Concentration (molecule cm^{-3})	Uptake coefficient	Techniques
TiO_2	El Zein and Bedjanian, 2012	275-320	$(0.3\text{-}3.3)\times10^{12}$	γ_0 was determined to be ~4.2×10^{-6} at 10% RH and 300 K, showing negative dependence on RH (up to 12.6%) and *T* (275-320 K).	CRFT-MS
	El Zein et al., 2013a	275-320	$(0.5\text{-}5)\times10^{12}$	Under illuminated condition, γ_0 increased to ~3.5×10^{-4} at 10% RH and 280 K, showing negative dependence on RH (up to 60%) and *T* (275-320 K). Though illumination enhanced HONO uptake compared to dark conditions, further increase in illumination intensity for $J(NO_2)$ in the range of 0.002-0.012 s^{-1} did not affect γ_0.	CRFT-MS
Al_2O_2	Romanias et al., 2012b	275-320	$(0.6\text{-}3.5)\times10^{12}$	At 10% RH, γ_0 was determined to be ~1.2×10^{-6} and ~6.2×10^{-6} under dark and illuminated conditions, respectively. γ_0 was found to increase linearly with $J(NO_2)$ in the range of 0.002-0.012 s^{-1}. In addition, γ_0 decreased with RH, and no dependence on temperature was observed.	CRFT-MS
Fe_2O_3	El Zein et al., 2013b	275-320	$(0.6\text{-}15.0)\times10^{12}$	No significant effect of UV illumination, with $J(NO_2)$ up to 0.012 s^{-1}, was observed. γ_0 was determined to be ~4.1×10^{-7} at 10% RH and 300 K, showing negative dependence on RH (up to 14.4 %) and no dependence on *T* (275-320 K).	CRFT-MS
ATD	El Zein et al., 2013b	275-320	$(0.6\text{-}15.0)\times10^{12}$	No significant effect of UV illumination, with $J(NO_2)$ up to 0.012 s^{-1}, was observed. γ_0 was determined to be ~9.3×10^{-7} at 10% RH and 275 K, showing negative dependence on RH (up to 84.1%) and no dependence on *T* (275-320 K).	CRFT-MS

El Zein and Bedjanian (2012) measured heterogeneous uptake of HONO by TiO_2 particles under dark conditions. Upon exposure to HONO, heterogeneous reactivity of TiO_2 was progressively reduced, and the steady-state uptake coefficients were at least one order of magnitude smaller than the corresponding initial uptake coefficients, γ_0 (El Zein and Bedjanian, 2012). γ_0, independent of initial HONO concentrations in the range of (0.3-3.3)×10^{12} molecule cm^{-3}, showed strong dependence on RH and a slightly negative dependence on temperature. The effects of temperature (275-320 K) at 0.001% RH and of RH at 300 K on γ_0 are given by (El Zein and Bedjanian, 2012):

$$\gamma_0 = (1.4 \pm 0.5) \times 10^{-5} \times \exp[(1405 \pm 110)/T] \quad (21)$$

$$\gamma_0 = 1.8 \times 10^{-5} \times RH^{-0.63} \quad (22)$$

HONO uptaken by TiO_2 undergoes chemical conversion on the surface, and molecularly adsorbed HONO is insignificant (El Zein and Bedjanian, 2012). This was confirmed by gas phase production analysis, showing that the total yield of NO and NO_2 is equal to 1 within the experimental uncertainties. The yields of NO and NO_2 were determined to be 0.42±0.07 and 0.60±0.09, respectively, independent of RH, temperature, and the initial HONO concentration (El Zein and Bedjanian, 2012).

In a following study, El Zein et al. (2013a) examined the effect of illumination on the uptake of HONO by TiO_2, and found that under illuminated conditions HONO uptake rates also decreased with reaction time. Compared to dark conditions, HONO uptake was enhanced, though no difference in the γ_0 was observed by varying UV illumination from 0.002 to 0.012 s^{-1} (El Zein et al., 2013a). Under illuminated conditions, γ_0 is independent of initial HONO concentration but depends inversely on temperature and RH. The effects of temperature (275-320 K) at 0.002% RH and of RH (0.001-60%) at 280 K can be described by (El Zein et al., 2013a):

$$\gamma_0 = (3.0 \pm 1.5) \times 10^{-5} \times \exp[(1390 \pm 150)/T] \quad (23)$$

$$\gamma_0 = 6.9 \times 10^{-4} \times RH^{-0.3} \quad (24)$$

Similar to dark conditions, all the HONO molecules removed from the gas phase have been converted NO and NO_2. Yields of NO and NO_2 were determined to be 0.48±0.07 and 0.52±0.08, respectively (El Zein et al., 2013a), independent of RH, temperature, and initial HONO concentration.

The uptake of HONO by γ-Al_2O_3, Fe_2O_3, and ATD particles was also investigated under dark and illuminated conditions as a function of temperature and RH. Progressive surface deactivation was observed in all the experiments. For uptake onto γ-Al_2O_3, under both dark and irradiated conditions γ_0(HONO) were found to be independent of initial HONO concentration (0.3×10^{12} to 3.3×10^{12} molecule cm^{-3}) and temperature (275-320 K), though RH has a profound influence. Under dark conditions, γ_0 is given by (Romanias et al., 2012b):

$$\gamma_0 = 4.8 \times 10^{-6} \times RH^{-0.61} \quad (25)$$

for RH in the range of 0.00014% to 10.5%. UV illumination linearly enhances initial HONO uptake, with γ_0 under illumination with $J(NO_2)$ equal to 0.012 s^{-1} given by (Romanias et al., 2012b):

$$\gamma_0 = 1.7 \times 10^{-5} \times RH^{-0.44} \quad (26)$$

for RH in the range of 0.0003% to 35.4%. NO and NO_2 yields were determined to be 0.40±0.06 and 0.60±0.09 for all the experimental conditions.

No significant effects of UV irradiation with $J(NO_2)$ up to 0.012 s^{-1} were observed for heterogeneous reaction of HONO with Fe_2O_3 and ATD particles (El Zein et al., 2013b). γ_0(HONO) were found to be independent of initial HONO concentration (0.6×10^{12} to 15.0×10^{12} molecule cm^{-3}) and temperature (275-320 K), while RH has a significant impact, given by (El Zein et al., 2013b):

$$\gamma_0 = 1.7 \times 10^{-6} \times RH^{-0.62} \quad (27)$$

for Fe_2O_3 and RH in the range of 0.0003% to 14.4%, and

$$\gamma_0 = 3.8 \times 10^{-6} \times RH^{-0.61} \quad (28)$$

for ATD and RH in the range of 0.00039% to 84.1%. NO and NO_2 yields, independent of experimental conditions, were reported to be 0.40±0.06 and 0.60±0.09, respectively (El Zein et al., 2013b).

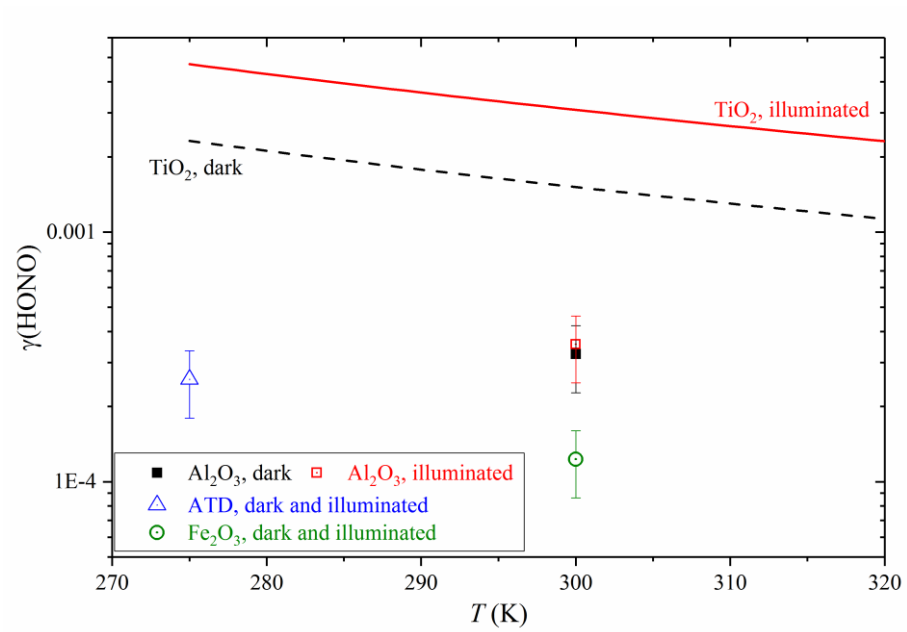

Figure 15. Temperature dependence of γ_0(HONO) for TiO_2 (El Zein and Bedjanian, 2012; El Zein et al., 2013a), Al_2O_3 (Romanias et al., 2012b), ATD (El Zein et al., 2013b) and Fe_2O_3 (El Zein et al., 2013b) under dark and illuminated conditions. Data at 0.001% RH were presented except for illuminated TiO_2 at 0.002% RH. Please note that no significant temperature (275-320 K) effect was found for Al_2O_3, ATD, and Fe_2O_3. In addition, no difference in uptake kinetics was observed between dark and illuminated conditions for ATD and Fe_2O_3.

The dependence of γ_0(HONO) on temperature is displayed in Figure 15 for different mineral dust under dark and illuminated conditions. No significant effect of temperature was observed for uptake onto Al_2O_3, Fe_2O_3, and ATD. When temperature increases from 275 K to 320 K, γ_0(HONO) is reduced by a factor of about 2 under both dark and illuminated conditions for TiO_2. It is interesting to note that UV illumination has different impacts on HONO uptake

for different minerals. HONO uptake onto Al_2O_3 is enhanced by UV radiation, and the extent of enhancement shows linear dependence on illumination intensity for $J(NO_2)$ in the range of 0.002-0.012 s^{-1} (Romanias et al., 2012b). In contrast, photo-enhancement was found to be insignificant for ATD and Fe_2O_3 with $J(NO_2)$ up to 0.012 s^{-1} (El Zein et al., 2013b). Significant enhancement in γ_0(HONO) was observed for illuminated TiO_2 with $J(NO_2)$ of 0.002 s^{-1} when compared to dark conditions, especially at evaluated RH as shown in Figure 16; however, further increase in illumination intensity with $J(NO_2)$ up to 0.012 s^{-1} did not lead to further increase in γ_0(HONO) (El Zein et al., 2013a). In addition, we note that NO and NO_2 yields were found to be ~0.40 and 0.60 for all the four types of minerals investigated, independent of experimental conditions.

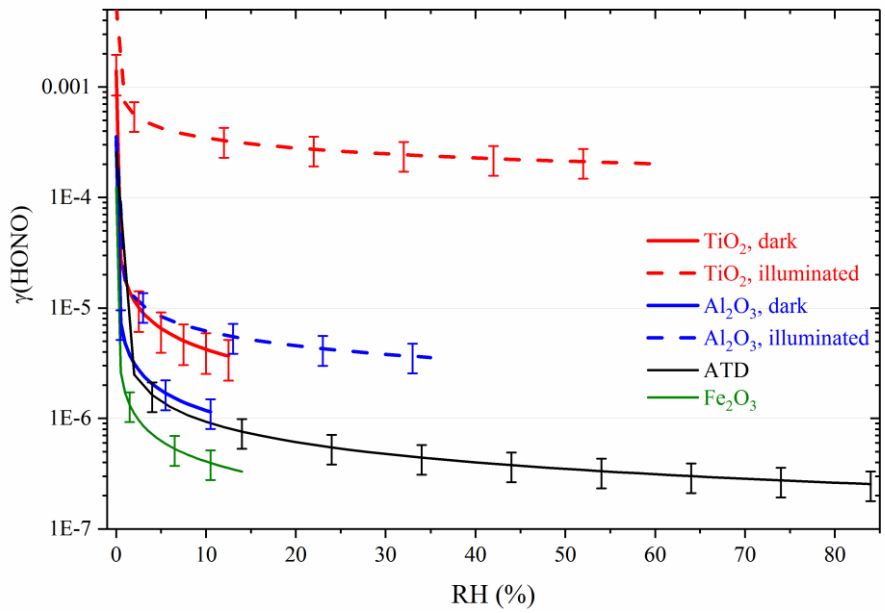

Figure 16. RH dependence of γ_0(HONO) for TiO_2 (El Zein and Bedjanian, 2012; El Zein et al., 2013a), Al_2O_3 (Romanias et al., 2012b), ATD (El Zein et al., 2013b) and Fe_2O_3 (El Zein et al., 2013b) under dark and illuminated conditions at around room temperature.

Figure 16 shows effects of RH on γ_0(HONO) at around room temperature for TiO_2, Al_2O_3, ATD, and Fe_2O_3. Most of measurements were only carried out at low RH (<15%), and

thus their atmospheric relevance is rather limited. Experiments using ATD and illuminated TiO_2 particles were conducted at RH over a wide range, and a negative dependence of γ_0(HONO) on RH was observed. When RH increases from 10% to 60%, γ_0(HONO) is reduced by ~66% and ~42% for ATD and illuminated TiO_2, respectively.

3.5.1 Discussion and atmospheric implication

All the fours studies, as shown in Figures 15 and 16, were carried out by the same group. Furthermore, heterogeneous interactions of HONO with authentic dust and clay minerals which are the major components for tropospheric dust, have not been explored yet. Future studies can provide more scientific insights to reaction mechanisms and better quantify uptake kinetics.

In this work we use γ_0(HONO) for ATD, the only authentic dust sample investigated, to preliminarily assess the significance of heterogeneous uptake by mineral dust as a HONO sink. As shown in Figure 16, γ_0(HONO) decreases from 9.3×10^{-7} at 10% to 2.6×10^{-7} at 80%. A γ(HONO) value of 1×10^{-6} is adopted here to calculate τ_{het}(HONO) with respect to heterogeneous reaction with mineral dust. This may represent an upper limit for its atmospheric significance, because i) at typical RH found in the troposphere, γ_0(HONO) should be $<1\times10^{-6}$ according to the work by El Zein et al. (2013b); ii) surface deactivation was observed, and thus the average γ(HONO) should be smaller than γ_0(HONO) (El Zein et al., 2013b). Using Eq. (6), τ_{het}(HONO) is calculated to be ~57 days for dust mass concentration of 1000 μg m^{-3} which can only occur during dust storms. For comparison, typical HONO lifetimes in the troposphere are estimated to be 10-20 min, with the major sink being photolysis (in Section 2.1). Therefore, heterogeneous uptake by mineral dust is a negligible sink for HONO in the troposphere.

3.6 N_2O_5 and NO_3 radicals

N_2O_5 and NO_3 in the troposphere are in the dynamic equilibrium, as introduced in Section 2.1.3. Therefore, their heterogeneous reactions with mineral dust are discussed together in this section.

3.6.1 N_2O_5

Heterogeneous reaction of N_2O_5 with mineral dust particles was investigated for the first time by Seisel et al. (2005), using DRIFTS and a Knudsen cell reactor coupled to quadruple mass spectrometry. The initial uptake coefficient of N_2O_5 on Saharan dust was determined to be 0.080±0.003 at 298 K, and slowly decreased to a steady-state value of 0.013±0.003 (Seisel et al., 2005). Formation of nitrate on dust particles was observed, and N_2O_5 uptake was suggested to proceed with two mechanisms, i.e. heterogeneous hydrolysis and its reaction with surface OH groups (Seisel et al., 2005). A Knudsen cell reactor was also used by Karagulian et al. (2006) to investigate heterogeneous uptake of N_2O_5 by several different types of mineral dust. Both the initial and steady-state uptake coefficient were found to decrease with increasing initial N_2O_5 concentrations. When N_2O_5 concentration was $(4.0\pm1.0)\times10^{11}$ molecule cm^{-3}, γ_0 and γ_{ss} were determined to be 0.30±0.08 and 0.20±0.05 for Saharan dust, 0.12±0.04 and 0.021±0.006 for $CaCO_3$, 0.20±0.06 and 0.11±0.03 for ATD, 0.16±0.04 and 0.021±0.006 for kaolinite, and 0.43±0.13 and 0.043±0.013 for natural limestone, respectively. When N_2O_5 concentration increased to $(3.8\pm0.5)\times10^{12}$ molecule cm^{-3}, γ_0 and γ_{ss} were determined to be 0.090±0.026 and 0.059±0.016 for Saharan dust, 0.033±0.010 and 0.0062±0.0018 for $CaCO_3$, 0.064±0.019 and 0.016±0.004 for ATD, 0.14±0.04 and 0.022±0.006 for kaolinite, and 0.011±0.003 and 0.0022±0.0006 for natural limestone, respectively (Karagulian et al., 2006). Formation of HNO_3 in the gas phase was detected, with production yield varying with dust mineralogy. The postulated reason is that partitioning of formed HNO_3 between gas and particle phases may vary for different dust samples (Karagulian et al., 2006).

Wagner et al. (2008) utilized a Knudsen cell reactor to study heterogeneous uptake of N_2O_5 by Saharan dust, ATD, and $CaCO_3$ particles at 296±2 K. Interestingly, surface deactivation was only observed for $CaCO_3$ under their experimental conditions. Therefore, γ_0 and γ_{ss} are equal for the other two types of dust, being 0.037±0.012 for Saharan dust and

0.022±0.008 for ATD, respectively (Wagner et al., 2008). The initial uptake coefficient was reported to be 0.05±0.02 for $CaCO_3$; pre-heating could reduce its heterogeneous reactivity towards N_2O_5 (Wagner et al., 2008), very likely due to the loss of surface adsorbed water and surface OH groups. It should be noted that all the uptake coefficients measured by using Knudsen cell reactors are based on the projected area of dust samples (Seisel et al., 2005; Karagulian et al., 2006; Wagner et al., 2008).

Heterogeneous reactions of N_2O_5 with airborne mineral dust particles were also investigated by several previous studies, with the first one being carried out by Mogili et al. (2006b). In this study, in-situ FTIR measurements was carried out to determine N_2O_5 loss due to reactions with dust particles in an environmental chamber at 290 K. The uptake coefficients of N_2O_5, based on the BET area of dust particles, increase with RH for SiO_2, from $(4.4\pm0.4)\times10^{-5}$ at <1% RH, to $(9.3\pm0.1)\times10^{-5}$ at 11% RH, $(1.2\pm0.2)\times10^{-4}$ at 19% RH, and $(1.8\pm0.4)\times10^{-4}$ at 43% RH (Mogili et al., 2006b). In addition, $\gamma(N_2O_5)$ at <1% RH were determined to be for $(1.9\pm0.2)\times10^{-4}$ for $CaCO_3$, $(9.8\pm0.1)\times10^{-4}$ for kaolinite, $(4.0\pm0.4)\times10^{-4}$ for α-Fe_2O_3, and $(1.9\pm0.2)\times10^{-4}$ for montmorillonite, respectively (Mogili et al., 2006b).

Table 9: Summary of previous laboratory studies on heterogeneous reactions of mineral dust with N_2O_5

Dust	Reference	*T* (K)	Concentration (molecule cm^{-3})	Uptake coefficient	Techniques
Saharan dust	Seisel et al., 2005	298	$(0.03\text{-}5)\times10^{12}$	γ_0: 0.080±0.003 and γ_{ss}: 0.013±0.003	KC, DRIFTS
	Karagulian et al., 2006	298±2	$(0.4\text{-}3.8)\times10^{12}$	When $[N_2O_5]$ was $(4.0\pm1.0)\times10^{11}$ molecule cm^{-3}, γ_0 = 0.30±0.08 and γ_{ss} = 0.20±0.05; when $[N_2O_5]$ was $(3.8\pm0.5)\times10^{12}$ molecule cm^{-3}, γ_0 = 0.090±0.026 and γ_{ss} = 0.059±0.016.	KC
	Wagner et al., 2008	296±2	KC: $(3.0\text{-}11.0)\times10^{9}$; AFT: $(5\text{-}20)\times10^{12}$	KC measurements: $\gamma_0 = \gamma_{ss}$ =0.037±0.012; AFT measurements: 0.026±0.004 at 0% RH, 0.016±0.004 at 29% RH, and 0.010±0.004 at 58% RH.	KC-MS, AFT-CLD
	Tang et al., 2012	297±1	$(0.5\text{-}30)\times10^{12}$	0.02±0.01, independent of RH (0-67%)	AFT-CRDS
ATD	Karagulian et al., 2006	298±2	$(0.4\text{-}3.8)\times10^{12}$	When $[N_2O_5]$ was $(4.0\pm1.0)\times10^{11}$ molecule cm^{-3}, γ_0 = 0.20±0.06 and γ_{ss} = 0.11±0.03; when $[N_2O_5]$ was $(3.8\pm0.5)\times10^{12}$ molecule cm^{-3}, γ_0 = 0.064±0.019 and γ_{ss} = 0.016±0.004.	KC
	Wagner et al., 2008	296±2	$(3.3\text{-}10.4)\times10^{9}$	$\gamma_0 = \gamma_{ss}$ =0.022±0.008	KC-MS
	Wagner et al., 2009	296±2	$(10\text{-}44)\times10^{12}$	0.0098±0.0010 at 0% RH and 0.0073±0.0007 at 29% RH	AFT-CLD
	Tang et al., 2014c	297±1	$(11\text{-}22)\times10^{12}$	$(7.7\pm1.0)\times10^{-3}$ at 0% RH, $(6.0\pm2.0)\times10^{-3}$ at 17% RH, $(7.4\pm0.7)\times10^{-3}$ at 33% RH, $(4.9\pm1.3)\times10^{-3}$ at 50% RH, and $(5.0\pm0.3)\times10^{-3}$ at 67% RH.	AFT-CRDS
$CaCO_3$	Karagulian et al., 2006	298±2	$(0.4\text{-}3.8)\times10^{12}$	When $[N_2O_5]$ was $(4.0\pm1.0)\times10^{11}$ molecule cm^{-3}, γ_0 = 0.12±0.04 and γ_{ss} = 0.021±0.006; when $[N_2O_5]$ was $(3.8\pm0.5)\times10^{12}$ molecule cm^{-3}, γ_0 = 0.033±0.010 and γ_{ss} = 0.0062±0.0018.	KC
	Mogili et al., 2006b	290	$(2\text{-}3)\times10^{15}$	$(1.9\pm0.2)\times10^{-4}$ at <1% RH	EC

	Wagner et al., 2008	296±2	$(1.7\text{-}4.5)\times10^{9}$	γ_0 = 0.05±0.02	KC-MS
	Wagner et al., 2009	296±2	$(1\text{-}40)\times10^{12}$	0.0048±0.0007 at 0% RH, 0.0053±0.0010 at 29% RH, 0.0113±0.0016 at 58% RH, and 0.0194±0.0022 at 71% RH.	AFT-CLD
SiO_2	Mogili et al., 2006b	290	$(2\text{-}3)\times10^{15}$	$(4.4\pm0.4)\times10^{-5}$ at <1% RH, $(9.3\pm0.1)\times10^{-5}$ at 11% RH, $(1.2\pm0.2)\times10^{-4}$ at 19% RH, and $(1.8\pm0.4)\times10^{-4}$ at 43% RH.	EC
	Wagner et al., 2009	296±2	$(0.5\text{-}30)\times10^{12}$	0.0086±0.0006 at 0% RH and 0.0045±0.0005 at 29%	AFT-CLD
	Tang et al., 2014a	296±2	$(10\text{-}50)\times10^{12}$	$(7.2\pm0.6)\times10^{-3}$ at (7±2)% RH, $(5.6\pm0.6)\times10^{-3}$ at (26±2)% RH, and $(5.3\pm0.8)\times10^{-3}$ at (40±3)% RH.	AFT-CLD
kaolinite	Karagulian et al., 2006	298±2	$(0.4\text{-}3.8)\times10^{12}$	When $[N_2O_5]$ was $(4.0\pm1.0)\times10^{11}$ molecule cm^{-3}, γ_0 = 0.16±0.04 and γ_{ss} = 0.021±0.006; when $[N_2O_5]$ was $(3.8\pm0.5)\times10^{12}$ molecule cm^{-3}, γ_0 = 0.14±0.04 and γ_{ss} = 0.022±0.006.	KC
	Mogili et al., 2006b	290	$(2\text{-}3)\times10^{15}$	$(9.8\pm0.1)\times10^{-4}$ at <1% RH	EC
natural limestone	Karagulian et al., 2006	298±2	$(0.4\text{-}3.8)\times10^{12}$	When $[N_2O_5]$ was $(4.0\pm1.0)\times10^{11}$ molecule cm^{-3}, γ_0 = 0.43±0.13 and γ_{ss} = 0.043±0.013; when $[N_2O_5]$ was $(3.8\pm0.5)\times10^{12}$ molecule cm^{-3}, γ_0 = 0.011±0.003 and γ_{ss} = 0.0022±0.0006.	KC
montmorillonite	Mogili et al., 2006b	290	$(2\text{-}3)\times10^{15}$	$(1.8\pm0.2)\times10^{-4}$ at <1% RH	EC
illite	Tang et al., 2014c	297±1	$(8\text{-}24)\times10^{12}$	0.091±0.039 at 0% RH and 0.093±0.008 at 17% RH, 0.072±0.021 at 33% RH, 0.049±0.006 at 50% RH, and 0.039±0.012 at 67% RH.	AFT-CRDS
TiO_2	Tang et al., 2014d	296±2	$(10\text{-}50)\times10^{12}$	$(1.83\pm0.32)\times10^{-3}$ at (5±1)% RH, $(2.01\pm0.27)\times10^{-3}$ at (12±2)% RH, $(1.02\pm0.20)\times10^{-3}$ at (23±2)% RH, $(1.29\pm0.26)\times10^{-3}$ at (33±2)% RH, $(2.28\pm0.51)\times10^{-3}$ at (45±3)% RH, and $(4.47\pm2.04)\times10^{-3}$ at (30±3)% RH.	AFT-CLD
Fe_2O_3	Mogili et al., 2006b	290	$(2\text{-}3)\times10^{15}$	$(4.0\pm0.4)\times10^{-4}$ at <1% RH	EC

An atmospheric pressure aerosol flow tube was deployed by Wagner et al. (2008, 2009) to investigate heterogeneous reactions of N_2O_5 with Saharan dust, ATD, calcite, and SiO_2 aerosol particles at 296±2 K, and N_2O_5 decays in the flow tube were detected by using a modified chemiluminescence method. Slightly negative dependence of $\gamma(N_2O_5)$ on RH was observed for Saharan dust, ATD, and SiO_2 aerosol particles. $\gamma(N_2O_5)$ was determined to be 0.026±0.004 at 0% RH, 0.016±0.004 at 29% RH, and 0.010±0.004 at 58% RH for Saharan dust (Wagner et al., 2008), 0.0086±0.0006 at 0% RH and 0.0045±0.0005 at 29% for SiO_2 (Wagner et al., 2009), and 0.0098±0.0010 at 0% RH and 0.0073±0.0007 at 29% RH for ATD (Wagner et al., 2009), respectively. In contrast, $\gamma(N_2O_5)$ increases with RH for $CaCO_3$, from 0.0048±0.0007 at 0% RH to 0.0194±0.0022 at 71% RH (Wagner et al., 2009). It should be pointed out that in the original paper (Wagner et al., 2008) the uptake coefficients for Saharan dust were based on the aerosol surface area concentrations after the shape factor correction was applied. In order to keep consistence with other studies, $\gamma(N_2O_5)$ reported by Wagner et al. (2008) have been recalculated in this review without taking into account the shape factor of Saharan dust.

Tang and co-workers systematically investigated the dependence of $\gamma(N_2O_5)$ on RH and dust mineralogy, using aerosol flow tubes with N_2O_5 measured by a modified chemiluminescence method (Tang et al., 2012; Tang et al., 2014c) or cavity ring-down spectroscopy (Tang et al., 2014a; Tang et al., 2014d). Within experimental uncertainties, $\gamma(N_2O_5)$ was determined to be 0.02±0.01 for Saharan dust (Tang et al., 2012), independent of RH (0-67%) and initial N_2O_5 concentration (5×10^{11} to 3×10^{13} molecule cm^{-3}). Products analysis suggests that N_2O_5 is converted to particulate nitrate after heterogeneous reaction with Saharan dust, and that the formation of NO_2 in the gas phase is negligible (Tang et al., 2012). It has also been shown that if pretreated with high levels of gaseous HNO_3, heterogeneous reactivity of Saharan dust towards N_2O_5 would be substantially reduced (Tang et al., 2012). A

strong negative effect of RH on $\gamma(N_2O_5)$ was found for uptake onto illite, with $\gamma(N_2O_5)$ decreasing from 0.091±0.039 at 0% RH to 0.039±0.012 at 67% RH. The negative effect of RH is much smaller for ATD, with $\gamma(N_2O_5)$ determined to be 0.0077±0.0010 at 0% RH and 0.0050±0.0003 at 67% RH (Tang et al., 2014c). $\gamma(N_2O_5)$ on SiO_2 particles decreases from 0.0072±0.0006 at (7±2)% RH to 0.0053±0.0008 at (40±2)% RH (Tang et al., 2014a), also showing a weak negative RH dependence. RH exhibits complex effects on heterogeneous reaction of N_2O_5 with TiO_2 particles, and the reported $\gamma(N_2O_5)$ first decreases with RH from $(1.83\pm0.32)\times10^{-3}$ at (5±1)% RH to $(1.02\pm0.20)\times10^{-3}$ at (23±2)% RH, and then increases with RH to $(4.47\pm2.04)\times10^{-3}$ at (60±3)% RH (Tang et al., 2014e). Analysis of optically levitated single micrometer sized SiO_2 particles using Raman spectroscopy during their reaction with N_2O_5 (Tang et al., 2014a) suggests that HNO_3 formed in this reaction can partition between gas and particle phases, with partitioning largely governed by RH.

Figure 17 summarizes $\gamma(N_2O_5)$ onto Saharan dust reported by previous work. $\gamma(N_2O_5)$ reported by the three studies using Knudsen cell reactors (Seisel et al., 2005; Karagulian et al., 2006; Wagner et al., 2008) show large variation, with $\gamma_{ss}(N_2O_5)$ ranging from 0.013±0.003 to 0.20±0.05. This comparison demonstrates that sample preparation methods could largely influence reported uptake coefficients using particles supported on a substrate, even though they all used Knudsen cell reactor (as discussed in Section 2.2.1). In addition, significant surface saturation was observed by Seisel et al. (2005) and Karagulian et al. (2006), but not by Wagner et al. (2008). For the same reason, $\gamma(N_2O_5)$ reported by two Knudsen studies (Karagulian et al., 2006; Wagner et al., 2008) exhibit significant discrepancy for Arizona Test Dust (and reasonably good agreement is found for $CaCO_3$). Instead, the two aerosol flow tube studies (Wagner et al., 2008; Tang et al., 2012) show good agreement in $\gamma(N_2O_5)$ onto Saharan dust considering experimental uncertainties, though RH was found to have a slightly negative effect by Wagner et al. (2008) while no significant effect of RH was observed by Tang et al.

(2012). Since cavity ring-down spectroscopy used by Tang et al. (2012) to detect N_2O_5 is more sensitive and selective than the chemiluminescence method used by Wagner et al. (2008), in this work we choose to use the uptake coefficient (0.02±0.01) reported by Tang et al. (2012), as recommended by the IUPAC task group, to assess $\tau_{het}(N_2O_5)$ in the troposphere.

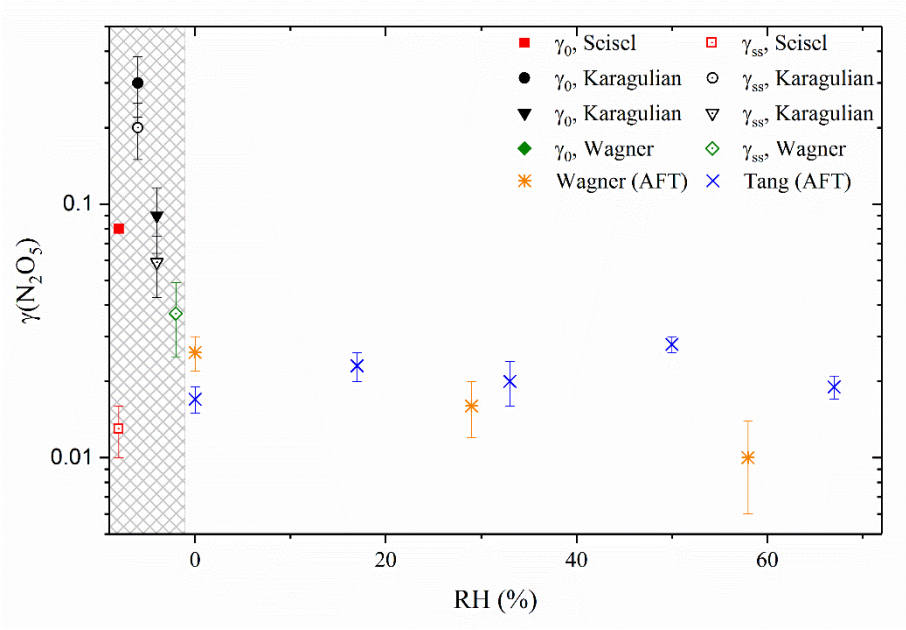

Figure 17. Uptake coefficients of N_2O_5 for Saharan dust, as reported by previous studies. Knudsen cell studies were all carried out under vacuum conditions (i.e. 0% RH), and for better readability these results are plotted in the region of RH <0% (shadowed region). Karagulian et al. (2006) reported γ_0 and γ_{ss} at two different N_2O_5 concentrations (circles: ~4×10^{11} molecule cm^{-3}; triangles: ~4×10^{12} molecule cm^{-3}); γ_0 and γ_{ss} reported by Wagner et al. (2008) using a Knudsen cell reactor are equal and thus overlapped with each other in Figure 17.

It is somehow unexpected that $\gamma(N_2O_5)$ onto SiO_2 reported by the first two studies (Mogili et al., 2006b; Wagner et al., 2009), both using aerosol samples, differ by about two orders of magnitude. A third study (Tang et al., 2014a), using an aerosol flow tube, concluded that this discrepancy is largely due to the fact that SiO_2 particles are likely to be porous. Mogili et al. (2006b) and Wagner et al. (2009) used BET surface area and the Stokes diameter to

calculate the aerosol surface area, respectively. If BET surface area is used, $\gamma(N_2O_5)$ reported by Tang et al. (2014a) show good agreement with those determined by Mogili et al. (2006b); if mobility diameters are used to derive aerosol surface area, they agree well with those reported by Wagner et al. (2009). Nevertheless, some discrepancies still remain: Wagner et al. (2009) and Tang et al. (2014a) suggested a small negative dependence of $\gamma(N_2O_5)$ on RH, and Mogili et al. (2006b) found that $\gamma(N_2O_5)$ significantly increase with RH. In addition, $\gamma(N_2O_5)$ onto $CaCO_3$ aerosol particles at <1% RH, as reported by Mogili et al. (2006b) and Wagner et al. (2009), differ by a factor of >20. It is not yet clear if the difference in calculating surface area (BET surface area versus Stokes diameter based surface area) could explain such a large difference, and further work is required to resolve this issue.

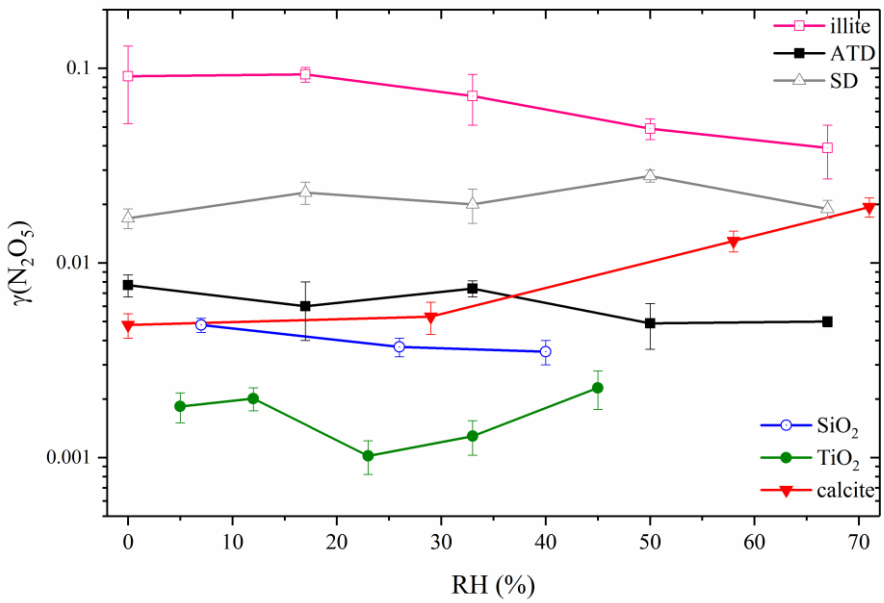

Figure 18. Uptake coefficients of N_2O_5 for Saharan dust (Tang et al., 2012), ATD (Tang et al., 2014c), illite (Tang et al., 2014c), $CaCO_3$ (Wagner et al., 2009), SiO_2 (Tang et al., 2014a), and TiO_2 (Tang et al., 2014d), as reported by aerosol flow tube studies.

Aerosol flow tubes have been deployed to investigate heterogeneous interactions of N_2O_5 with different types of mineral dust, with reported $\gamma(N_2O_5)$ summarized in Figure 18.

Two distinctive features can be identified. First, different minerals exhibit very different heterogeneous reactivity towards N_2O_5. $\gamma(N_2O_5)$ at <10% RH increase from $(1.83\pm0.32)\times10^{-3}$ for TiO_2 to 0.091±0.039 for illite, spanning over almost two orders of magnitude. Second, RH (and thus surface adsorbed water) plays important and various roles in uptake kinetics. For example, increasing RH significantly suppresses N_2O_5 uptake onto illite but largely enhances its uptake onto $CaCO_3$, while it does not show a significant effect for Saharan dust. In this paper $\gamma(N_2O_5)$ onto Saharan dust is used to assess the significance of heterogeneous reaction of N_2O_5 with mineral dust. Mineralogy of Asian dust is different from Saharan dust, and thus their heterogeneous reactivity (and probably the effect of RH) towards N_2O_5 can be different. Considering that Asian dust is transported over East Asia with high levels of NOx and O_3 (Zhang et al., 2007; Geng et al., 2008; Shao et al., 2009; Ding et al., 2013; Itahashi et al., 2014) and thus also N_2O_5 (Brown et al., 2016; Tham et al., 2016; Wang et al., 2016), heterogeneous reaction of N_2O_5 with Asian dust deserves further investigation.

Using $\gamma(N_2O_5)$ of 0.02, $\tau_{het}(N_2O_5)$ are estimated to be ~10 h, ~1 h, and ~6 min for dust loading of 10, 100, and 1000 μm m^{-3}, respectively. N_2O_5 lifetimes in the troposphere is typically in the range of several minutes to several hours, as shown in Table 1. Therefore, heterogeneous uptake by mineral dust could contribute significantly to and in some regions even dominate tropospheric N_2O_5 removal. Since uptake of N_2O_5 leads to the formation of nitrate, it can also substantially modify chemical composition and physicochemical properties of mineral dust.

A global modelling study (Dentener and Crutzen, 1993) suggested that including heterogeneous reaction of N_2O_5 with tropospheric aerosol particles with $\gamma(N_2O_5)$ equal to 0.1 could reduce modelled yearly average global NOx burden by 50%. It is found by other global and regional modelling studies (Evans and Jacob, 2005; Chang et al., 2016) that modelled NOx and O_3 concentrations agree better with observations if $\gamma(N_2O_5)$ parameterization based on new laboratory results is adopted. In the study by Evans and Jacob (2005), $\gamma(N_2O_5)$ was set to be

0.01 for mineral dust, independent of RH. A recent modelling study (Macintyre and Evans, 2010) suggests that simulated NOx, O_3, and OH concentrations are very sensitive to the choice of $\gamma(N_2O_5)$ in the range of 0.001-0.02, which significantly overlaps with the range of laboratory measured $\gamma(N_2O_5)$ for mineral dust particles. Therefore, in order to better assess the impacts of heterogeneous reaction of N_2O_5 with mineral dust on tropospheric oxidation capacity, $\gamma(N_2O_5)$ and its dependence on mineralogy and RH should be better understood.

Mineralogy and composition of mineral dust aerosol particles in the ambient air are always more complex than those for dust samples used in laboratory studies. Measurements of NO_3, N_2O_5, and other trace gases and aerosols in the troposphere enable steady-state NO_3 and N_2O_5 lifetimes to be determined and $\gamma(N_2O_5)$ onto ambient aerosol particles to be derived (Brown et al., 2006; Brown et al., 2009; Morgan et al., 2015; Phillips et al., 2016). It will be very beneficial to investigate N_2O_5 uptake (and other reactive trace gases as well) by ambient mineral dust aerosol. Recently such experimental apparatus, based on the aerosol flow tube technique, has been developed and deployed to directly measure $\gamma(N_2O_5)$ onto ambient aerosol particles (Bertram et al., 2009a; Bertram et al., 2009b). To our knowledge these measurements have never been carried out in dust-impacted regions yet, though they will undoubtedly improve our understanding of heterogeneous reaction of N_2O_5 with mineral dust in the troposphere.

Table 10: Summary of previous laboratory studies on heterogeneous reactions of mineral dust with NO_3 radicals

Dust	Reference	*T* (K)	Concentration (molecule cm^{-3})	Uptake coefficient	Techniques
Saharan dust	Karagulian and Rossi, 2005	298±2	$(0.7\text{-}4.0)\times10^{10}$	γ_0 = 0.23±0.20 and γ_{ss} = 0.12±0.08 when $[NO_3]_0 = (7.0\pm1.0)\times10^{11}$ cm^{-3}; γ_0 = 0.16±0.05 and γ_{ss} = 0.065±0.012 when $[NO_3]_0 = (4.0\pm1.0)\times10^{12}$ cm^{-3}.	KC
	Tang et al., 2010	296±2	$(0.4\text{-}1.6)\times10^{10}$	$\gamma(NO_3)/\gamma(N_2O_5)$ was reported to be 0.9±0.4, independent of RH (up to 70%).	CRDS
$CaCO_3$	Karagulian and Rossi, 2005	298±2	$(0.4\text{-}3.8)\times10^{12}$	γ_0 = 0.13±0.10 and γ_{ss} = 0.067±0.040 when $[NO_3]_0 = (7.0\pm1.0)\times10^{11}$ cm^{-3}; γ_0 = 0.14±0.05 and γ_{ss} = 0.014±0.004 when $[NO_3]_0 = (4.0\pm1.0)\times10^{12}$ cm^{-3}.	KC
kaolinite	Karagulian and Rossi, 2005	298±2	$(0.4\text{-}3.8)\times10^{12}$	γ_0 = 0.11±0.08 and γ_{ss} = 0.14±0.02 when $[NO_3]_0 = (7.0\pm1.0)\times10^{11}$ cm^{-3}; γ_0 = 0.12±0.04 and γ_{ss} = 0.065±0.012 when $[NO_3]_0 = (4.0\pm1.0)\times10^{12}$ cm^{-3}.	KC
limestone	Karagulian and Rossi, 2005	298±2	$(0.4\text{-}3.8)\times10^{12}$	γ_0 = 0.12±0.08 and γ_{ss} = 0.034±0.016 when $[NO_3]_0 = (7.0\pm1.0)\times10^{11}$ cm^{-3}; γ_0 = 0.20±0.07 and γ_{ss} = 0.022±0.005 when $[NO_3]_0 = (4.0\pm1.0)\times10^{12}$ cm^{-3}.	KC
ATD	Karagulian and Rossi, 2005	298±2	$(0.4\text{-}3.8)\times10^{12}$	γ_0 = 0.2±0.1 and γ_{ss} = 0.10±0.016 when $[NO_3]_0 = (7.0\pm1.0)\times10^{11}$ cm^{-3}; γ_0 = 0.14±0.04 and γ_{ss} = 0.025±0.007 when $[NO_3]_0 = (4.0\pm1.0)\times10^{12}$ cm^{-3}.	KC

3.6.2 NO_3 radicals

To our knowledge only two previous studies have explored heterogeneous uptake of NO_3 radicals by mineral dust particles. Heterogeneous reaction of NO_3 radicals with mineral dust was investigated for the first time at 298±2 K, using a Knudsen cell reactor (Karagulian and Rossi, 2005). Products observed in the gas phase include N_2O_5 (formed in the Eley-Rideal reaction of NO_3 with NO_2 on the dust surface) and HNO_3 (formed in the heterogeneous reaction of N_2O_5 and subsequently released into the gas phase) (Karagulian and Rossi, 2005). Surface deactivation occurred for all types of dust particles investigated. Dependence of uptake kinetics on the initial NO_3 concentration was observed (Karagulian and Rossi, 2005). When $[NO_3]_0$ was $(7.0\pm1.0)\times10^{11}$ cm^{-3}, the initial and steady-state uptake coefficients (γ_0 and γ_{ss}) were determined to be 0.13±0.10 and 0.067±0.040 for $CaCO_3$, 0.12±0.08 and 0.034±0.016 for natural limestone, 0.11±0.08 and 0.14±0.02 for kaolinite, 0.23±0.20 and 0.12±0.08 for Saharan dust, and 0.2±0.1 and 0.10±0.06 for ATD, respectively. When $[NO_3]_0$ was $(4.0\pm1.0)\times10^{12}$ cm^{-3}, γ_0 and γ_{ss} were determined to be 0.14±0.05 and 0.014±0.004 for $CaCO_3$, 0.20±0.07 and 0.022±0.005 for natural limestone, 0.12±0.04 and 0.050±0.014 for kaolinite, 0.16±0.05 and 0.065±0.012 for Saharan dust, and 0.14±0.04 and 0.025±0.007 for ATD, respectively.

In the second study (Tang et al., 2010), a novel relative rate method was developed to investigate heterogeneous uptake of NO_3 and N_2O_5 by mineral dust. Changes in NO_3 and N_2O_5 concentrations due to reactions with dust particles (loaded on filters) were simultaneously detected by cavity ring-down spectroscopy. Experiments were carried out at room temperature (296±2 K) and at different RH up to 70%. $\gamma(NO_3)/\gamma(N_2O_5)$ was reported to be 0.9±0.4 for Saharan dust particles, independent of RH within the experimental uncertainties (Tang et al., 2010). In addition, even though very low levels of NO_3 and N_2O_5 (a few hundred pptv) were used, surface deactivation was still observed for both species (Tang et al., 2010).

With the reported $\gamma(NO_3)/\gamma(N_2O_5)$ ratio of 0.9 (Tang et al., 2010), $\gamma(NO_3)$ of 0.018 is thus adopted to evaluate $\tau_{het}(NO_3)$ due to its heterogeneous uptake by mineral dust, based on the $\gamma(N_2O_5)$ value of 0.02 (Section 3.6.1). Using Eq. (6), mineral dust mass concentrations of 10, 100, and 1000 μm m^{-3} result in $\tau_{het}(NO_3)$ of ~9 h, ~52 min, and ~5 min, respectively. Field measurements, as summarized in Table 1, suggest that tropospheric NO_3 lifetimes are typically several minutes. Therefore, uptake by mineral dust is unlikely to be a significant sink for NO_3 in the troposphere, except for regions which are close to dust sources and thus heavily impacted by dust storms. Similar conclusions were drawn by Tang et al. (2010a) who used an uptake coefficient of 0.009 which is a factor of 2 smaller than the value used here. 3D GEOS-Chem model simulations suggest that modelled O_3 appears to be insensitive to the choice of $\gamma(NO_3)$ in the range of 0.0001 to 0.1 (Mao et al., 2013b). To conclude, heterogeneous reaction with mineral dust is not an important sink for tropospheric NO_3 radicals unless in regions with heavy dust loadings.

4. Summary and outlook

It has been widely recognized that heterogeneous reactions with mineral dust particles can significantly affect tropospheric oxidation capacity directly and indirectly. These reactions can also change the composition of dust particles, thereby modifying their physicochemical properties important for direct and indirect radiative forcing. In the past two decades there have been a large number of laboratory (as well as field and modelling) studies which have examined these reactions. In this paper we provide a comprehensive and timely review of laboratory studies of heterogeneous reactions of mineral dust aerosol with OH, NO_3, and O_3 as well as several other reactive species (including HO_2, H_2O_2, HCHO, HONO, and N_2O_5) which are directly related to OH, NO_3, and O_3. Lifetimes of these species with respect to heterogeneous uptake by mineral dust are compared to their lifetimes due to other major loss processes in the troposphere in order to provide a quick assessment of atmospheric significance of

heterogeneous reactions as sinks for these species. In addition, representative field and modelling work is also discussed to further illustrate the roles these heterogeneous reactions play in tropospheric oxidation capacity. As shown in Section 3, these studies have significantly improved our understanding of the effects of these reactions on tropospheric oxidation capacity. Nevertheless, there are still a number of open questions which cannot be answered by laboratory work alone but only by close collaboration among laboratory, field, and modelling studies. Several major challenges, and strategies we proposed to address these challenges, are outlined below.

1) Mineral dust in the troposphere are in fact mineralogically complex and its mineralogy vary with dust sources and also residence time in the troposphere (Claquin et al., 1999; Ta et al., 2003; Zhang et al., 2003a; Nickovic et al., 2012; Journet et al., 2014; Scanza et al., 2015). Different minerals can exhibit large variabilities in heterogeneous reactivity towards trace gases, as shown by Tables 4-10. However, Tables 4-10 also reveal that simple oxides (e.g., SiO_2 and Al_2O_3) and $CaCO_3$ have been much more widely investigated compared to authentic dust samples (probably except ATD) and clay minerals which are the major components of mineral dust aerosol particles (Claquin et al., 1999). The relative importance of clay minerals will be increased after long-range transport due to their smaller sizes compared to SiO_2 and $CaCO_3$. Therefore, more attention should be paid in future work to heterogeneous reactions of clay minerals and authentic dust samples.

2) In the last several years, important roles that RH (and thus surface adsorbed water) plays in heterogeneous reactions of mineral dust have been widely recognized by many studies and discussed in a recent review paper (Rubasinghege and Grassian, 2013). Tables 4-10 show that most of previous studies have been conducted at RH <80%, and heterogeneous reactivity at higher RH largely remain unknown. In addition, effects of RH on heterogeneous reactions of mineral dust with a few important reactive trace gases, such as HO_2 radicals (Bedjanian et

al., 2013a; Matthews et al., 2014) and O_3 (Sullivan et al., 2004; Chang et al., 2005; Mogili et al., 2006a), are still under debate. It has been known that heterogeneous processing can modify chemical composition and hygroscopicity of mineral dust particles (Tang et al., 2016a), and at evaluated RH aged dust particles may consist of a solid core and an aqueous shell (Krueger et al., 2003b; Laskin et al., 2005a; Liu et al., 2008b; Shi et al., 2008; Li and Shao, 2009; Ma et al., 2012). Under such circumstances, reactions are no longer limited to particle surface but instead involve gas, liquid, and solid phases and their interfaces, and hence mutual influence among chemical reactivity, composition, and physiochemical properties has to be taken into account (Tang et al., 2016a).

3) Temperature in the troposphere varies from <200 K to >300 K. However, most of laboratory studies of heterogeneous reactions of mineral dust were carried out at room temperature (around 296 K). Once lifted into the atmosphere, mineral dust aerosol is mainly transported in the free troposphere in which temperature is much lower than that at the ground level. Some work has started to examine the influence of temperature on heterogeneous uptake by mineral dust (Michel et al., 2003; Xu et al., 2006; Xu et al., 2010; Wu et al., 2011; Xu et al., 2011; Romanias et al., 2012a; Romanias et al., 2012b; Zhou et al., 2012; Bedjanian et al., 2013a; El Zein et al., 2013a; El Zein et al., 2013b; Romanias et al., 2013; Wu et al., 2013b; El Zein et al., 2014; Hou et al., 2016; Zhou et al., 2016). It has been found temperature may have significant effects on some reactions. However, to the best of our knowledge, no study has explored the influence of temperature on heterogeneous reactions of airborne mineral dust particles.

4) Laboratory studies may not entirely mimic actual heterogeneous reactions in the troposphere due to several reasons. First of all, laboratory studies are typically carried out with time scales of <1 min to several hours, compared to lifetimes of a few days for mineral dust in the troposphere. Secondly, it is not uncommon that concentrations of reactive trace gases used

in laboratory work are several orders of magnitude larger than those in the troposphere. These two aspects can make it non-trivial to extrapolate laboratory results to the real atmosphere. In addition, dust samples used in laboratory studies, even when authentic dust samples are used, do not exactly mimic the complexity of ambient dust particles in composition and mineralogy. Very recently a new type of experiments, sometimes called "laboratory work in the field", can at least partly provide solutions to this challenge. For example, an aerosol flow tube has been deployed to explore heterogeneous uptake of N_2O_5 by ambient aerosol particles at a few locations (Bertram et al., 2009a; Bertram et al., 2009b; Ryder et al., 2014), revealing the roles of RH and particle composition in heterogeneous reactivity of ambient aerosol particles. To our knowledge, this technique has not been used to investigate heterogeneous uptake of N_2O_5 by ambient mineral dust aerosol. This technique can also be extended to examine heterogeneous reactions of ambient aerosol particles with other reactive trace gases, especially those whose heterogeneous reactions are anticipated to be efficient (e.g., HO_2 and H_2O_2).

5) Decrease in heterogeneous reactivity due to surface passivation has been observed by many studies using dust powders supported by substrates. On the other hand, increase in heterogeneous reactivity, due to conversion of solid particles to aqueous droplets with solid cores (caused by formation of hygroscopic materials), has also been reported. In addition, it has been widely recognized that the co-presence of two or more reactive trace gases may change the rates of heterogeneous reactions of each individual gases (Li et al., 2006; Raff et al., 2009; Liu et al., 2012; Rubasinghege and Grassian, 2012; Wu et al., 2013a; Zhao et al., 2015; Yang et al., 2016a), typically termed as synergistic effects. Parameterization of these complex processes is very difficult, and lack of sophisticated bulk parameterizations impedes us from a quantitative assessment of their atmospheric significance via modelling studies. Kinetic models have been developed to integrate physical and chemical processes in and between different phases (Pöschl et al., 2007; Shiraiwa et al., 2012; Berkemeier et al., 2013),

and these models have been successfully used to investigate multiphase chemistry of aqueous aerosol particles and cloud droplets (Shiraiwa et al., 2011; Arangio et al., 2015; Pöschl and Shiraiwa, 2015). Future efforts devoted to development and application of comprehensive kinetic models to study heterogeneous and multiphase reactions of mineral dust particles would largely improve our understanding in the field.

6) It has been found that UV and visible radiation can substantially enhance the heterogeneous reactivity of mineral dust towards several trace gases, including but not limited to H_2O_2, O_3, and HCHO, and in some cases even reactivate mineral surfaces which have been passivated (Cwiertny et al., 2008; Chen et al., 2012; George et al., 2015). In addition, photolysis of materials (such as nitrate) formed on mineral surface can also be sources for some trace gases (Nanayakkara et al., 2013; Gankanda and Grassian, 2014; Nanayakkara et al., 2014). Although the effects of photo-radiation in heterogeneous reactions with mineral dust have been recognized for more than one decade, it largely remains unclear to which extent these reactions are photo-enhanced under ambient solar radiation and thus quantitative evaluation of impacts of heterogeneous photochemistry on tropospheric oxidation capacity is lacking.

7) There still exists a considerably large gap between laboratory work and modelling studies used to explain field measurements and predict future changes. One reason is that the communication and collaboration between laboratory and modelling communities, though enhanced in the past few decades, are still not enough and should be further encouraged and stimulated in future. Furthermore, many laboratory studies have been designed from the perspective of classical chemical kinetics such that although experimental results are beautiful, they are difficult to be parameterized and then included in models. As mentioned, heterogeneous reactivity is highly dependent on temperature, RH, co-presence of other trace gases and mutual influences among these factors. Given that most models are capable of resolving/assimilating meteorological variables and trace gas concentrations at high temporal

resolution, multivariate analysis and integrated numerical expressions are encouraged to be conducted in laboratory studies so as to better characterize heterogeneous chemistry and its climate and environmental effects in numerical models. Therefore, it is suggested that when a laboratory study is designed, it should be kept in mind how experimental results can be used by modelling studies. On the other hand, modelling work is encouraged to include new laboratory results in numerical simulations and to identify missing reactions and key parameters which deserve further laboratory investigation. Field campaigns which are specifically designed to assess the impacts of mineral dust aerosol on tropospheric oxidation capacity have been proved to be very beneficial (de Reus et al., 2000; Galy-Lacaux et al., 2001; Seinfeld et al., 2004; Tang et al., 2004; de Reus et al., 2005; Umann et al., 2005; Arimoto et al., 2006; Song et al., 2007), and more campaigns of this types should be organized. Overall, as urged by a few recent articles (Kolb et al., 2010; Abbatt et al., 2014; Burkholder et al., 2017), the three-legged stool approach (laboratory studies, field observations, and modelling studies) adopted by atmospheric chemistry research for a long time should be emphasized, and mutual communication and active collaboration among these three “legs” should be further enhanced.

Acknowledgement

The preparation of this manuscript was inspired by the first International Workshop on Heterogeneous Atmospheric Chemistry (August 2015, Beijing, China) endorsed by the International Global Atmospheric Chemistry (IGAC) Project, and Mingjin Tang and Tong Zhu would like to thank all the participants for their valuable presentations and discussion. Financial support provided by Chinese National Science Foundation (41675140 and 21522701), Chinese Academy of Sciences international collaborative project (132744KYSB20160036), and State Key Laboratory of Organic Geochemistry (SKLOGA201603A) is acknowledged. Mingjin Tang is also sponsored by Chinese Academy of Sciences Pioneer Hundred Talents Program.

Reference

Abbatt, J., George, C., Melamed, M., Monks, P., Pandis, S., and Rudich, Y.: New Directions: Fundamentals of atmospheric chemistry: Keeping a three-legged stool balanced, Atmos. Environ., 84, 390-391, 2014.

Abbatt, J. P. D., Lee, A. K. Y., and Thornton, J. A.: Quantifying trace gas uptake to tropospheric aerosol: recent advances and remaining challenges, Chem. Soc. Rev., 41, 6555-6581, 2012.

Akimoto, H.: Heterogeneous Reactions in the Atmosphere and Uptake Coefficients, in: Atmospheric Reaction Chemistry, Springer Japan, Tokyo, 239-284, 2016.

Aldener, M., Brown, S. S., Stark, H., Williams, E. J., Lerner, B. M., Kuster, W. C., Goldan, P. D., Quinn, P. K., Bates, T. S., Fehsenfeld, F. C., and Ravishankara, A. R.: Reactivity and loss mechanisms of NO3 and N2O5 in a polluted marine environment: Results from in situ measurements during New England Air Quality Study 2002, J. Geophys. Res.-Atmos., 111, D23S73, DOI: 10.1029/2006JD007252, 2006.

Alebić-Juretić, A., Cvitaš, T., and Klasinc, L.: Ozone Destruction on Powders, Ber. Bunsenges. Phys. Chem., 96, 493-495, 1992.

Alfaro, S. C., Gomes, L., Rajot, J. L., Lafon, S., Gaudichet, A., Chatenet, B., Maille, M., Cautenet, G., Lasserre, F., Cachier, H., and Zhang, X. Y.: Chemical and optical characterization of aerosols measured in spring 2002 at the ACE-Asia supersite, Zhenbeitai, China, J. Geophys. Res.-Atmos., 108, 2003.

Alicke, B., Geyer, A., Hofzumahaus, A., Holland, F., Konrad, S., Patz, H. W., Schafer, J., Stutz, J., Volz-Thomas, A., and Platt, U.: OH formation by HONO photolysis during the BERLIOZ experiment, J. Geophys. Res.-Atmos., 108, 8247, doi: 8210.1029/2001jd000579, 2003.

Ammann, M., and Poschl, U.: Kinetic model framework for aerosol and cloud surface chemistry and gas-particle interactions - Part 2: Exemplary practical applications and numerical simulations, Atmos. Chem. Phys., 7, 6025-6045, 2007.

Ammann, M., Cox, R. A., Crowley, J. N., Jenkin, M. E., Mellouki, A., Rossi, M. J., Troe, J., and Wallington, T. J.: Evaluated kinetic and photochemical data for atmospheric chemistry: Volume VI - heterogeneous reactions with liquid substrates, Atmos. Chem. Phys., 12, 8045-8228, 2013.

Ammar, R., Monge, M. E., George, C., and D'Anna, B.: Photoenhanced NO2 Loss on Simulated Urban Grime, ChemPhysChem, 11, 3956-3961, 2010.

Ao, C. H., Lee, S. C., Yu, J. Z., and Xu, J. H.: Photodegradation of formaldehyde by photocatalyst TiO_2: effects on the presences of NO, SO_2 and VOCs, Appl. Catal., B: Environ., 54, 41-50, 2004.

Arangio, A. M., Slade, J. H., Berkemeier, T., Poschl, U., Knopf, D. A., and Shiraiwa, M.: Multiphase Chemical Kinetics of OH Radical Uptake by Molecular Organic Markers of Biomass Burning Aerosols: Humidity and Temperature Dependence, Surface Reaction, and Bulk Diffusion, J. Phys. Chem. A, 119, 4533-4544, 2015.

Arimoto, R., Kim, Y. J., Kim, Y. P., Quinn, P. K., Bates, T. S., Anderson, T. L., Gong, S., Uno, I., Chin, M., Huebert, B. J., Clarke, A. D., Shinozuka, Y., Weber, R. J., Anderson, J. R., Guazzotti, S. A., Sullivan, R. C., Sodeman, D. A., Prather, K. A., and Sokolik, I. N.: Characterization of Asian Dust during ACE-Asia, Glob. Planet. Change, 52, 23-56, 2006.

Atkinson, R., Baulch, D. L., Cox, R. A., Crowley, J. N., Hampson, R. F., Hynes, R. G., Jenkin, M. E., Rossi, M. J., and Troe, J.: Evaluated kinetic and photochemical data for atmospheric chemistry: Volume I - gas phase reactions of Ox, HOx, NOx and SOx species, Atmos. Chem. Phys., 4, 1461-1738, 2004.

Atkinson, R., Baulch, D. L., Cox, R. A., Crowley, J. N., Hampson, R. F., Hynes, R. G., Jenkin, M. E., Rossi, M. J., and Troe, J.: Evaluated kinetic and photochemical data for atmospheric chemistry: Volume II - gas phase reactions of organic species, Atmos. Chem. Phys., 6, 3625-4055, 2006.

Baergen, A. M., and Donaldson, D. J.: Formation of reactive nitrogen oxides from urban grime photochemistry, Atmos. Chem. Phys., 16, 6355-6363, 2016.

Balkanski, Y., Schulz, M., Claquin, T., and Guibert, S.: Reevaluation of Mineral Aerosol Radiative Forcings Suggests a Better Agreement with Satellite and AERONET Data, Atmos. Chem. Phys., 7, 81-95, 2007.

Bauer, S. E., Balkanski, Y., Schulz, M., Hauglustaine, D. A., and Dentener, F.: Global modeling of heterogeneous chemistry on mineral aerosol surfaces: Influence on tropospheric ozone chemistry and comparison to observations, J. Geophys. Res.-Atmos., 109, D02304, doi: 02310.01029/02003JD003868, 2004.

Bedjanian, Y., Romanias, M. N., and El Zein, A.: Uptake of HO_2 Radicals on Arizona Test Dust, Atmos. Chem. Phys., 12, 6461-6471, 2013a.

Bedjanian, Y., Romanias, M. N., and El Zein, A.: Interaction of OH Radicals with Arizona Test Dust: Uptake and Products, J. Phys. Chem. A, 117, 393-400, 2013b.

Berkemeier, T., Huisman, A. J., Ammann, M., Shiraiwa, M., Koop, T., and Pöschl, U.: Kinetic regimes and limiting cases of gas uptake and heterogeneous reactions in atmospheric aerosols and clouds: a general classification scheme, Atmos. Chem. Phys., 13, 6663-6686, 2013.

Bertram, A. K., Ivanov, A. V., Hunter, M., Molina, L. T., and Molina, M. J.: The Reaction Probability of OH on Organic Surfaces of Tropospheric Interest, J. Phys. Chem. A, 105, 9415-9421, 2001.

Bertram, T. H., Thornton, J. A., and Riedel, T. P.: An experimental technique for the direct measurement of N_2O_5 reactivity on ambient particles, Atmos. Meas. Tech., 2, 231-242, 2009a.

Bertram, T. H., Thornton, J. A., Riedel, T. P., Middlebrook, A. M., Bahreini, R., Bates, T. S., Quinn, P. K., and Coffman, D. J.: Direct observations of N_2O_5 reactivity on ambient aerosol particles, Geophys. Res. Lett., 36, L19803, 19810.11029/12009gl040248, 2009b.

Bi, J., Huang, J., Holben, B., and Zhang, G.: Comparison of key absorption and optical properties between pure and transported anthropogenic dust over East and Central Asia, Atmos. Chem. Phys., 16, 15501-15516, 2016.

Bi, J., Huang, J., Shi, J., Hu, Z., Zhou, T., Zhang, G., Huang, Z., Wang, X., and Jin, H.: Measurement of scattering and absorption properties of dust aerosol in a Gobi farmland region of northwestern China – a potential anthropogenic influence, Atmos. Chem. Phys., 17, 7775-7792, 2017.

Bian, H. S., and Zender, C. S.: Mineral dust and global tropospheric chemistry: Relative roles of photolysis and heterogeneous uptake, J. Geophys. Res.-Atmos., 108, 2003.

Bogart, K. H. A., Cushing, J. P., and Fisher, E. R.: Effects of Plasma Processing Parameters on the Surface Reactivity of OH(X2Π) in Tetraethoxysilane/O_2 Plasmas during Deposition of SiO_2, J. Phys. Chem. B, 101, 10016-10023, 1997.

Boyd, P. W., and Ellwood, M. J.: The biogeochemical cycle of iron in the ocean, Nature Geosci, 3, 675-682, 2010.

Brauers, T., Hausmann, M., Bister, A., Kraus, A., and Dorn, H.-P.: OH radicals in the boundary layer of the Atlantic Ocean: 1. Measurements by long-path laser absorption spectroscopy, J. Geophys. Res.-Atmos, 106, 7399-7414, 2001.

Brown, S. S., Ryerson, T. B., Wollny, A. G., Brock, C. A., Peltier, R., Sullivan, A. P., Weber, R. J., Dube, W. P., Trainer, M., Meagher, J. F., Fehsenfeld, F. C., and Ravishankara, A. R.:

Variability in nocturnal nitrogen oxide processing and its role in regional air quality, Science, 311, 67-70, 2006.

Brown, S. S., Dube, W. P., Fuchs, H., Ryerson, T. B., Wollny, A. G., Brock, C. A., Bahreini, R., Middlebrook, A. M., Neuman, J. A., Atlas, E., Roberts, J. M., Osthoff, H. D., Trainer, M., Fehsenfeld, F. C., and Ravishankara, A. R.: Reactive uptake coefficients for N2O5 determined from aircraft measurements during the Second Texas Air Quality Study: Comparison to current model parameterizations, J. Geophys. Res.-Atmos., 114, D00F10, DOI: 10.1029/2008JD011679, 2009.

Brown, S. S., and Stutz, J.: Nighttime radical observations and chemistry, Chem. Soc. Rev., 41, 6405-6447, 2012.

Brown, S. S., Dube, W. P., Tham, Y. J., Zha, Q. Z., Xue, L. K., Poon, S., Wang, Z., Blake, D. R., Tsui, W., Parrish, D. D., and Wang, T.: Nighttime chemistry at a high altitude site above Hong Kong, J. Geophys. Res.-Atmos., 121, 2457-2475, 2016.

Burkholder, J. B., Sander, S. P., Abbatt, J. P. D., Barker, J. R., Huie, R. E., Kolb, C. E., Kurylo, M. J., Orkin, V. L., Wilmouth, D. M., and Wine, P. H.: Chemical Kinetics and Photochemical Data for Use in Atmospheric Studies, Evaluation No. 18, JPL Publication 15-10, Jet Propulsion Lab., Pasadena, CA, 2015.

Burkholder, J. B., Abbatt, J. P. D., Barnes, I., Roberts, J. M., Melamed, M. L., Ammann, M., Bertram, A. K., Cappa, C. D., Carlton, A. G., Carpenter, L. J., Crowley, J. N., Dubowski, Y., George, C., Heard, D. E., Herrmann, H., Keutsch, F. N., Kroll, J. H., McNeill, V. F., Ng, N. L., Nizkorodov, S. A., Orlando, J. J., Percival, C. J., Picquet-Varrault, B., Rudich, Y., Seakins, P. W., Surratt, J. D., Tanimoto, H., Thornton, J. A., Tong, Z., Tyndall, G. S., Wahner, A., Weschler, C. J., Wilson, K. R., and Ziemann, P. J.: The Essential Role for Laboratory Studies in Atmospheric Chemistry, Environ. Sci. Technol., 51, 2519-2528, 2017.

Carlos-Cuellar, S., Li, P., Christensen, A. P., Krueger, B. J., Burrichter, C., and Grassian, V. H.: Heterogeneous Uptake Kinetics of Volatile Organic Compounds on Oxide Surfaces Using a Knudsen Cell Reactor: Adsorption of Acetic Acid, Formaldehyde, and Methanol on α-Fe_2O_3, α-Al_2O_3, and SiO_2, J. Phys. Chem. A, 107, 4250-4261, 2003.

Chang, R. Y. W., Sullivan, R. C., and Abbatt, J. P. D.: Initial uptake of ozone on Saharan dust at atmospheric relative humidities, Geophys. Res. Lett., 32, L14815, doi: 14810.11029/12005GL023317, 2005.

Chang, W. L., Brown, S. S., Stutz, J., Middlebrook, A. M., Bahreini, R., Wagner, N. L., Dubé, W. P., Pollack, I. B., Ryerson, T. B., and Riemer, N.: Evaluating N2O5 heterogeneous hydrolysis parameterizations for CalNex 2010, J. Geophys. Res.-Atmos, 121, 5051-5070, 2016.

Chatani, S., Shimo, N., Matsunaga, S., Kajii, Y., Kato, S., Nakashima, Y., Miyazaki, K., Ishii, K., and Ueno, H.: Sensitivity analyses of OH missing sinks over Tokyo metropolitan area in the summer of 2007, Atmos. Chem. Phys., 9, 8975-8986, 2009.

Chen, H. H., Navea, J. G., Young, M. A., and Grassian, V. H.: Heterogeneous Photochemistry of Trace Atmospheric Gases with Components of Mineral Dust Aerosol, J. Phys. Chem. A, 115, 490-499, 2011a.

Chen, H. H., Stanier, C. O., Young, M. A., and Grassian, V. H.: A Kinetic Study of Ozone Decomposition on Illuminated Oxide Surfaces, J. Phys. Chem. A, 115, 11979-11987, 2011b.

Chen, H. H., Nanayakkara, C. E., and Grassian, V. H.: Titanium Dioxide Photocatalysis in Atmospheric Chemistry, Chem. Rev., 112, 5919-5948, 2012.

Chen, Z. M., Jie, C. Y., Li, S., Wang, H. L., Wang, C. X., Xu, J. R., and Hua, W.: Heterogeneous reactions of methacrolein and methyl vinyl ketone: Kinetics and mechanisms of uptake and ozonolysis on silicon dioxide, J. Geophys. Res.-Atmos, 113, D22303, doi: 22310.21029/22007JD009754, 2008.

Chernoff, D. I., and Bertram, A. K.: Effects of sulfate coatings on the ice nucleation properties of a biological ice nucleus and several typs of minerals, J. Geophys. Res.-Atmos., 115, D20205, doi: 20210.21029/22010JD014254, 2010.

Chou, C., Formenti, P., Maille, M., Ausset, P., Helas, G., Harrison, M., and Osborne, S.: Size distribution, shape, and composition of mineral dust aerosols collected during the African Monsoon Multidisciplinary Analysis Special Observation Period 0: Dust and Biomass-Burning Experiment field campaign in Niger, January 2006, J. Geophys. Res.-Atmos., 113, D00C10, doi: 10.1029/2008jd009897, 2008.

Claquin, T., Schulz, M., and Balkanski, Y. J.: Modeling the mineralogy of atmospheric dust sources, J. Geophys. Res.-Atmos., 104, 22243-22256, 1999.

Creamean, J. M., Suski, K. J., Rosenfeld, D., Cazorla, A., DeMott, P. J., Sullivan, R. C., White, A. B., Ralph, F. M., Minnis, P., Comstock, J. M., Tomlinson, J. M., and Prather, K. A.: Dust and Biological Aerosols from the Sahara and Asia Influence Precipitation in the Western U.S, Science, 339, 1572-1578, 2013.

Crowley, J. N., Ammann, M., Cox, R. A., Hynes, R. G., Jenkin, M. E., Mellouki, A., Rossi, M. J., Troe, J., and Wallington, T. J.: Evaluated Kinetic and Photochemical Data for Atmospheric Chemistry: Volume V - Heterogeneous Reactions on Solid Substrates, Atmos. Chem. Phys., 10, 9059-9223, 2010a.

Crowley, J. N., Schuster, G., Pouvesle, N., Parchatka, U., Fischer, H., Bonn, B., Bingemer, H., and Lelieveld, J.: Nocturnal nitrogen oxides at a rural mountain-site in south-western Germany, Atmos. Chem. Phys., 10, 2795-2812, 2010b.

Crutzen, P. J.: Albedo enhancement by stratospheric sulfur injections: A contribution to resolve a policy dilemma?, Clim. Change, 77, 211-219, 2006.

Cwiertny, D. M., Young, M. A., and Grassian, V. H.: Chemistry and photochemistry of mineral dust aerosol, Annu. Rev. Phys. Chem., 59, 27-51, 2008.

Cziczo, D. J., Froyd, K. D., Hoose, C., Jensen, E. J., Diao, M., Zondlo, M. A., Smith, J. B., Twohy, C. H., and Murphy, D. M.: Clarifying the Dominant Sources and Mechanisms of Cirrus Cloud Formation, Science, 340, 1320-1324, 2013.

Davidovits, P., Kolb, C. E., Williams, L. R., Jayne, J. T., and Worsnop, D. R.: Update 1 of: Mass Accommodation and Chemical Reactions at Gas-Liquid Interfaces, Chem. Rev., 111, PR76-PR109, 2011.

De Laurentiis, E., Socorro, J., Vione, D., Quivet, E., Brigante, M., Mailhot, G., Wortham, H., and Gligorovski, S.: Phototransformation of 4-phenoxyphenol sensitised by 4-carboxybenzophenone: Evidence of new photochemical pathways in the bulk aqueous phase and on the surface of aerosol deliquescent particles, Atmos. Environ., 81, 569-578, 2013.

De Longueville, F., Hountondji, Y.-C., Henry, S., and Ozer, P.: What do we know about effects of desert dust on air quality and human health in West Africa compared to other regions?, Sci. Total Environ., 409, 1-8, 2010.

de Longueville, F., Ozer, P., Doumbia, S., and Henry, S.: Desert dust impacts on human health: an alarming worldwide reality and a need for studies in West Africa, Int. J. Biometeorol., 57, 1-19, 2013.

de Reus, M., Dentener, F., Thomas, A., Borrmann, S., Strom, J., and Lelieveld, J.: Airborne observations of dust aerosol over the North Atlantic Ocean during ACE 2: Indications for heterogeneous ozone destruction, J. Geophys. Res.-Atmos., 105, 15263-15275, 2000.

de Reus, M., Fischer, H., Sander, R., Gros, V., Kormann, R., Salisbury, G., Van Dingenen, R., Williams, J., Zollner, M., and Lelieveld, J.: Observations and model calculations of trace gas scavenging in a dense Saharan dust plume during MINATROC, Atmos. Chem. Phys., 5, 1787-1803, 2005.

DeMott, P. J., Sassen, K., Poellot, M. R., Baumgardner, D., Rogers, D. C., Brooks, S. D., Prenni, A. J., and Kreidenweis, S. M.: African dust aerosols as atmospheric ice nuclei, Geophys. Res. Lett., 30, 1732, doi: 1710.1029/2003gl017410, 2003.

DeMott, P. J., Prenni, A. J., McMeeking, G. R., Sullivan, R. C., Petters, M. D., Tobo, Y., Niemand, M., Möhler, O., Snider, J. R., Wang, Z., and Kreidenweis, S. M.: Integrating laboratory and field data to quantify the immersion freezing ice nucleation activity of mineral dust particles, Atmos. Chem. Phys., 15, 393-409, 2015.

Dentener, F. J., and Crutzen, P. J.: Reaction of N_2O_5 on tropospheric aerosols: Impact on the global distributions of NOx , O_3, and OH, J. Geophys. Res.-Atmos., 98, 7149-7163, 1993.

Dentener, F. J., Carmichael, G. R., Zhang, Y., Lelieveld, J., and Crutzen, P. J.: Role of Mineral Aerosol as a Reactive Surface in the Global Troposphere, J. Geophys. Res.-Atmos., 101, 22869-22889, 1996.

Dhandapani, B., and Oyama, S. T.: Gas phase ozone decomposition catalysts, Appl. Catal., B: Environ., 11, 129-166, 1997.

Ding, A. J., Fu, C. B., Yang, X. Q., Sun, J. N., Zheng, L. F., Xie, Y. N., Herrmann, E., Nie, W., Petäjä, T., Kerminen, V. M., and Kulmala, M.: Ozone and fine particle in the western Yangtze River Delta: an overview of 1 yr data at the SORPES station, Atmos. Chem. Phys., 13, 5813-5830, 2013.

Donaldson, M. A., Berke, A. E., and Raff, J. D.: Uptake of Gas Phase Nitrous Acid onto Boundary Layer Soil Surfaces, Environ. Sci. Technol., 48, 375-383, 2014.

Dusanter, S., Vimal, D., Stevens, P. S., Volkamer, R., Molina, L. T., Baker, A., Meinardi, S., Blake, D., Sheehy, P., Merten, A., Zhang, R., Zheng, J., Fortner, E. C., Junkermann, W., Dubey, M., Rahn, T., Eichinger, B., Lewandowski, P., Prueger, J., and Holder, H.: Measurements of OH and HO2 concentrations during the MCMA-2006 field campaign - Part 2: Model comparison and radical budget, Atmos. Chem. Phys., 9, 6655-6675, 2009.

Duvall, R. M., Majestic, B. J., Shafer, M. M., Chuang, P. Y., Simoneit, B. R. T., and Schauer, J. J.: The water-soluble fraction of carbon, sulfur, and crustal elements in Asian aerosols and Asian soils, Atmos. Environ., 42, 5872-5884, 2008.

Edwards, P. M., Brown, S. S., Roberts, J. M., Ahmadov, R., Banta, R. M., deGouw, J. A., Dube, W. P., Field, R. A., Flynn, J. H., Gilman, J. B., Graus, M., Helmig, D., Koss, A., Langford, A. O., Lefer, B. L., Lerner, B. M., Li, R., Li, S.-M., McKeen, S. A., Murphy, S. M., Parrish, D. D., Senff, C. J., Soltis, J., Stutz, J., Sweeney, C., Thompson, C. R., Trainer, M. K., Tsai, C., Veres, P. R., Washenfelder, R. A., Warneke, C., Wild, R. J., Young, C. J., Yuan, B., and Zamora, R.: High winter ozone pollution from carbonyl photolysis in an oil and gas basin, Nature, 514, 351-354, 2014.

Ehhalt, D. H.: Photooxidation of trace gases in the troposphere Plenary Lecture, Phys. Chem. Chem. Phys., 1, 5401-5408, 1999.

El Zein, A., and Bedjanian, Y.: Reactive Uptake of HONO to TiO_2 Surface: "Dark" Reaction, J. Phys. Chem. A, 116, 3665-3672, 2012.

El Zein, A., Bedjanian, Y., and Romanias, M. N.: Kinetics and products of HONO interaction with TiO_2 surface under UV irradiation, Atmos. Environ., 67, 203-210, 2013a.

El Zein, A., Romanias, M. N., and Bedjanian, Y.: Kinetics and Products of Heterogeneous Reaction of HONO with Fe_2O_3 and Arizona Test Dust, Environ. Sci. Technol., 47, 6325-6331, 2013b.

El Zein, A., Romanias, M. N., and Bedjanian, Y.: Heterogeneous Interaction of H_2O_2 with Arizona Test Dust, J. Phys. Chem. A, 118, 441-448, 2014.

Evans, M. J., and Jacob, D. J.: Impact of new laboratory studies of N_2O_5 hydrolysis on global model budgets of tropospheric nitrogen oxides, ozone, and OH, Geophys. Res. Lett., 32, L09813, doi:09810.01029/02005GL022469, 2005.

Fitzgerald, E., Ault, A. P., Zauscher, M. D., Mayol-Bracero, O. L., and Prather, K. A.: Comparison of the mixing state of long-range transported Asian and African mineral dust, Atmos. Environ., 115, 19-25, 2015.
Formenti, P., Schutz, L., Balkanski, Y., Desboeufs, K., Ebert, M., Kandler, K., Petzold, A., Scheuvens, D., Weinbruch, S., and Zhang, D.: Recent progress in understanding physical and chemical properties of African and Asian mineral dust, Atmos. Chem. Phys., 11, 8231-8256, 2011.
Formenti, P., Caquineau, S., Desboeufs, K., Klaver, A., Chevaillier, S., Journet, E., and Rajot, J. L.: Mapping the physico-chemical properties of mineral dust in western Africa: mineralogical composition, Atmos. Chem. Phys., 14, 10663-10686, 2014.
Fuller, E. N., Schettle.Pd, and Giddings, J. C.: A new method for prediction of binary gas-phase diffusion coefficients, Ind. Eng. Chem., 58, 19-27, 1966.
Galy-Lacaux, C., Carmichael, G. R., Song, C. H., Lacaux, J. P., Al Ourabi, H., and Modi, A. I.: Heterogeneous processes involving nitrogenous compounds and Saharan dust inferred from measurements and model calculations, J. Geophys. Res.-Atmos., 106, 12559-12578, 2001.
Gankanda, A., and Grassian, V. H.: Nitrate Photochemistry on Laboratory Proxies of Mineral Dust Aerosol: Wavelength Dependence and Action Spectra, J. Phys. Chem. C, 118, 29117-29125, 2014.
Garimella, S., Huang, Y. W., Seewald, J. S., and Cziczo, D. J.: Cloud condensation nucleus activity comparison of dry- and wet-generated mineral dust aerosol: the significance of soluble material, Atmos. Chem. Phys., 14, 6003-6019, 2014.
Ge, M. F., Wu, L. Y., Tong, S. R., Liu, Q. F., and Wang, W. G.: Heterogeneous chemistry of trace atmospheric gases on atmospheric aerosols: an overview, Science Foundation in China, 23, 62-80, 2015.
Geng, F., Tie, X., Xu, J., Zhou, G., Peng, L., Gao, W., Tang, X., and Zhao, C.: Characterizations of ozone, NOx, and VOCs measured in Shanghai, China, Atmos. Environ., 42, 6873-6883, 2008.
George, C., Ammann, M., D'Anna, B., Donaldson, D. J., and Nizkorodov, S. A.: Heterogeneous Photochemistry in the Atmosphere, Chem. Rev., 115, 4218-4258, 2015.
George, C., Beeldens, A., Barmpas, F., Doussin, J.-F., Manganelli, G., Herrmann, H., Kleffmann, J., and Mellouki, A.: Impact of photocatalytic remediation of pollutants on urban air quality, Front. Environ. Sci. Eng., 10, 1-11, 2016.
Gershenzon, Y. M., Ivanov, A. V., Kucheryavyi, S. I., and Rozenshtein, V. B.: Annihilation of OH radicals on the surfaces of substances chemically similar to atmospheric aerosol particles, Kinet. Catal., 27, 1069-1074, 1986.
Geyer, A., Alicke, B., Konrad, S., Schmitz, T., Stutz, J., and Platt, U.: Chemistry and oxidation capacity of the nitrate radical in the continental boundary layer near Berlin, J. Geophys. Res.-Atmos, 106, 8013-8025, 2001.
Geyer, A., Bachmann, K., Hofzumahaus, A., Holland, F., Konrad, S., Klupfel, T., Patz, H. W., Perner, D., Mihelcic, D., Schafer, H. J., Volz-Thomas, A., and Platt, U.: Nighttime formation of peroxy and hydroxyl radicals during the BERLIOZ campaign: Observations and modeling studies, J. Geophys. Res.-Atmos., 108, 8249, DOI: 8210.1029/2001JD000656, 2003.
Giannadaki, D., Pozzer, A., and Lelieveld, J.: Modeled global effects of airborne desert dust on air quality and premature mortality, Atmos. Chem. Phys., 14, 957-968, 2014.
Ginoux, P., Prospero, J. M., Gill, T. E., Hsu, N. C., and Zhao, M.: Global-scale Attribution of Anthropogenic and Natural Dust Sources and Their Emission Rates Based on MODIS Deep Blue Aerosol Products, Rev. Geophys., 50, RG3005, doi: 3010.1029/2012RG000388, 2012.

Gobbi, G. P., Barnaba, F., Giorgi, R., and Santacasa, A.: Altitude-resolved properties of a Saharan dust event over the Mediterranean, Atmos. Environ., 34, 5119-5127, 2000.
Goodman, A. L., Underwood, G. M., and Grassian, V. H.: A Laboratory Study of the Heterogeneous Reaction of Nitric Acid on Calcium Carbonate Particles, J. Geophys. Res.-Atmos., 105, 29053-29064, 2000.
Graedel, T. E., Mandich, M. L., and Weschler, C. J.: Kinetic model studies of atmospheric droplet chemistry: 2. Homogeneous transition metal chemistry in raindrops, J. Geophys. Res.-Atmos, 91, 5205-5221, 1986.
Hall, B. D., and Claiborn, C. S.: Measurements of the dry deposition of peroxides to a Canadian boreal forest, J. Geophys. Res.-Atmos, 102, 29343-29353, 1997.
Hanisch, F., and Crowley, J. N.: Heterogeneous Reactivity of Gaseous Nitric Acid on Al_2O_3, $CaCO_3$, and Atmospheric Dust Samples: A Knudsen Cell Study, J. Phys. Chem. A, 105, 3096-3106, 2001.
Hanisch, F., and Crowley, J. N.: Ozone decomposition on Saharan dust: an experimental investigation, Atmos. Chem. Phys., 3, 119-130, 2003a.
Hanisch, F., and Crowley, J. N.: Heterogeneous reactivity of NO and HNO3 on mineral dust in the presence of ozone, Phys. Chem. Chem. Phys., 5, 883-887, 2003b.
Hanning-Lee, M. A., Brady, B. B., Martin, L. R., and Syage, J. A.: Ozone decomposition on alumina: Implications for solid rocket motor exhaust, Geophys. Res. Lett., 23, 1961-1964, 1996.
Harris, E., Sinha, B., Foley, S., Crowley, J. N., Borrmann, S., and Hoppe, P.: Sulfur isotope fractionation during heterogeneous oxidation of SO2 on mineral dust, Atmos. Chem. Phys., 12, 4867-4884, 2012.
Harrison, R. M., and Kitto, A. M. N.: EVIDENCE FOR A SURFACE SOURCE OF ATMOSPHERIC NITROUS-ACID, Atmos. Environ., 28, 1089-1094, 1994.
Harrison, R. M., Peak, J. D., and Collins, G. M.: Tropospheric cycle of nitrous acid, J. Geophys. Res.-Atmos., 101, 14429-14439, 1996.
He, H., Wang, Y., Ma, Q., Ma, J., Chu, B., Ji, D., Tang, G., Liu, C., Zhang, H., and Hao, J.: Mineral Dust and NOx Promote the Conversion of SO_2 to Sulfate in Heavy Pollution Days, Sci. Rep., 4, 4172, doi: 4110.1038/srep04172, 2014.
Heard, D. E., Carpenter, L. J., Creasey, D. J., Hopkins, J. R., Lee, J. D., Lewis, A. C., Pilling, M. J., Seakins, P. W., Carslaw, N., and Emmerson, K. M.: High levels of the hydroxyl radical in the winter urban troposphere, Geophys. Res. Lett., 31, L18112, DOI: 18110.11029/12004GL020544, 2004.
Highwood, E., and Ryder, C.: Radiative Effects of Dust, in: Mineral Dust, edited by: Knippertz, P., and Stuut, J.-B. W., Springer, Netherlands, 267-286, 2014.
Hoffman, R. C., Gebel, M. E., Fox, B. S., and Finlayson-Pitts, B. J.: Knudsen cell studies of the reactions of N2O5 and ClONO2 with NaCl: development and application of a model for estimating available surface areas and corrected uptake coefficients, Phys. Chem. Chem. Phys., 5, 1780-1789, 2003a.
Hoffman, R. C., Kaleuati, M. A., and Finlayson-Pitts, B. J.: Knudsen cell studies of the reaction of gaseous HNO3 with NaCl using less than a single layer of particles at 298 K: A modified mechanism, J. Phys. Chem. A, 107, 7818-7826, 2003b.
Hofzumahaus, A., Rohrer, F., Lu, K. D., Bohn, B., Brauers, T., Chang, C. C., Fuchs, H., Holland, F., Kita, K., Kondo, Y., Li, X., Lou, S. R., Shao, M., Zeng, L. M., Wahner, A., and Zhang, Y. H.: Amplified Trace Gas Removal in the Troposphere, Science, 324, 1702-1704, 2009.
Holland, F., Hofzumahaus, A., Schäfer, J., Kraus, A., and Pätz, H.-W.: Measurements of OH and HO2 radical concentrations and photolysis frequencies during BERLIOZ, J. Geophys. Res.-Atmos, 108, 8246, doi: 8210.1029/2001JD001393, 2003.

Hoose, C., Kristjansson, J. E., and Burrows, S. M.: How important is biological ice nucleation in clouds on a global scale?, Environ. Res. Lett., 5, 024009, 2010.
Hoose, C., and Moehler, O.: Heterogeneous ice nucleation on atmospheric aerosols: a review of results from laboratory experiments, Atmos. Chem. Phys., 12, 9817–9854, 2012.
Hou, S. Q., Tong, S. R., Zhang, Y., Tan, F., Guo, Y. C., and Ge, M. F.: Heterogeneous uptake of gas-phase acetic acid on α-Al_2O_3 particle surface: the impact of temperature, Chem. Asian J., doi: 10.1002/asia.201600402, 2016.
Hua, W., Chen, Z. M., Jie, C. Y., Kondo, Y., Hofzumahaus, A., Takegawa, N., Chang, C. C., Lu, K. D., Miyazaki, Y., Kita, K., Wang, H. L., Zhang, Y. H., and Hu, M.: Atmospheric hydrogen peroxide and organic hydroperoxides during PRIDE-PRD'06, China: their concentration, formation mechanism and contribution to secondary aerosols, Atmos. Chem. Phys., 8, 6755-6773, 2008.
Huang, J., Yu, H., Guan, X., Wang, G., and Guo, R.: Accelerated dryland expansion under climate change, Nature Clim. Change, 6, 166-171, 2016.
Huang, J. P., Wang, T. H., Wang, W. C., Li, Z. Q., and Yan, H. R.: Climate effects of dust aerosols over East Asian arid and semiarid regions, J. Geophys. Res.-Atmos., 119, 11398-11416, 2014.
Huang, L., Zhao, Y., Li, H., and Chen, Z.: Kinetics of Heterogeneous Reaction of Sulfur Dioxide on Authentic Mineral Dust: Effects of Relative Humidity and Hydrogen Peroxide, Environ. Sci. Technol., 49, 10797-10805, 2015a.
Huang, X., Song, Y., Zhao, C., Cai, X., Zhang, H., and Zhu, T.: Direct Radiative Effect by Multicomponent Aerosol over China, J. Climate, 28, 3472-3495, 2015b.
Huff, D. M., Joyce, P. L., Fochesatto, G. J., and Simpson, W. R.: Deposition of dinitrogen pentoxide, N2O5, to the snowpack at high latitudes, Atmos. Chem. Phys., 11, 4929-4938, 2011.
Huneeus, N., Schulz, M., Balkanski, Y., Griesfeller, J., Prospero, J., Kinne, S., Bauer, S., Boucher, O., Chin, M., Dentener, F., Diehl, T., Easter, R., Fillmore, D., Ghan, S., Ginoux, P., Grini, A., Horowitz, L., Koch, D., Krol, M. C., Landing, W., Liu, X., Mahowald, N., Miller, R., Morcrette, J. J., Myhre, G., Penner, J., Perlwitz, J., Stier, P., Takemura, T., and Zender, C. S.: Global dust model intercomparison in AeroCom phase I, Atmos. Chem. Phys., 11, 7781-7816, 2011.
Ingham, T., Goddard, A., Whalley, L. K., Furneaux, K. L., Edwards, P. M., Seal, C. P., Self, D. E., Johnson, G. P., Read, K. A., Lee, J. D., and Heard, D. E.: A flow-tube based laser-induced fluorescence instrument to measure OH reactivity in the troposphere, Atmos. Meas. Tech., 2, 465-477, 2009.
Itahashi, S., Uno, I., Irie, H., Kurokawa, J. I., and Ohara, T.: Regional modeling of tropospheric NO₂ vertical column density over East Asia during the period 2000–2010: comparison with multisatellite observations, Atmos. Chem. Phys., 14, 3623-3635, 2014.
Ito, A., and Xu, L.: Response of acid mobilization of iron-containing mineral dust to improvement of air quality projected in the future, Atmos. Chem. Phys., 14, 3441-3459, 2014.
Jacob, D. J.: Heterogeneous chemistry and tropospheric ozone, Atmos. Environ., 34, 2131-2159, 2000.
James, A. D., Moon, D. R., Feng, W., Lakey, P. S. J., Frankland, V. L., Heard, D. E., and Plane, J. M. C.: The uptake of HO2 on meteoric smoke analogues, J. Geophys. Res.-Atmos, 122, 554-565, 2017.
Jeong, G. R., and Sokolik, I. N.: Effect of mineral dust aerosols on the photolysis rates in the clean and polluted marine environments, J. Geophys. Res.-Atmos., 112, D21308, doi: 21310.21029/22007jd008442, 2007.

Jeong, G. Y.: Bulk and single-particle mineralogy of Asian dust and a comparison with its source soils, J. Geophys. Res.-Atmos., 113, D02208, doi: 02210.01029/02007jd008606, 2008.

Jickells, T., Boyd, P., and Hunter, K.: Biogeochemical Impacts of Dust on the Global Carbon Cycle, in: Mineral Dust, edited by: Knippertz, P., and Stuut, J.-B. W., Springer, Netherlands, 359-384, 2014.

Jickells, T. D., An, Z. S., Andersen, K. K., Baker, A. R., Bergametti, G., Brooks, N., Cao, J. J., Boyd, P. W., Duce, R. A., Hunter, K. A., Kawahata, H., Kubilay, N., laRoche, J., Liss, P. S., Mahowald, N., Prospero, J. M., Ridgwell, A. J., Tegen, I., and Torres, R.: Global Iron Connections between Desert Dust, Ocean Biogeochemistry, and Climate, Science, 308, 67-71, 2005.

Journet, E., Desboeufs, K. V., Caquineau, S., and Colin, J.-L.: Mineralogy as a critical factor of dust iron solubility, Geophys. Res. Lett., 35, L07805, doi: 07810.01029/02007GL031589, 2008.

Journet, E., Balkanski, Y., and Harrison, S. P.: A New Data Set of Soil Mineralogy for Dust-cycle Modeling, Atmos. Chem. Phys., 14, 3801-3816, 2014.

Jung, J., Kim, Y. J., Lee, K. Y., Cayetano, M. G., Batmunkh, T., Koo, J. H., and Kim, J.: Spectral optical properties of long-range transport Asian dust and pollution aerosols over Northeast Asia in 2007 and 2008, Atmos. Chem. Phys., 10, 5391-5408, 2010.

Kaiser, E. W., and Wu, C. H.: A kinetic study of the gas phase formation and decomposition reactions of nitrous acid, J. Phys. Chem., 81, 1701-1706, 1977.

Kanaya, Y., Cao, R., Akimoto, H., Fukuda, M., Komazaki, Y., Yokouchi, Y., Koike, M., Tanimoto, H., Takegawa, N., and Kondo, Y.: Urban photochemistry in central Tokyo: 1. Observed and modeled OH and HO2 radical concentrations during the winter and summer of 2004, J. Geophys. Res.-Atmos, 112, D21312, doi: 21310.21029/22007JD008670, 2007a.

Kanaya, Y., Cao, R. Q., Akimoto, H., Fukuda, M., Komazaki, Y., Yokouchi, Y., Koike, M., Tanimoto, H., Takegawa, N., and Kondo, Y.: Urban photochemistry in central Tokyo: 1. Observed and modeled OH and HO2 radical concentrations during the winter and summer of 2004, J. Geophys. Res.-Atmos., 112, D21312, DOI: 21310.21029/22007JD008670, 2007b.

Kandler, K., Schutz, L., Deutscher, C., Ebert, M., Hofmann, H., Jackel, S., Jaenicke, R., Knippertz, P., Lieke, K., Massling, A., Petzold, A., Schladitz, A., Weinzierl, B., Wiedensohler, A., Zorn, S., and Weinbruch, S.: Size distribution, mass concentration, chemical and mineralogical composition and derived optical parameters of the boundary layer aerosol at Tinfou, Morocco, during SAMUM 2006, Tellus Ser. B-Chem. Phys. Meteorol., 61, 32-50, 2009.

Karagulian, F., and Rossi, M. J.: The heterogeneous chemical kinetics of NO_3 on atmospheric mineral dust surrogates, Phys. Chem. Chem. Phys., 7, 3150-3162, 2005.

Karagulian, F., and Rossi, M. J.: The heterogeneous decomposition of ozone on atmospheric mineral dust surrogates at ambient temperature, Int. J. Chem. Kinet., 38, 407-419, 2006.

Karagulian, F., Santschi, C., and Rossi, M. J.: The heterogeneous chemical kinetics of N_2O_5 on $CaCO_3$ and other atmospheric mineral dust surrogates, Atmos. Chem. Phys., 6, 1373-1388, 2006.

Keyser, L. F., Moore, S. B., and Leu, M. T.: Surface-Reaction and Pore Diffusion in Flow-Tube Reactors, J. Phys. Chem., 95, 5496-5502, 1991.

Keyser, L. F., Leu, M. T., and Moore, S. B.: Comment on porosities of ice films used to simulate stratospheric cloud surfaces, J. Phys. Chem., 97, 2800-2801, 1993.

Koehler, K. A., Kreidenweis, S. M., DeMott, P. J., Petters, M. D., Prenni, A. J., and Carrico, C. M.: Hygroscopicity and cloud droplet activation of mineral dust aerosol, Geophys. Res. Lett., 36, L08805, doi: 08810.01029/02009gl037348, 2009.

Kok, J. F., Ridley, D. A., Zhou, Q., Miller, R. L., Zhao, C., Heald, C. L., Ward, D. S., Albani, S., and Haustein, K.: Smaller desert dust cooling effect estimated from analysis of dust size and abundance, Nature Geosci, 10, 274-278, 2017.

Kolb, C. E., Cox, R. A., Abbatt, J. P. D., Ammann, M., Davis, E. J., Donaldson, D. J., Garrett, B. C., George, C., Griffiths, P. T., Hanson, D. R., Kulmala, M., McFiggans, G., Pöschl, U., Riipinen, I., Rossi, M. J., Rudich, Y., Wagner, P. E., Winkler, P. M., Worsnop, D. R., and O' Dowd, C. D.: An overview of current issues in the uptake of atmospheric trace gases by aerosols and clouds, Atmos. Chem. Phys., 10, 10561-10605, 2010.

Kong, L. D., Zhao, X., Sun, Z. Y., Yang, Y. W., Fu, H. B., Zhang, S. C., Cheng, T. T., Yang, X., Wang, L., and Chen, J. M.: The effects of nitrate on the heterogeneous uptake of sulfur dioxide on hematite, Atmos. Chem. Phys., 14, 9451-9467, 2014.

Krieger, U. K., Marcolli, C., and Reid, J. P.: Exploring the complexity of aerosol particle properties and processes using single particle techniques, Chem. Soc. Rev., 41, 6631-6662, 2012.

Krueger, B. J., Grassian, V. H., Iedema, M. J., Cowin, J. P., and Laskin, A.: Probing heterogeneous chemistry of individual atmospheric particles using scanning electron microscopy and energy-dispersive X-ray analysis, Anal. Chem., 75, 5170-5179, 2003a.

Krueger, B. J., Grassian, V. H., Laskin, A., and Cowin, J. P.: The Transformation of Solid Atmospheric Particles into Liquid Droplets through Heterogeneous Chemistry: Laboratory Insights into the Processing of Calcium Containing Mineral Dust Aerosol in the Troposphere, Geophys. Res. Lett., 30, 1148, doi: 1110.1029/2002gl016563, 2003b.

Kulkarni, G., Zhang, K., Zhao, C., Nandasiri, M., Shutthanandan, V., Liu, X., Fast, J., and Berg, L.: Ice Formation on Nitric Acid Coated Dust Particles: Laboratory and Modeling Studies, J. Geophys. Res.-Atmos, 120, 7682-7698, 2015.

Kumar, P., Sokolik, I. N., and Nenes, A.: Parameterization of cloud droplet formation for global and regional models: including adsorption activation from insoluble CCN, Atmos. Chem. Phys., 9, 2517-2532, 2009.

Kumar, R., Barth, M. C., Madronich, S., Naja, M., Carmichael, G. R., Pfister, G. G., Knote, C., Brasseur, G. P., Ojha, N., and Sarangi, T.: Effects of dust aerosols on tropospheric chemistry during a typical pre-monsoon season dust storm in northern India, Atmos. Chem. Phys., 14, 6813-6834, 2014.

Ladino, L. A., Stetzer, O., and Lohmann, U.: Contact freezing: a review of experimental studies, Atmos. Chem. Phys., 13, 9745-9769, 2013.

Lampimaki, M., Zelenay, V., Krepelova, A., Liu, Z., Chang, R., Bluhm, H., and Ammann, M.: Ozone-Induced Band Bending on Metal-Oxide Surfaces Studied under Environmental Conditions, ChemPhysChem, 14, 2419 – 2425, 2013.

Langridge, J. M., Gustafsson, R. J., Griffiths, P. T., Cox, R. A., Lambert, R. M., and Jones, R. L.: Solar driven nitrous acid formation on building material surfaces containing titanium dioxide: A concern for air quality in urban areas?, Atmos. Environ., 43, 5128-5131, 2009.

Laskin, A., Iedema, M. J., Ichkovich, A., Graber, E. R., Taraniuk, I., and Rudich, Y.: Direct Observation of Completely Processed Calcium Carbonate Dust Particles, Faraday Discuss., 130, 453-468, 2005a.

Laskin, A., Wietsma, T. W., Krueger, B. J., and Grassian, V. H.: Heterogeneous chemistry of individual mineral dust particles with nitric acid: A combined CCSEM/EDX, ESEM, and ICP-MS study, J. Geophys. Res.-Atmos., 110, 2005b.

Laufs, S., Burgeth, G., Duttlinger, W., Kurtenbach, R., Maban, M., Thomas, C., Wiesen, P., and Kleffmann, J.: Conversion of nitrogen oxides on commercial photocatalytic dispersion paints, Atmos. Environ., 44, 2341-2349, 2010.

Lee, A. K. Y., and Chan, C. K.: Heterogeneous Reactions of Linoleic Acid and Linolenic Acid Particles with Ozone: Reaction Pathways and Changes in Particle Mass, Hygroscopicity, and Morphology, J. Phys. Chem. A, 111, 6285-6295, 2007.

Lee, A. K. Y., Ling, T. Y., and Chan, C. K.: Understanding hygroscopic growth and phase transformation of aerosols using single particle Raman spectroscopy in an electrodynamic balance, Faraday Discuss., 137, 245-263, 2008.

Lelieveld, J., Butler, T. M., Crowley, J. N., Dillon, T. J., Fischer, H., Ganzeveld, L., Harder, H., Lawrence, M. G., Martinez, M., Taraborrelli, D., and Williams, J.: Atmospheric oxidation capacity sustained by a tropical forest, Nature, 452, 737-740, 2008.

Lemaitre, C., Flamant, C., Cuesta, J., Raut, J. C., Chazette, P., Formenti, P., and Pelon, J.: Radiative heating rates profiles associated with a springtime case of Bodele and Sudan dust transport over West Africa, Atmos. Chem. Phys., 10, 8131-8150, 2010.

Li, G., Su, H., Li, X., Kuhn, U., Meusel, H., Hoffmann, T., Ammann, M., Poschl, U., Shao, M., and Cheng, Y. F.: Uptake of gaseous formaldehyde by soil surfaces: a combination of adsorption/desorption equilibrium and chemical reactions, Atmos. Chem. Phys., 16, 10299-10311, 2016.

Li, H. J., Zhu, T., Zhao, D. F., Zhang, Z. F., and Chen, Z. M.: Kinetics and mechanisms of heterogeneous reaction of NO_2 on $CaCO_3$ surfaces under dry and wet conditions, Atmos. Chem. Phys., 10, 463-474, 2010.

Li, L., Chen, Z. M., Zhang, Y. H., Zhu, T., Li, J. L., and Ding, J.: Kinetics and mechanism of heterogeneous oxidation of sulfur dioxide by ozone on surface of calcium carbonate, Atmos. Chem. Phys., 6, 2453-2464, 2006.

Li, P., Al-Abadleh, H. A., and Grassian, V. H.: Measuring heterogeneous uptake coefficients of gases on solid particle surfaces with a Knudsen cell reactor: Complications due to surface saturation and gas diffusion into underlying layers, J. Phys. Chem. A, 106, 1210-1219, 2002.

Li, W., Gibbs, G. V., and Oyama, S. T.: Mechanism of ozone decomposition on a manganese oxide catalyst. I. In situ Raman spectroscopy and ab initio molecular orbital calculations, J. Am. Chem. Soc., 120, 9041-9046, 1998.

Li, W., and Oyama, S. T.: Mechanism of ozone decomposition on a manganese oxide catalyst. 2. Steady-state and transient kinetic studies, J. Am. Chem. Soc., 120, 9047-9052, 1998.

Li, W. J., and Shao, L. Y.: Observation of Nitrate Coatings on Atmospheric Mineral Dust Particles, Atmos. Chem. Phys., 9, 1863-1871, 2009.

Li, X., Brauers, T., Haseler, R., Bohn, B., Fuchs, H., Hofzumahaus, A., Holland, F., Lou, S., Lu, K. D., Rohrer, F., Hu, M., Zeng, L. M., Zhang, Y. H., Garland, R. M., Su, H., Nowak, A., Wiedensohler, A., Takegawa, N., Shao, M., and Wahner, A.: Exploring the atmospheric chemistry of nitrous acid (HONO) at a rural site in Southern China, Atmos. Chem. Phys., 12, 1497-1513, 2012.

Liao, H., Yung, Y. L., and Seinfeld, J. H.: Effects of aerosols on tropospheric photolysis rates in clear and cloudy atmospheres, J. Geophys. Res.-Atmos., 104, 23697-23707, 1999.

Liao, J., Huey, L. G., Liu, Z., Tanner, D. J., Cantrell, C. A., Orlando, J. J., Flocke, F. M., Shepson, P. B., Weinheimer, A. J., Hall, S. R., Ullmann, K., Beine, H. J., Wang, Y., Ingall, E. D., Stephens, C. R., Hornbrook, R. S., Apel, E. C., Riemer, D., Fried, A., Mauldin Iii, R. L., Smith, J. N., Staebler, R. M., Neuman, J. A., and Nowak, J. B.: High levels of molecular chlorine in the Arctic atmosphere, Nature Geosci., 7, 91-94, 2014.

Lipfert, F. W.: Atmospheric damage to calcareous stones: Comparison and reconciliation of recent experimental findings, Atmos. Environ., 23, 415-429, 1989.

Liu, C., Ma, Q., Liu, Y., Ma, J., and He, H.: Synergistic reaction between SO2 and NO2 on mineral oxides: a potential formation pathway of sulfate aerosol, Phys. Chem. Chem. Phys., 14, 1668-1676, 2012.

Liu, H. M., Lian, Z. W., Ye, X. J., and Shangguan, W. F.: Kinetic analysis of photocatalytic oxidation of gas-phase formaldehyde over titanium dioxide, Chemosphere, 60, 630-635, 2005.

Liu, Y., Ma, J., and He, H.: Heterogeneous reactions of carbonyl sulfide on mineral oxides: mechanism and kinetics study, Atmos. Chem. Phys., 10, 10335-10344, 2010.

Liu, Y., Han, C., Ma, J., Bao, X., and He, H.: Influence of relative humidity on heterogeneous kinetics of NO2 on kaolin and hematite, Phys. Chem. Chem. Phys., 17, 19424-19431, 2015.

Liu, Y. C., He, H., and Mu, Y. J.: Heterogeneous reactivity of carbonyl sulfide on α-Al_2O_3 and γ-A_l2O_3, Atmos. Environ., 42, 960-969, 2008a.

Liu, Y. J., Zhu, T., Zhao, D. F., and Zhang, Z. F.: Investigation of the hygroscopic properties of $Ca(NO_3)_2$ and internally mixed $Ca(NO_3)_2/CaCO_3$ particles by micro-Raman spectrometry, Atmos. Chem. Phys., 8, 7205-7215, 2008b.

Lohmann, U., and Feichter, J.: Global indirect aerosol effects: a review, Atmos. Chem. Phys., 5, 715-737, 2005.

Lou, S., Holland, F., Rohrer, F., Lu, K., Bohn, B., Brauers, T., Chang, C. C., Fuchs, H., Häseler, R., Kita, K., Kondo, Y., Li, X., Shao, M., Zeng, L., Wahner, A., Zhang, Y., Wang, W., and Hofzumahaus, A.: Atmospheric OH reactivities in the Pearl River Delta – China in summer 2006: measurement and model results, Atmos. Chem. Phys., 10, 11243-11260, 2010.

Lu, K. D., Rohrer, F., Holland, F., Fuchs, H., Bohn, B., Brauers, T., Chang, C. C., Haseler, R., Hu, M., Kita, K., Kondo, Y., Li, X., Lou, S. R., Nehr, S., Shao, M., Zeng, L. M., Wahner, A., Zhang, Y. H., and Hofzumahaus, A.: Observation and modelling of OH and HO2 concentrations in the Pearl River Delta 2006: a missing OH source in a VOC rich atmosphere, Atmos. Chem. Phys., 12, 1541-1569, 2012.

Lu, K. D., Hofzumahaus, A., Holland, F., Bohn, B., Brauers, T., Fuchs, H., Hu, M., Haseler, R., Kita, K., Kondo, Y., Li, X., Lou, S. R., Oebel, A., Shao, M., Zeng, L. M., Wahner, A., Zhu, T., Zhang, Y. H., and Rohrer, F.: Missing OH source in a suburban environment near Beijing: observed and modelled OH and HO2 concentrations in summer 2006, Atmos. Chem. Phys., 13, 1057-1080, 2013.

Lu, K. D., Rohrer, F., Holland, F., Fuchs, H., Brauers, T., Oebel, A., Dlugi, R., Hu, M., Li, X., Lou, S. R., Shao, M., Zhu, T., Wahner, A., Zhang, Y. H., and Hofzumahaus, A.: Nighttime observation and chemistry of HOx in the Pearl River Delta and Beijing in summer 2006, Atmos. Chem. Phys., 14, 4979-4999, 2014.

Ma, Q. X., Liu, Y. C., Liu, C., and He, H.: Heterogeneous Reaction of Acetic Acid on MgO, α-Al_2O_3, and $CaCO_3$ and the Effect on the Hygroscopic Behavior of These Particles, Phys. Chem. Chem. Phys., 14, 8403-8409, 2012.

Macintyre, H. L., and Evans, M. J.: Sensitivity of a global model to the uptake of N_2O_5 by tropospheric aerosol, Atmos. Chem. Phys., 10, 7409-7414, 2010.

Macintyre, H. L., and Evans, M. J.: Parameterisation and impact of aerosol uptake of HO2 on a global tropospheric model, Atmos. Chem. Phys., 11, 10965-10974, 2011.

Mahowald, N., Jickells, T. D., Baker, A. R., Artaxo, P., Benitez-Nelson, C. R., Bergametti, G., Bond, T. C., Chen, Y., Cohen, D. D., Herut, B., Kubilay, N., Losno, R., Luo, C., Maenhaut, W., McGee, K. A., Okin, G. S., Siefert, R. L., and Tsukuda, S.: Global distribution of atmospheric phosphorus sources, concentrations and deposition rates, and anthropogenic impacts, Glob. Biogeochem. Cycle, 22, GB4026, doi: 4010.1029/2008GB003240., 2008.

Mahowald, N.: Aerosol Indirect Effect on Biogeochemical Cycles and Climate, Science, 334, 794-796, 2011.

Mahowald, N., Ward, D. S., Kloster, S., Flanner, M. G., Heald, C. L., Heavens, N. G., Hess, P. G., Lamarque, J.-F., and Chuang, P. Y.: Aerosol Impacts on Climate and Biogeochemistry, Annu. Rev. Environ. Resour., 36, 45-74, 2011.

Mahowald, N. M., Baker, A. R., Bergametti, G., Brooks, N., Duce, R. A., Jickells, T. D., Kubilay, N., Prospero, J. M., and Tegen, I.: Atmospheric Global Dust Cycle and Iron Inputs to the Ocean, Glob. Biogeochem. Cycle, 19, GB4025, doi:4010.1029/2004GB002402, 2005.

Mahowald, N. M., Ballantine, J. A., Feddema, J., and Ramankutty, N.: Global trends in visibility: implications for dust sources, Atmos. Chem. Phys., 7, 3309-3339, 2007.

Mao, J., Jacob, D. J., Evans, M. J., Olson, J. R., Ren, X., Brune, W. H., Clair, J. M. S., Crounse, J. D., Spencer, K. M., Beaver, M. R., Wennberg, P. O., Cubison, M. J., Jimenez, J. L., Fried, A., Weibring, P., Walega, J. G., Hall, S. R., Weinheimer, A. J., Cohen, R. C., Chen, G., Crawford, J. H., McNaughton, C., Clarke, A. D., Jaeglé, L., Fisher, J. A., Yantosca, R. M., Le Sager, P., and Carouge, C.: Chemistry of hydrogen oxide radicals (HOx) in the Arctic troposphere in spring, Atmos. Chem. Phys., 10, 5823-5838, 2010a.

Mao, J., Ren, X., Chen, S., Brune, W. H., Chen, Z., Martinez, M., Harder, H., Lefer, B., Rappenglück, B., Flynn, J., and Leuchner, M.: Atmospheric oxidation capacity in the summer of Houston 2006: Comparison with summer measurements in other metropolitan studies, Atmos. Environ., 44, 4107-4115, 2010b.

Mao, J., Ren, X., Zhang, L., Van Duin, D. M., Cohen, R. C., Park, J. H., Goldstein, A. H., Paulot, F., Beaver, M. R., Crounse, J. D., Wennberg, P. O., DiGangi, J. P., Henry, S. B., Keutsch, F. N., Park, C., Schade, G. W., Wolfe, G. M., Thornton, J. A., and Brune, W. H.: Insights into hydroxyl measurements and atmospheric oxidation in a California forest, Atmos. Chem. Phys., 12, 8009-8020, 2012.

Mao, J., Fan, S., Jacob, D. J., and Travis, K. R.: Radical loss in the atmosphere from Cu-Fe redox coupling in aerosols, Atmos. Chem. Phys., 12, 509-519, 2013a.

Mao, J. Q., Paulot, F., Jacob, D. J., Cohen, R. C., Crounse, J. D., Wennberg, P. O., Keller, C. A., Hudman, R. C., Barkley, M. P., and Horowitz, L. W.: Ozone and organic nitrates over the eastern United States: Sensitivity to isoprene chemistry, J. Geophys. Res.-Atmos., 118, 11256-11268, 2013b.

Martinez, M., Perner, D., Hackenthal, E. M., Kulzer, S., and Schutz, L.: NO3 at Helgoland during the NORDEX campaign in October 1996, J. Geophys. Res.-Atmos., 105, 22685-22695, 2000.

Matsuki, A., Iwasaka, Y., Shi, G. Y., Zhang, D. Z., Trochkine, D., Yamada, M., Kim, Y. S., Chen, B., Nagatani, T., Miyazawa, T., Nagatani, M., and Nakata, H.: Morphological and chemical modification of mineral dust: Observational insight into the heterogeneous uptake of acidic gases, Geophys. Res. Lett., 32, L22806, doi: 22810.21029/22005gl024176, 2005.

Matthews, P. S. J., Baeza-Romero, M. T., Whalley, L. K., and Heard, D. E.: Uptake of HO_2 radicals onto Arizona test dust particles using an aerosol flow tube, Atmos. Chem. Phys., 14, 7397-7408, 2014.

Mauldin III, R. L., Berndt, T., Sipila, M., Paasonen, P., Petaja, T., Kim, S., Kurten, T., Stratmann, F., Kerminen, V. M., and Kulmala, M.: A new atmospherically relevant oxidant of sulphur dioxide, Nature, 488, 193-196, 2012.

Meng, Z., and Lu, B.: Dust events as a risk factor for daily hospitalization for respiratory and cardiovascular diseases in Minqin, China, Atmos. Environ., 41, 7048-7058, 2007.

Meskhidze, N., Chameides, W. L., and Nenes, A.: Dust and pollution: A recipe for enhanced ocean fertilization?, J. Geophys. Res.-Atmos., 110, D03301, doi: 03310.01029/02004jd005082, 2005.

Michel, A. E., Usher, C. R., and Grassian, V. H.: Heterogeneous and catalytic uptake of ozone on mineral oxides and dusts: A Knudsen cell investigation, Geophys. Res. Lett., 29, 1665, 10.1029/2002gl014896, 2002.

Michel, A. E., Usher, C. R., and Grassian, V. H.: Reactive uptake of ozone on mineral oxides and mineral dusts, Atmos. Environ., 37, 3201-3211, 2003.

Mihelcic, D., Holland, F., Hofzumahaus, A., Hoppe, L., Konrad, S., Müsgen, P., Pätz, H. W., Schäfer, H. J., Schmitz, T., Volz-Thomas, A., Bächmann, K., Schlomski, S., Platt, U., Geyer, A., Alicke, B., and Moortgat, G. K.: Peroxy radicals during BERLIOZ at Pabstthum: Measurements, radical budgets and ozone production, J. Geophys. Res.-Atmos, 108, 8254, doi: 8210.1029/2001JD001014, 2003.

Mogili, P. K., Kleiber, P. D., Young, M. A., and Grassian, V. H.: Heterogeneous uptake of ozone on reactive components of mineral dust aerosol: An environmental aerosol reaction chamber study, J. Phys. Chem. A, 110, 13799-13807, 2006a.

Mogili, P. K., Kleiber, P. D., Young, M. A., and Grassian, V. H.: N_2O_5 hydrolysis on the components of mineral dust and sea salt aerosol: Comparison study in an environmental aerosol reaction chamber, Atmos. Environ., 40, 7401-7408, 2006b.

Moon, D. R., Taverna, G. S., Anduix-Canto, C., Ingham, T., Chipperfield, M. P., Seakins, P. W., Baeza-Romero, M. T., and Heard, D. E.: Heterogeneous reaction of HO2 with airborne TiO2 particles and its implication for climate change mitigation strategies, Atmos. Chem. Phys. Discuss., 2017, 1-20, 10.5194/acp-2017-439, 2017.

Morgan, W. T., Ouyang, B., Allan, J. D., Aruffo, E., Di Carlo, P., Kennedy, O. J., Lowe, D., Flynn, M. J., Rosenberg, P. D., Williams, P. I., Jones, R., McFiggans, G. B., and Coe, H.: Influence of aerosol chemical composition on N2O5 uptake: airborne regional measurements in northwestern Europe, Atmos. Chem. Phys., 15, 973-990, 2015.

Morman, S., and Plumlee, G.: Dust and Human Health, in: Mineral Dust, edited by: Knippertz, P., and Stuut, J.-B. W., Springer, Netherlands, 385-409, 2014.

Moteki, N., Adachi, K., Ohata, S., Yoshida, A., Harigaya, T., Koike, M., and Kondo, Y.: Anthropogenic iron oxide aerosols enhance atmospheric heating, 8, 15329, 10.1038/ncomms15329, 2017.

Murray, B. J., O'Sullivan, D., Atkinson, J. D., and Webb, M. E.: Ice nucleation by particles immersed in supercooled cloud droplets, Chem. Soc. Rev., 41, 6519-6554, 2012.

Nölscher, A. C., Williams, J., Sinha, V., Custer, T., Song, W., Johnson, A. M., Axinte, R., Bozem, H., Fischer, H., Pouvesle, N., Phillips, G., Crowley, J. N., Rantala, P., Rinne, J., Kulmala, M., Gonzales, D., Valverde-Canossa, J., Vogel, A., Hoffmann, T., Ouwersloot, H. G., Vilà-Guerau de Arellano, J., and Lelieveld, J.: Summertime total OH reactivity measurements from boreal forest during HUMPPA-COPEC 2010, Atmos. Chem. Phys., 12, 8257-8270, 2012.

Naderi, M.: Chapter Fourteen - Surface Area: Brunauer–Emmett–Teller (BET) A2 - Tarleton, Steve, in: Progress in Filtration and Separation, Academic Press, Oxford, 585-608, 2015.

Nanayakkara, C. E., Jayaweera, P. M., Rubasinghege, G., Baltrusaitis, J., and Grassian, V. H.: Surface Photochemistry of Adsorbed Nitrate: The Role of Adsorbed Water in the Formation of Reduced Nitrogen Species on α-Fe2O3 Particle Surfaces, J. Phys. Chem. A, 118, 158-166, 2013.

Nanayakkara, C. E., Dillon, J. K., and Grassian, V. H.: Surface Adsorption and Photochemistry of Gas-Phase Formic Acid on TiO_2 Nanoparticles: The Role of Adsorbed Water in Surface Coordination, Adsorption Kinetics, and Rate of Photoproduct Formation, J. Phys. Chem. C, 118, 25487-25495, 2014.

Ndour, M., Nicolas, M., D'Anna, B., Ka, O., and George, C.: Photoreactivity of NO_2 on mineral dusts originating from different locations of the Sahara desert, Phys. Chem. Chem. Phys., 11, 1312-1319, 2009.

Nenes, A., Krom, M. D., Mihalopoulos, N., Van Cappellen, P., Shi, Z., Bougiatioti, A., Zarmpas, P., and Herut, B.: Atmospheric acidification of mineral aerosols: a source of bioavailable phosphorus for the oceans, Atmos. Chem. Phys., 11, 6265-6272, 2011.

Net, S., Nieto-Gligorovski, L., Gligorovski, S., Temime-Rousell, B., Barbati, S., Lazarou, Y. G., and Wortharn, H.: Heterogeneous light-induced ozone processing on the organic coatings in the atmosphere, Atmos. Environ., 43, 1683-1692, 2009.

Net, S., Gligorovski, S., Pietri, S., and Wortham, H.: Photoenhanced degradation of veratraldehyde upon the heterogeneous ozone reactions, Phys. Chem. Chem. Phys., 12, 7603-7611, 2010a.

Net, S., Gligorovski, S., and Wortham, H.: Light-induced heterogeneous ozone processing on organic coated particles: Kinetics and condensed-phase products, Atmos. Environ., 44, 3286-3294, 2010b.

Net, S., Gomez Alvarez, E., Balzer, N., Wortham, H., Zetzsch, C., and Gligorovski, S.: Photolysis and Heterogeneous Reaction of Coniferyl Aldehyde Adsorbed on Silica Particles with Ozone, ChemPhysChem, 11, 4019-4027, 2010c.

Net, S., Nieto-Gligorovski, L., Gligorovski, S., and Wortham, H.: Heterogeneous ozonation kinetics of 4-phenoxyphenol in the presence of photosensitizer, Atmos. Chem. Phys., 10, 1545-1554, 2010d.

Net, S., Alvarez, E. G., Gligorovski, S., and Wortham, H.: Heterogeneous reactions of ozone with methoxyphenols, in presence and absence of light, Atmos. Environ., 45, 3007-3014, 2011.

Nickovic, S., Vukovic, A., Vujadinovic, M., Djurdjevic, V., and Pejanovic, G.: Technical Note: High-resolution mineralogical database of dust-productive soils for atmospheric dust modeling, Atmos. Chem. Phys., 12, 845-855, 2012.

Nicolas, M., Ndour, M., Ka, O., D'anna, B., and George, C.: Photochemistry of Atmospheric Dust: Ozone Decomposition on Illuminatd Titanium Dioxide, Environ. Sci. Technol., 43, 7347-7442, 2009.

Nie, W., Ding, A., Wang, T., Kerminen, V.-M., George, C., Xue, L., Wang, W., Zhang, Q., Petaja, T., Qi, X., Gao, X., Wang, X., Yang, X., Fu, C., and Kulmala, M.: Polluted dust promotes new particle formation and growth, Sci. Rep., 4, 6634, doi: 6610.1038/srep06634, 2014.

Noguchi, T., Fujishima, A., Sawunyama, P., and Hashimoto, K.: Photocatalytic Degradation of Gaseous Formaldehyde Using TiO_2 Film, Environ. Sci. Technol., 32, 3831-3833, 1998.

Obee, T. N., and Brown, R. T.: TiO2 Photocatalysis for Indoor Air Applications: Effects of Humidity and Trace Contaminant Levels on the Oxidation Rates of Formaldehyde, Toluene, and 1,3-Butadiene, Environ. Sci. Technol., 29, 1223-1231, 1995.

Okada, K., Heintzenberg, J., Kai, K. J., and Qin, Y.: Shape of atmospheric mineral particles collected in three Chinese arid-regions, Geophys. Res. Lett., 28, 3123-3126, 2001.

Osthoff, H. D., Roberts, J. M., Ravishankara, A. R., Williams, E. J., Lerner, B. M., Sommariva, R., Bates, T. S., Coffman, D., Quinn, P. K., Dibb, J. E., Stark, H., Burkholder, J. B., Talukdar, R. K., Meagher, J., Fehsenfeld, F. C., and Brown, S. S.: High levels of nitryl chloride in the polluted subtropical marine boundary layer, Nature Geosci., 1, 324-328, 2008.

Ouyang, B., McLeod, M. W., Jones, R. L., and Bloss, W. J.: NO3 radical production from the reaction between the Criegee intermediate CH2OO and NO2, Phys. Chem. Chem. Phys., 15, 17070-17075, 2013.

Pöschl, U., Rudich, Y., and Ammann, M.: Kinetic model framework for aerosol and cloud surface chemistry and gas-phase interaction-Part 1: General equation, parameters, and terminology, Atmos. Chem. Phys., 7, 5989-6023, 2007.

Pöschl, U.: Gas–particle interactions of tropospheric aerosols: Kinetic and thermodynamic perspectives of multiphase chemical reactions, amorphous organic substances, and the activation of cloud condensation nuclei, Atmos. Res., 101, 562-573, 2011.

Pöschl, U., and Shiraiwa, M.: Multiphase Chemistry at the Atmosphere–Biosphere Interface Influencing Climate and Public Health in the Anthropocene, Chem. Rev., 115, 4440-4475, 2015.

Park, J.-H., Ivanov, A. V., and Molina, M. J.: Effect of Relative Humidity on OH Uptake by Surfaces of Atmospheric Importance, J. Phys. Chem. A, 112, 6968-6977, 2008.

Percival, C. J., Welz, O., Eskola, A. J., Savee, J. D., Osborn, D. L., Topping, D. O., Lowe, D., Utembe, S. R., Bacak, A., McFiggans, G., Cooke, M. C., Xiao, P., Archibald, A. T., Jenkin, M. E., Derwent, R. G., Riipinen, I., Mok, D. W. K., Lee, E. P. F., Dyke, J. M., Taatjes, C. A., and Shallcross, D. E.: Regional and global impacts of Criegee intermediates on atmospheric sulphuric acid concentrations and first steps of aerosol formation, Faraday Discuss., 165, 45-73, 2013.

Phillips, G. J., Tang, M. J., Thieser, J., Brickwedde, B., Schuster, G., Bohn, B., Lelieveld, J., and Crowley, J. N.: Significant concentrations of nitryl chloride observed in rural continental Europe associated with the influence of sea salt chloride and anthropogenic emissions, Geophys. Res. Lett., 39, L10811, 10.1029/2012gl051912, 2012.

Phillips, G. J., Thieser, J., Tang, M. J., Sobanski, N., Schuster, G., Fachinger, J., Drewnick, F., Borrmann, S., Bingemer, H., Lelieveld, J., and Crowley, J. N.: Estimating N2O5 uptake coefficients using ambient measurements of NO3, N2O5, ClNO2 and particle-phase nitrate, Atmos. Chem. Phys. Discuss., 2016, 1-34, 10.5194/acp-2016-693, 2016.

Pope, F. D., Dennis-Smither, B. J., Griffiths, P. T., Clegg, S. L., and Cox, R. A.: Studies of Single Aerosol Particles Containing Malonic Acid, Glutaric Acid, and Their Mixtures with Sodium Chloride. I. Hygroscopic Growth, J. Phys. Chem. A, 114, 5335-5341, 2010.

Pope, F. D., Braesicke, P., Grainger, R. G., Kalberer, M., Watson, I. M., Davidson, P. J., and Cox, R. A.: Stratospheric aerosol particles and solar-radiation management, Nature Clim. Change, 2, 713-719, 2012.

Pradhan, M., Kalberer, M., Griffiths, P. T., Braban, C. F., Pope, F. D., Cox, R. A., and Lambert, R. M.: Uptake of Gaseous Hydrogen Peroxide by Submicrometer Titanium Dioxide Aerosol as a Function of Relative Humidity, Environ. Sci. Technol., 44, 1360-1365, 2010a.

Pradhan, M., Kyriakou, G., Archibald, A. T., Papageorgiou, A. C., Kalberer, M., and Lambert, R. M.: Heterogeneous uptake of gaseous hydrogen peroxide by Gobi and Saharan dust aerosols: a potential missing sink for H_2O_2 in the troposphere, Atmos. Chem. Phys., 10, 7127-7136, 2010b.

Prospero, J. M.: Mineral and sea salt aerosol concentrations in various ocean regions, J. Geophys. Res.-Atmos, 84, 725-731, 1979.

Prospero, J. M.: Long-range Transport of Mineral Dust in the Global Atmosphere: Impact of African Dust on the Environment of the Southeastern United States, Proc. Natl. Acad. Sci. U. S. A., 96, 3396-3403, 1999.

Raff, J. D., Njegic, B., Chang, W. L., Gordon, M. S., Dabdub, D., Gerber, R. B., and Finlayson-Pitts, B. J.: Chrorine Activation Indoors and Outdoors via Surface-mediated Reactions of Nitrogen Oxides with Hydrogen Chloride, Proc. Natl. Acad. Sci. U. S. A., 106, 13647-13654, 2009.

Real, E., and Sartelet, K.: Modeling of photolysis rates over Europe: impact on chemical gaseous species and aerosols, Atmos. Chem. Phys., 11, 1711-1727, 2011.

Ren, X., Harder, H., Martinez, M., Lesher, R. L., Oliger, A., Simpas, J. B., Brune, W. H., Schwab, J. J., Demerjian, K. L., He, Y., Zhou, X., and Gao, H.: OH and HO2 Chemistry in the urban atmosphere of New York City, Atmos. Environ., 37, 3639-3651, 2003.

Rkiouak, L., Tang, M. J., Camp, J. C. J., McGregor, J., Watson, I. M., Cox, R. A., Kalberer, M., Ward, A. D., and Pope, F. D.: Optical trapping and Raman Spectroscopy of solid aerosol particles, Phys. Chem. Chem. Phys., 16, 11426-11434, 2014.

Ro, C. U., Hwang, H., Chun, Y., and Van Grieken, R.: Single-particle characterization of four "Asian Dust" samples collected in Korea, using low-Z particle electron probe X-ray microanalysis, Environ. Sci. Technol., 39, 1409-1419, 2005.

Rohrer, F., Lu, K. D., Hofzumahaus, A., Bohn, B., Brauers, T., Chang, C. C., Fuchs, H., Haseler, R., Holland, F., Hu, M., Kita, K., Kondo, Y., Li, X., Lou, S. R., Oebel, A., Shao, M., Zeng, L. M., Zhu, T., Zhang, Y. H., and Wahner, A.: Maximum efficiency in the hydroxyl-radical-based self-cleansing of the troposphere, Nature Geoscience, 7, 559-563, 2014.

Romanias, M. N., El Zein, A., and Bedjanian, Y.: Heterogeneous Interaction of H_2O_2 with TiO_2 Surface under Dark and UV Light Irradiation Conditions, J. Phys. Chem. A, 116, 8191-8200, 2012a.

Romanias, M. N., El Zein, A., and Bedjanian, Y.: Reactive uptake of HONO on aluminium oxide surface, J. Photochem. Photobiol. A-Chem., 250, 50-57, 2012b.

Romanias, M. N., El Zein, A., and Bedjanian, Y.: Uptake of hydrogen peroxide on the surface of Al_2O_3 and Fe_2O_3, Atmos. Environ., 77, 1-8, 2013.

Roscoe, J. M., and Abbatt, J. P. D.: Diffuse reflectance FTIR study of the interaction of alumina surfaces with ozone and water vapor, J. Phys. Chem. A, 109, 9028-9034, 2005.

Rosenfeld, D., Rudich, Y., and Lahav, R.: Desert dust suppressing precipitation: A possible desertification feedback loop, Proc. Natl. Acad. Sci. U. S. A., 98, 5975-5980, 2001.

Rosenfeld, D., Lohmann, U., Raga, G. B., O'Dowd, C. D., Kulmala, M., Fuzzi, S., Reissell, A., and Andreae, M. O.: Flood or drought: How do aerosols affect precipitation?, Science, 321, 1309-1313, 2008.

Rubasinghege, G., and Grassian, V. H.: Surface-Catalyzed Chlorine and Nitrogen Activation: Mechanisms for the Heterogeneous Formation of ClNO, NO, NO2, HONO, and N2O from HNO3 and HCl on Aluminum Oxide Particle Surfaces, J. Phys. Chem. A, 116, 5180-5192, 2012.

Rubasinghege, G., and Grassian, V. H.: Role(s) of Adsorbed Water in the Surface Chemistry of Environmental Interfaces, Chem. Commun., 49, 3071-3094, 2013.

Ryder, O. S., Ault, A. P., Cahill, J. F., Guasco, T. L., Riedel, T. P., Cuadra-Rodriguez, L. A., Gaston, C. J., Fitzgerald, E., Lee, C., Prather, K. A., and Bertram, T. H.: On the Role of Particle Inorganic Mixing State in the Reactive Uptake of N2O5 to Ambient Aerosol Particles, Environ. Sci. Technol., 10.1021/es4042622, 2014.

Sassine, M., Burel, L., D'Anna, B., and George, C.: Kinetics of the tropospheric formaldehyde loss onto mineral dust and urban surfaces, Atmos. Environ., 44, 5468-5475, 2010.

Scanza, R. A., Mahowald, N., Ghan, S., Zender, C. S., Kok, J. F., Liu, X., Zhang, Y., and Albani, S.: Modeling Dust as Component Minerals in the Community Atmosphere Model: Development of Framework and Impact on Radiative Forcing, Atmos. Chem. Phys., 15, 537-561, 2015.

Scheuvens, D., Schütz, L., Kandler, K., Ebert, M., and Weinbruch, S.: Bulk composition of northern African dust and its source sediments - A compilation, Earth-Sci. Rev., 116, 170-194, 2013.

Schulz, M., Prospero, J. M., Baker, A. R., Dentener, F., Ickes, L., Liss, P. S., Mahowald, N. M., Nickovic, S., García-Pando, C. P., Rodríguez, S., Sarin, M., Tegen, I., and Duce, R. A.: Atmospheric Transport and Deposition of Mineral Dust to the Ocean: Implications for Research Needs, Environ. Sci. Technol., 46, 10390-10404, 2012.

Seinfeld, J. H., Carmichael, G. R., Arimoto, R., Conant, W. C., Brechtel, F. J., Bates, T. S., Cahill, T. A., Clarke, A. D., Doherty, S. J., Flatau, P. J., Huebert, B. J., Kim, J., Markowicz, K. M., Quinn, P. K., Russell, L. M., Russell, P. B., Shimizu, A., Shinozuka, Y., Song, C. H., Tang, Y., Uno, I., Vogelmann, A. M., Weber, R. J., Woo, J.-H., and Zhang, X. Y.: ACE-

ASIA: Regional Climatic and Atmospheric Chemical Effects of Asian Dust and Pollution, Bull. Amer. Meteorol. Soc., 85, 367-380, 2004.
Seinfeld, J. H., and Pandis, S. N.: Atmospheric Chemistry and Physics: From Air Pollution to Climate Change, Wiley Interscience, New York, 2006.
Seisel, S., Borensen, C., Vogt, R., and Zellner, R.: Kinetics and Mechanism of the Uptake of N_2O_5 on Mineral Dust at 298 K, Atmos. Chem. Phys., 5, 3423-3432, 2005.
Seyfioglu, R., Odabasi, M., and Cetin, E.: Wet and dry deposition of formaldehyde in Izmir, Turkey, Sci. Total Environ., 366, 809-818, 2006.
Shao, M., Zhang, Y., Zeng, L., Tang, X., Zhang, J., Zhong, L., and Wang, B.: Ground-level ozone in the Pearl River Delta and the roles of VOC and NOx in its production, Journal of Environmental Management, 90, 512-518, 2009.
Shen, X., Zhao, Y., Chen, Z., and Huang, D.: Heterogeneous reactions of volatile organic compounds in the atmosphere, Atmos. Environ., 68, 297-314, 2013.
Shi, Z., Zhang, D., Hayashi, M., Ogata, H., Ji, H., and Fujiie, W.: Influences of sulfate and nitrate on the hygroscopic behaviour of coarse dust particles, Atmos. Environ., 42, 822-827, 2008.
Shi, Z. B., Krom, M. D., Jickells, T. D., Bonneville, S., Carslaw, K. S., Mihalopoulos, N., Baker, A. R., and Benning, L. G.: Impacts on iron solubility in the mineral dust by processes in the source region and the atmosphere: A review, Aeolian Res., 5, 21-42, 2012.
Shiraiwa, M., Ammann, M., Koop, T., and Poschl, U.: Gas uptake and chemical aging of semisolid organic aerosol particles, Proc. Natl. Acad. Sci. U. S. A., 108, 11003-11008, 2011.
Shiraiwa, M., Pfrang, C., Koop, T., and Poschl, U.: Kinetic multi-layer model of gas-particle interactions in aerosols and clouds (KM-GAP): linking condensation, evaporation and chemical reactions of organics, oxidants and water, Atmos. Chem. Phys., 12, 2777-2794, 2012.
Shirley, T. R., Brune, W. H., Ren, X., Mao, J., Lesher, R., Cardenas, B., Volkamer, R., Molina, L. T., Molina, M. J., Lamb, B., Velasco, E., Jobson, T., and Alexander, M.: Atmospheric oxidation in the Mexico City Metropolitan Area (MCMA) during April 2003, Atmos. Chem. Phys., 6, 2753-2765, 2006.
Sihvonen, S. K., Schill, G. P., Lyktey, N. A., Veghte, D. P., Tolbert, M. A., and Freedman, M. A.: Chemical and Physical Transformations of Aluminosilicate Clay Minerals Due to Acid Treatment and Consequences for Heterogeneous Ice Nucleation, J. Phys. Chem. A, 118, 8787-8796, 2014.
Simpson, W. R., Brown, S. S., Saiz-Lopez, A., Thornton, J. A., and Glasow, R. v.: Tropospheric Halogen Chemistry: Sources, Cycling, and Impacts, Chem. Rev., 115, 4035-4062, 2015.
Sing, K. S. W.: 7 - Assessment of Surface Area by Gas Adsorption, in: Adsorption by Powders and Porous Solids (Second Edition), Academic Press, Oxford, 237-268, 2014.
Sinha, V., Williams, J., Crowley, J. N., and Lelieveld, J.: The Comparative Reactivity Method – a new tool to measure total OH Reactivity in ambient air, Atmos. Chem. Phys., 8, 2213-2227, 2008.
Sobanski, N., Tang, M. J., Thieser, J., Schuster, G., Pöhler, D., Fischer, H., Song, W., Sauvage, C., Williams, J., Fachinger, J., Berkes, F., Hoor, P., Platt, U., Lelieveld, J., and Crowley, J. N.: Chemical and meteorological influences on the lifetime of NO3 at a semi-rural mountain site during PARADE, Atmos. Chem. Phys., 16, 4867-4883, 2016.
Song, C. H., Kim, C. M., Lee, Y. J., Carmichael, G. R., Lee, B. K., and Lee, D. S.: An evaluation of reaction probabilities of sulfate and nitrate precursors onto East Asian dust particles, J. Geophys. Res.-Atmos., 112, D18206, 10.1029/2006jd008092, 2007.

Spicer, C. W., Chapman, E. G., Finlayson-Pitts, B. J., Plastridge, R. A., Hubbe, J. M., Fast, J. D., and Berkowitz, C. M.: Unexpectedly high concentrations of molecular chlorine in coastal air, Nature, 394, 353-356, 1998.

Stockwell, W. R.: On the HO2+HO2 reaction: its misapplication in atmospheric chemistry models, J. Geophys. Res.-Atmos., 100, 11695-11698, 10.1029/94jd03107, 1995.

Stockwell, W. R., Kirchner, F., Kuhn, M., and Seefeld, S.: A new mechanism for regional atmospheric chemistry modeling, J. Geophys. Res.-Atmos, 102, 25847-25879, 1997.

Stone, D., Whalley, L. K., and Heard, D. E.: Tropospheric OH and HO2 radicals: field measurements and model comparisons, Chem. Soc. Rev., 41, 6348-6404, 2012.

Striegel, M. F., Bede Guin, E., Hallett, K., Sandoval, D., Swingle, R., Knox, K., Best, F., and Fornea, S.: Air pollution, coatings, and cultural resources, Progress in Organic Coatings, 48, 281-288, 2003.

Stutz, J., Alicke, B., and Neftel, A.: Nitrous acid formation in the urban atmosphere: Gradient measurements of NO2 and HONO over grass in Milan, Italy, J. Geophys. Res.-Atmos., 107, 8192, doi: 8110.1029/2001jd000390, 2002.

Su, H., Cheng, Y. F., Shao, M., Gao, D. F., Yu, Z. Y., Zeng, L. M., Slanina, J., Zhang, Y. H., and Wiedensohler, A.: Nitrous acid (HONO) and its daytime sources at a rural site during the 2004 PRIDE-PRD experiment in China, J. Geophys. Res.-Atmos., 113, D14312, doi: 14310.11029/12007jd009060, 2008.

Suh, M., Bagus, P. S., Pak, S., Rosynek, M. P., and Lunsford, J. H.: Reactions of hydroxyl radicals on titania, silica, alumina, and gold surfaces, J. Phys. Chem. B, 104, 2736-2742, 2000.

Sullivan, R. C., Thornberry, T., and Abbatt, J. P. D.: Ozone decomposition kinetics on alumina: effects of ozone partial pressure, relative humidity and repeated oxidation cycles, Atmos. Chem. Phys., 4, 1301-1310, 2004.

Sullivan, R. C., Guazzotti, S. A., Sodeman, D. A., and Prather, K. A.: Direct Observations of the Atmospheric Processing of Asian Mineral Dust, Atmos. Chem. Phys., 7, 1213-1236, 2007.

Sullivan, R. C., and Prather, K. A.: Investigations of the diurnal cycle and mixing state of oxalic acid in individual particles in Asian aerosol outflow, Environ. Sci. Technol., 41, 8062-8069, 2007.

Sullivan, R. C., Moore, M. J. K., Petters, M. D., Kreidenweis, S. M., Roberts, G. C., and Prather, K. A.: Timescale for Hygroscopic Conversion of Calcite Mineral Particles through Heterogeneous Reaction with Nitric Acid, Phys. Chem. Chem. Phys., 11, 7826-7837, 2009a.

Sullivan, R. C., Moore, M. J. K., Petters, M. D., Kreidenweis, S. M., Roberts, G. C., and Prather, K. A.: Effect of Chemical Mixing State on the Hygroscopicity and Cloud Nucleation Properties of Calcium Mineral Dust Particles, Atmos. Chem. Phys., 9, 3303-3316, 2009b.

Sun, S., Ding, J., Bao, J., Gao, C., Qi, Z., and Li, C.: Photocatalytic Oxidation of Gaseous Formaldehyde on TiO_2: An In Situ DRIFTS Study, Catal. Lett., 137, 239-246, 2010.

Syomin, D. A., and Finlayson-Pitts, B. J.: HONO decomposition on borosilicate glass surfaces: implications for environmental chamber studies and field experiments, Phys. Chem. Chem. Phys., 5, 5236-5242, 2003.

Ta, W. Q., Xiao, Z., Qu, J. J., Yang, G. S., and Wang, T.: Characteristics of dust particles from the desert/Gobi area of northwestern China during dust-storm periods, Environmental Geology, 43, 667-679, 2003.

Taatjes, C. A., Welz, O., Eskola, A. J., Savee, J. D., Scheer, A. M., Shallcross, D. E., Rotavera, B., Lee, E. P. F., Dyke, J. M., Mok, D. K. W., Osborn, D. L., and Percival, C. J.: Direct Measurements of Conformer-Dependent Reactivity of the Criegee Intermediate CH3CHOO, Science, 340, 177-180, 2013.

Taatjes, C. A., Shallcross, D. E., and Percival, C. J.: Research frontiers in the chemistry of Criegee intermediates and tropospheric ozonolysis, Phys. Chem. Chem. Phys., 16, 1704-1718, 2014.

Tang, M. J., Thieser, J., Schuster, G., and Crowley, J. N.: Uptake of NO_3 and N_2O_5 to Saharan dust, ambient urban aerosol and soot: a relative rate study, Atmos. Chem. Phys., 10, 2965-2974, 2010.

Tang, M. J., Thieser, J., Schuster, G., and Crowley, J. N.: Kinetics and Mechanism of the Heterogeneous Reaction of N_2O_5 with Mineral Dust Particles, Phys. Chem. Chem. Phys., 14, 8551-8561, 2012.

Tang, M. J., Camp, J. C. J., Rkiouak, L., McGregor, J., Watson, I. M., Cox, R. A., Kalberer, M., Ward, A. D., and Pope, F. D.: Heterogeneous Interaction of SiO_2 with N_2O_5: Aerosol Flow Tube and Single Particle Optical Levitation-Raman Spectroscopy Studies, J. Phys. Chem. A, 118, 8817-8827, 2014a.

Tang, M. J., Cox, R. A., and Kalberer, M.: Compilation and evaluation of gas phase diffusion coefficients of reactive trace gases in the atmosphere: volume 1. Inorganic compounds, Atmos. Chem. Phys., 14, 9233-9247, 2014b.

Tang, M. J., Schuster, G., and Crowley, J. N.: Heterogeneous Reaction of N_2O_5 with Illite and Arizona Test Dust Particles, Atmos. Chem. Phys., 14, 245-254, 2014c.

Tang, M. J., Telford, P. J., Pope, F. D., Rkiouak, L., Abraham, N. L., Archibald, A. T., Braesicke, P., Pyle, J. A., McGregor, J., Watson, I. M., Cox, R. A., and Kalberer, M.: Heterogeneous reaction of N_2O_5 with airborne TiO_2 particles and its implication for stratospheric particle injection, Atmos. Chem. Phys., 14, 6035-6048, 2014d.

Tang, M. J., Telford, P. J., Pope, F. D., Rkiouak, L., Abraham, N. L., Archibald, A. T., Braesicke, P., Pyle, J. A., McGregor, J., Watson, I. M., Cox, R. A., and Kalberer, M.: Corrigendum to "Heterogeneous reaction of N2O5 with airborne TiO2 particles and its implication for stratospheric particle injection" published in Atmos. Chem. Phys., 14, 6035–6048, 2014, Atmos. Chem. Phys., 14, 8233-8234, 10.5194/acp-14-8233-2014, 2014e.

Tang, M. J., Shiraiwa, M., Pöschl, U., Cox, R. A., and Kalberer, M.: Compilation and evaluation of gas phase diffusion coefficients of reactive trace gases in the atmosphere: Volume 2. Diffusivities of organic compounds, pressure-normalised mean free paths, and average Knudsen numbers for gas uptake calculations, Atmos. Chem. Phys., 15, 5585-5598, 2015.

Tang, M. J., Cziczo, D. J., and Grassian, V. H.: Interactions of Water with Mineral Dust Aerosol: Water Adsorption, Hygroscopicity, Cloud Condensation and Ice Nucleation, Chem. Rev., 116, 4205–4259, 2016a.

Tang, M. J., Keeble, J., Telford, P. J., Pope, F. D., Braesicke, P., Griffiths, P. T., Abraham, N. L., McGregor, J., Watson, I. M., Cox, R. A., Pyle, J. A., and Kalberer, M.: Heterogeneous reaction of ClONO2 with TiO2 and SiO2 aerosol particles: implications for stratospheric particle injection for climate engineering, Atmos. Chem. Phys., 16, 15397-15412, 2016b.

Tang, Y., Carmichael, G. R., Kurata, G., Uno, I., Weber, R. J., Song, C. H., Guttikunda, S. K., Woo, J. H., Streets, D. G., Wei, C., Clarke, A. D., Huebert, B., and Anderson, T. L.: Impacts of Dust on Regional Tropospheric Chemistry during the ACE-Asia Experiment: a Model Study with Observations, J. Geophys. Res., 109, D19s21, doi: 10.1029/2003jd003806, 2004.

Ten Brink, H. M., and Spoelstra, H.: The dark decay of hono in environmental (SMOG) chambers, Atmos. Environ., 32, 247-251, 1998.

Textor, C., Schulz, M., Guibert, S., Kinne, S., Balkanski, Y., Bauer, S., Berntsen, T., Berglen, T., Boucher, O., Chin, M., Dentener, F., Diehl, T., Easter, R., Feichter, H., Fillmore, D., Ghan, S., Ginoux, P., Gong, S., Grini, A., Hendricks, J., Horowitz, L., Huang, P., Isaksen, I., Iversen, I., Kloster, S., Koch, D., Kirkevåg, A., Kristjansson, J. E., Krol, M., Lauer, A.,

Lamarque, J. F., Liu, X., Montanaro, V., Myhre, G., Penner, J., Pitari, G., Reddy, S., Seland, Ø., Stier, P., Takemura, T., and Tie, X.: Analysis and Quantification of the Diversities of Aerosol Life Cycles within AeroCom, Atmos. Chem. Phys., 6, 1777-1813, 2006.

Tham, Y. J., Wang, Z., Li, Q., Yun, H., Wang, W., Wang, X., Xue, L., Lu, K., Ma, N., Bohn, B., Li, X., Kecorius, S., Größ, J., Shao, M., Wiedensohler, A., Zhang, Y., and Wang, T.: Significant concentrations of nitryl chloride sustained in the morning: investigations of the causes and impacts on ozone production in a polluted region of northern China, Atmos. Chem. Phys., 16, 14959-14977, 2016.

Thornton, J., and Abbatt, J. P. D.: Measurements of HO2 uptake to aqueous aerosol: Mass accommodation coefficients and net reactive loss, J. Geophys. Res.-Atmos, 110, D08309, doi: 08310.01029/02004JD005402, 2005.

Thornton, J. A., Kercher, J. P., Riedel, T. P., Wagner, N. L., Cozic, J., Holloway, J., S., Dube, W. P., Wolfe, G. M., Quinn, P. K., Middlebrook, A. M., Alexander, B., and Brown, S. S.: A large atomic chlorine source inferred from mid-continental reactive nitrogen chemistry, Nature, 464, 271-174, 2010.

Tie, X., Brasseur, G., Emmons, L., Horowitz, L., and Kinnison, D.: Effects of aerosols on tropospheric oxidants: A global model study, J. Geophys. Res.-Atmos., 106, 22931-22964, 2001.

Tobo, Y., DeMott, P. J., Raddatz, M., Niedermeier, D., Hartmann, S., Kreidenweis, S. M., Stratmann, F., and Wex, H.: Impacts of chemical reactivity on ice nucleation of kaolinite particles: A case study of levoglucosan and sulfuric acid, Geophys. Res. Lett., 39, L19803, doi: 19810.11029/12012gl053007, 2012.

Tong, H. J., Reid, J. P., Bones, D. L., Luo, B. P., and Krieger, U. K.: Measurements of the timescales for the mass transfer of water in glassy aerosol at low relative humidity and ambient temperature, Atmos. Chem. Phys., 11, 4739-4754, 2011.

Tong, S. R., Wu, L. Y., Ge, M. F., Wang, W. G., and Pu, Z. F.: Heterogeneous Chemistry of Monocarboxylic Acids on α-Al_2O_3 at Different Relative Humidities, Atmos. Chem. Phys., 10, 7561-7574, 2010.

Twohy, C. H., Kreidenweis, S. M., Eidhammer, T., Browell, E. V., Heymsfield, A. J., Bansemer, A. R., Anderson, B. E., Chen, G., Ismail, S., DeMott, P. J., and Van den Heever, S. C.: Saharan Dust Particles Nucleate Droplets in Eastern Atlantic Clouds, Geophys. Res. Lett., 36, L01807, doi: 01810.01029/02008gl035846, 2009.

Ullerstam, M., Vogt, R., Langer, S., and Ljungstrom, E.: The kinetics and mechanism of SO_2 oxidation by O_3 on mineral dust, Phys. Chem. Chem. Phys., 4, 4694-4699, 2002.

Umann, B., Arnold, F., Schaal, C., Hanke, M., Uecker, J., Aufmhoff, H., Balkanski, Y., and Van Dingenen, R.: Interaction of mineral dust with gas phase nitric acid and sulfur dioxide during the MINATROC II field campaign: First estimate of the uptake coefficient gamma(HNO3) from atmospheric data, J. Geophys. Res.-Atmos., 110, D22306, 10.1029/2005jd005906, 2005.

Underwood, G. M., Li, P., Usher, C. R., and Grassian, V. H.: Determining accurate kinetic parameters of potentially important heterogeneous atmospheric reactions on solid particle surfaces with a Knudsen cell reactor, J. Phys. Chem. A, 104, 819-829, 2000.

Underwood, G. M., Li, P., Al-Abadleh, H., and Grassian, V. H.: A Knudsen Cell Study of the Heterogeneous Reactivity of Nitric Acid on Oxide and Mineral Dust Particles, J. Phys. Chem. A, 105, 6609-6620, 2001.

Uno, I., Eguchi, K., Yumimoto, K., Takemura, T., Shimizu, A., Uematsu, M., Liu, Z., Wang, Z., Hara, Y., and Sugimoto, N.: Asian Dust Transported One Full Circuit around the Globe, Nature Geosci., 2, 557-560, 2009.

Usher, C. R., Michel, A. E., and Grassian, V. H.: Reactions on Mineral Dust, Chem. Rev., 103, 4883-4939, 2003a.

Usher, C. R., Michel, A. E., Stec, D., and Grassian, V. H.: Laboratory studies of ozone uptake on processed mineral dust, Atmos. Environ., 37, 5337-5347, 2003b.
Vlasenko, A., Sjogren, S., Weingartner, E., Stemmler, K., Gaggeler, H. W., and Ammann, M.: Effect of Humidity on Nitric Acid Uptake to Mineral Dust Aerosol Particles, Atmos. Chem. Phys., 6, 2147-2160, 2006.
Vlasenko, A., Huthwelker, T., Gaggeler, H. W., and Ammann, M.: Kinetics of the heterogeneous reaction of nitric acid with mineral dust particles: an aerosol flow tube study, Phys. Chem. Chem. Phys., 11, 7921-7930, 2009.
Wagner, C., Hanisch, F., Holmes, N., de Coninck, H., Schuster, G., and Crowley, J. N.: The interaction of N_2O_5 with mineral dust: aerosol flow tube and Knudsen reactor studies, Atmos. Chem. Phys., 8, 91-109, 2008.
Wagner, C., Schuster, G., and Crowley, J. N.: An aerosol flow tube study of the interaction of N_2O_5 with calcite, Arizona dust and quartz, Atmos. Environ., 43, 5001-5008, 2009.
Wahner, A., Mentel, T. F., and Sohn, M.: Gas-phase reaction of N_2O_5 with water vapor: Importance of heterogeneous hydrolysis of N_2O_5 and surface desorption of HNO_3 in a large teflon chamber, Geophys. Res. Lett., 25, 2169-2172, 1998.
Walker, R. A., Wilson, K., Lee, A. F., Woodford, J., Grassian, V. H., Baltrusaitis, J., Rubasinghege, G., Cibin, G., and Dent, A.: Preservation of York Minster historic limestone by hydrophobic surface coatings, Sci. Rep., 2, 880, doi: 810.1038/srep00880, 2012.
Wang, K., Zhang, Y., Nenes, A., and Fountoukis, C.: Implementation of Dust Emission and Chemistry into the Community Multiscale Air Quality Modeling System and Initial Application to an Asian Dust Storm Episode, Atmos. Chem. Phys., 12, 10209-10237, 2012.
Wang, T., Tham, Y. J., Xue, L., Li, Q., Zha, Q., Wang, Z., Poon, S. C. N., Dubé, W. P., Blake, D. R., Louie, P. K. K., Luk, C. W. Y., Tsui, W., and Brown, S. S.: Observations of nitryl chloride and modeling its source and effect on ozone in the planetary boundary layer of southern China, J. Geophys. Res.-Atmos, 121, 2476-2489, 2016.
Wang, W. G., Ge, M. F., and Sun, Q.: Heterogeneous Uptake of Hydrogen Peroxide on Mineral Oxides, Chin. J. Chem. Phys., 24, 515-520, 2011.
Wang, Y. H., and Jacob, D. J.: Anthropogenic forcing on tropospheric ozone and OH since preindustrial times, J. Geophys. Res.-Atmos., 103, 31123-31135, 1998.
Wayne, R. P., Barnes, I., Biggs, P., Burrows, J. P., Canosamas, C. E., Hjorth, J., Lebras, G., Moortgat, G. K., Perner, D., Poulet, G., Restelli, G., and Sidebottom, H.: The nitrate radical-physics, chemistry, and the atmosphere, Atmos. Environ., 25A, 1-203, 1991.
Webb, A. H., Bawden, R. J., Busby, A. K., and Hopkins, J. N.: Studies on the effects of air pollution on limestone degradation in Great Britain, Atmos. Environ., 26, 165-181, 1992.
Weisenstein, D. K., Keith, D. W., and Dykema, J. A.: Solar geoengineering using solid aerosol in the stratosphere, Atmos. Chem. Phys., 15, 11835-11859, 2015.
Welz, O., Savee, J. D., Osborn, D. L., Vasu, S. S., Percival, C. J., Shallcross, D. E., and Taatjes, C. A.: Direct Kinetic Measurements of Criegee Intermediate (CH2OO) Formed by Reaction of CH2I with O-2, Science, 335, 204-207, 2012.
Wesely, M. L., and Hicks, B. B.: A review of the current status of knowledge on dry deposition, Atmos. Environ., 34, 2261-2282, 2000.
Wex, H., DeMott, P. J., Tobo, Y., Hartmann, S., Rösch, M., Clauss, T., Tomsche, L., Niedermeier, D., and Stratmann, F.: Kaolinite particles as ice nuclei: learning from the use of different kaolinite samples and different coatings, Atmos. Chem. Phys., 14, 5529-5546, 2014.
Whalley, L. K., Edwards, P. M., Furneaux, K. L., Goddard, A., Ingham, T., Evans, M. J., Stone, D., Hopkins, J. R., Jones, C. E., Karunaharan, A., Lee, J. D., Lewis, A. C., Monks, P. S., Moller, S. J., and Heard, D. E.: Quantifying the magnitude of a missing hydroxyl radical source in a tropical rainforest, Atmos. Chem. Phys., 11, 7223-7233, 2011.

Wood, E. C., Bertram, T. H., Wooldridge, P. J., and Cohen, R. C.: Measurements of N2O5, NO2, and O-3 east of the San Francisco Bay, Atmos. Chem. Phys., 5, 483-491, 2005.
Wu, L.-Y., Tong, S.-R., Zhou, L., Wang, W.-G., and Ge, M.-F.: Synergistic Effects between SO2 and HCOOH on α-Fe2O3, J. Phys. Chem. A, 117, 3972-3979, 2013a.
Wu, L., Tong, S., and Ge, M.: Heterogeneous Reaction of NO2 on Al2O3: The Effect of Temperature on the Nitrite and Nitrate Formation, J. Phys. Chem. A, 117, 4937-4944, 2013b.
Wu, L. Y., Tong, S. R., Wang, W. G., and Ge, M. F.: Effects of temperature on the heterogeneous oxidation of sulfur dioxide by ozone on calcium carbonate, Atmos. Chem. Phys., 11, 6593-6605, 2011.
Xu, B. Y., Zhu, T., Tang, X. Y., Ding, J., and Li, H. J.: Heterogeneous reaction of formaldehyde on surface of α-Al_2O_3 particles, Chemical Journal of Chinese Universities-Chinese, 27, 1912-1917, 2006.
Xu, B. Y., Zhu, T., Tang, X. Y., and Shang, J.: Heterogeneous reaction of formaldehyde on the surface of TiO_2 particles, Sci. China-Chem., 53, 2644-2651, 2010.
Xu, B. Y., Shang, J., Zhu, T., and Tang, X. Y.: Heterogeneous reaction of formaldehyde on the surface of γ-Al_2O_3 particles, Atmos. Environ., 45, 3569-3575, 2011.
Yang, W. W., He, H., Ma, Q. X., Ma, J. Z., Liu, Y. C., Liu, P. F., and Mu, Y. J.: Synergistic formation of sulfate and ammonium resulting from reaction between SO2 and NH3 on typical mineral dust, Phys. Chem. Chem. Phys., 18, 956-964, 2016a.
Yang, Y., Shao, M., Wang, X., Nölscher, A. C., Kessel, S., Guenther, A., and Williams, J.: Towards a quantitative understanding of total OH reactivity: A review, Atmos. Environ., 134, 147-161, 2016b.
Yang, Y., Russell, L. M., Lou, S., Liao, H., Guo, J., Liu, Y., Singh, B., and Ghan, S. J.: Dust-wind interactions can intensify aerosol pollution over eastern China, 8, 15333, 10.1038/ncomms15333, 2017.
Yi, J., Bahrini, C., Schoemaecker, C., Fittschen, C., and Choi, W.: Photocatalytic Decomposition of H_2O_2 on Different TiO_2 Surfaces Along with the Concurrent Generation of HO_2 Radicals Monitored Using Cavity Ring Down Spectroscopy, J. Phys. Chem. C, 116, 10090-10097, 2012.
Zhang, Q., Streets, D. G., He, K., Wang, Y., Richter, A., Burrows, J. P., Uno, I., Jang, C. J., Chen, D., Yao, Z., and Lei, Y.: NOx emission trends for China, 1995–2004: The view from the ground and the view from space, J. Geophys. Res.-Atmos, 112, D22306, doi: 22310.21029/22007JD008684, 2007.
Zhang, X. L., Wu, G. J., Zhang, C. L., Xu, T. L., and Zhou, Q. Q.: What is the real role of iron oxides in the optical properties of dust aerosols?, Atmos. Chem. Phys., 15, 12159-12177, 2015.
Zhang, X. Y., Gong, S. L., Shen, Z. X., Mei, F. M., Xi, X. X., Liu, L. C., Zhou, Z. J., Wang, D., Wang, Y. Q., and Cheng, Y.: Characterization of soil dust aerosol in China and its transport and distribution during 2001 ACE-Asia: 1. Network observations, J. Geophys. Res.-Atmos., 108, 4206, doi: 4210.1029/2002jd002632, 2003a.
Zhang, X. Y., Gong, S. L., Zhao, T. L., Arimoto, R., Wang, Y. Q., and Zhou, Z. J.: Sources of Asian dust and role of climate change versus desertification in Asian dust emission, Geophys. Res. Lett., 30, 2272, doi: 2210.1029/2003GL018206,, 2003b.
Zhang, Y., Young, S. W., Kotamarthi, V., and Carmichael, G. R.: Photochemical Oxidant Processes in the Presence of Dust: An Evaluation of the Impact of Dust on Particulate Nitrate and Ozone Formation, J. Appl. Met., 33, 813-824, 1994.
Zhao, D. F., Zhu, T., Chen, Q., Liu, Y. J., and Zhang, Z. F.: Raman micro-spectrometry as a technique for investigating heterogeneous reactions on individual atmospheric particles, Sci. China-Chem., 54, 154-160, 2011a.

Zhao, X., Kong, L. D., Sun, Z. Y., Ding, X. X., Cheng, T. T., Yang, X., and Chen, J. M.: Interactions between Heterogeneous Uptake and Adsorption of Sulfur Dioxide and Acetaldehyde on Hematite, J. Phys. Chem. A, 119, 4001-4008, 2015.

Zhao, Y., Chen, Z. M., Shen, X. L., and Zhang, X. A.: Kinetics and Mechanisms of Heterogeneous Reaction of Gaseous Hydrogen Peroxide on Mineral Oxide Particles, Environ. Sci. Technol., 45, 3317-3324, 2011b.

Zhao, Y., Chen, Z. M., Shen, X. L., and Huang, D.: Heterogeneous reactions of gaseous hydrogen peroxide on pristine and acidic gas-processed calcium carbonate particles: Effects of relative humidity and surface coverage of coating, Atmos. Environ., 67, 63-72, 2013.

Zhao, Y., Huang, D., Huang, L. B., and Chen, Z. M.: Hydrogen Peroxide Enhances the Oxidation of Oxygenated Volatile Organic Compounds on Mineral Dust Particles: A Case Study of Methacrolein, Environ. Sci. Technol., 48, 10614-10623, 2014.

Zhou, L., Wang, W. G., and Ge, M. F.: Temperature Dependence of Heterogeneous Uptake of Hydrogen Peroxide on Silicon Dioxide and Calcium Carbonate, J. Phys. Chem. A, 116, 7959-7964, 2012.

Zhou, L., Wang, W. G., Gai, Y. B., and Ge, M. F.: Knudsen cell and smog chamber study of the heterogeneous uptake of sulfur dioxide on Chinese mineral dust, J. Environ. Sci., 26, 2423-2433, 2014.

Zhou, L., Wang, W. G., Ge, M. F., and Tong, S. R.: Heterogeneous uptake of gaseous hydrogen peroxide on mineral dust, J. Environ. Sci., 28, 44-50, 2016.

Zhu, S., Butler, T., Sander, R., Ma, J., and Lawrence, M. G.: Impact of Dust on Tropospheric Chemistry over Polluted Regions: a Case Study of the Beijing Megacity, Atmos. Chem. Phys., 10, 3855-3873, 2010.

Zhu, T., Shang, J., and Zhao, D. F.: The roles of heterogeneous chemical processes in the formation of an air pollution complex and gray haze, Sci. China-Chem., 54, 145-153, 2011.